University of São Paulo
"Luiz de Queiroz" College of Agriculture

Insights on effector candidates of *Austropuccinia psidii*: identification, characterization and comparative genomic analysis

Carolina Alessandra de Almeida Hayashibara

Thesis presented to obtain the degree of Doctor in Science.
Area: Genetics and Plant Breeding

Piracicaba
2021

Carolina Alessandra de Almeida Hayashibara
Bsc in Biology Sciences

Insights on effector candidates of *Austropuccinia psidii*: identification, characterization and comparative genomic analysis

versão revisada de acordo com a resolução CoPGr 6018 de 2011

Advisor:
Profª Drª **MARIA CAROLINA QUECINE-VERDI**

Thesis presented to obtain the degree of Doctor in Science.
Area: Genetics and Plant Breeding

Piracicaba
2021

Dados Internacionais de Catalogação na Publicação
DIVISÃO DE BIBLIOTECA – DIBD/ESALQ/USP

Hayashibara, Carolina Alessandra de Almeida
Insights on effector candidates of *Austropuccinia psidii*: identification, characterization and comparative genomic analysis / Carolina Alessandra de Almeida Hayashibara. - - versão revisada de acordo com a resolução CoPGr 6018 de 2011 - - Piracicaba, 2021.
141 p.

Tese (Doutorado) - - USP / Escola Superior de Agricultura “Luiz de Queiroz”.

1. Efetorômica 2. Agroinfiltração 3. Ferrugem das mirtáceas 4. Biótipos I. Título

DECIDATORY

To my beloved family

ACKNOWLEDGEMENTS

It was a long way to finish the PhD, which takes a lot of effort and dedication, in addition to the support of essential people. Thus, I wish to express my sincere thanks to:

God and St Therese for life, protection, and for lighting my way. For having where to put my faith in moments of joy and difficulties.

My family, especially my mom (Sônia), my grandparents (José Victor and Sebastiana), my aunts (Sandra, Simone, and Silvia), and my cousins (Victória and Maria Fernanda) for all their support and unconditional belief during all these years.

My dear advisor Prof. Maria Carolina Quecine-Verdi for all knowledge, support, and encouragement. Thank you for the opportunity to have learned so much from you, for living together, for friendship, for counselling, for understanding and guidance. If I am a better professional today, that is on you. Thank you for always inspiring me to be a better person and professional.

Professor Robert Park, from the University of Sydney, who received me under his guidance, thank you for all your attention, availability, knowledge, and care.

Dr Peri Tobias, from the University of Sydney, for the guidance, help, and knowledge. You were very patient and caring the whole time I was there. Thank you for everything!

Professor João Lúcio, for the example of professional love, experience, knowledge, and coffee time.

My colleagues from the “Laboratory of Genetics of Microorganisms” and the extinct group “Puccinia”: Bruno, Isaneli, Jessica and Mariana. My gratitude to Everthon, Joelma, and Maurício, during the pandemic they were my companions from "Corujão", for their laughter, for their teachings, even for their stress at one time or another. I'm sure that without you I wouldn't have finished in time. Bruna Durante for received me in Australia, helped, and became a friend. To Zezo for the friendship and all the help.

My friends: Emanoel, Gabriel, Gleicy, Getúlio, Helena, Jaqueline, Jessica, João Nomura, Maiara, Maria Letícia, Mariana Marrafon, Patrícia and Willian. I am grateful that they made the walk happiest, encouraged me, listened to me, and supported me. My most sincere thanks!

My friends who are far away, but I carry them in my heart: Andreia, Anelise, Jaque, Luis Gustavo, Roxane, and Rafael.

Professor Paulo Teixeira, for his teachings, for his support in experiments conductions, and to provide structure for experiments.

Prof. Carlos Labate, Mônica, and Thaís from the “Max Feffer Laboratory of Plant Genetics” for the availability of equipment!

Prof. Luciana D. Silva and technicians Natanael and Sabino from the “Seedling nursery of the Department of Forestry Sciences” for their invaluable support in conducting seedlings and supply of plant material.

Professor Antônio Figueira and technician Felippe Campana from the Laboratory of Plant Breeding Plant at CENA / USP, for the structure, microscopy, and for the time dedicated. Dr. João Paulo Marques for his assistance during the microscopic analysis.

“Luiz de Queiroz” College of Agriculture, University of São Paulo, especially the Department of Genetics, colleagues, professors, and workers for all teachings, support, and professional opportunities.

GVENCK “Genetics and Plant Breeding Group “Roland Vencovsky”. I am immensely proud to have participated in the group foundation, to be part of it for 2 years, and for provided me with many moments of learning and sharing.

The University of Sydney, the Plant Breeding Institute, the University of Pretoria, Louise Shuey, Tuan Doung, and Alistair McTaggart for provided genetic material and genome information for analysis. "This work was made possible by the Australian Plant Biosecurity Science Foundation (PBSF018)."

Finally, I would like to acknowledge the financial support given by the São Paulo Research Foundation (FAPESP, Project number 2014/16804-4); the Conselho Nacional de Desenvolvimento Científico e Tecnológico (CNPq, grant number 140587/2018-7) and the Coordenação de Aperfeiçoamento de Pessoal de Nível Superior (CAPES, process number 88887.371006/2019-00).

EPÍGRAFE

“You cannot hope to build a better world without improving the individuals. To that end, each of us must work for our own improvement.”
Marie Curie

SUMMARY

RESUMO

Estudo dos efetores candidatos de *Austropuccina psidii*: identificação, caracterização e análise de genômica comparativa

A ferrugem das mirtáceas é uma doença causada pelo fungo biotrófico *Austropuccinia psidii.* Fungos biotróficos necessitam dos tecidos vivos do hospedeiro para obtenção de nutrientes e desenvolvimento, criando uma relação íntima com o hospedeiro. Desde o primeiro contato entre patógeno e hospedeiro diversas moléculas estão envolvidas nesta interação. Informações sobre a interação *A. psidii* e o hospedeiro são escassas, devido ao grande número de espécies de Mirtáceas infectadas, além do estilo de vida biotrófico de *A. psidii*, que limita a sua manipulação. Para superar os mecanismos de defesa das plantas, os fungos podem liberar efetores durante a infecção do hospedeiro. Em geral, efetores são moléculas secretadas pelo patógeno que podem alterar a fisiologia do hospedeiro para uma bem-sucedida infecção e colonização. Dessa forma, a caracterização de efetores é uma importante estratégia para compreender os mecanismos envolvidos durante a infecção do hospedeiro pelo patógeno. No Capítulo 1 foi realizado o primeiro estudo sobre candidatos a efetores do biótipo MF-1 de *A. psidii*. Primeiramente foi realizada a identificação de 255 efetores candidatos, e a predição da localização e funções dos mesmos, sendo a maioria dos candidatos preditos como apoplásticos e com funções hipotéticas. Foi realizada uma validação de expressão *in vitro* por RT-qPCR de sete efetores candidatos selecionados aleatoriamente, utilizando como estímulo ceras cuticulares extraídas de folhas de espécies de eucalipto resistentes e suscetíveis ao patógeno, *Eucalyptus urophylla* e *E. grandis*, respectivamente. Foi observado que a expressão dos sete efetores candidatos foi modulada de acordo com a espécie, as quais as ceras cuticulares eram provenientes. Dois efetores candidatos, Ap28303 e Ap30385, foram clonados em vetores binários contendo a proteína G3GFP (proteína verde fluorescente), e agroinfiltrados em folhas de *Nicotiana benthamiana*. A agroinfiltração foi realizada para observar a localização subcelular dos efetores candidatos, porém o efetor candidato Ap30385 não foi observado em nenhum compartimento, enquanto foi observado um acúmulo do efetor candidato Ap28303 no núcleo. Pela primeira vez foram identificados efetores candidatos de *A. psidii*, bem como a localização subcelular de um efetor candidato. No Capítulo 2, foi realizada a identificação e comparação de efetores de três biótipos de *A. psidii*, um biótipo pandêmico originário da Austrália (Au), um biótipo da África do Sul (SA) e o biótipo MF-1 do Brasil. Foi observado um número maior de efetores do biótipo pandêmico, em comparação aos demais, no entanto, não foram encontradas diferenças nas localizações preditas dos efetores candidatos. Nas análises de homologia, também se observou que o biótipo australiano se mostrou mais distante dos outros dois, em relação aos efetores candidatos, possuindo um maior número de proteínas exclusivas. A partir da validação por PCR, a maioria dos efetores candidatos mostraram-se conservados entre os biótipos testados, mas também foram encontrados polimorfismos. Portanto, estudos mais aprofundados sobre esses polimorfismos encontrados serão necessários para um melhor entendimento da importância dessas variações na amplitude de hospedeiros. Este estudo pioneiro certamente possibilita novos estudos acerca de efetores candidatos de *A. psidii*, em relação a evolução dos efetores quanto ao hospedeiro, bem como uma detalhada caracterização de outros efetores candidatos.

Palavras-chave: Efetorômica, Agroinfiltração, Ferrugem das mirtáceas, Biótipos

ABSTRACT

Insights on effector candidates of *Austropuccinia psidii*: identification, characterization and comparative genomic analysis

Myrtle rust is a disease caused by the biotrophic fungus *Austropuccinia psidii*. Biotrophic fungi require living tissues to obtain nutrients and to develop, establishing a close relationship with the host. Since the first contact between pathogen and host, several molecules of both are involved. Information on the interaction between *A. psidii* and the host is scarce, due to a large number of infected Myrtaceae species, in addition to the biotrophic lifestyle of *A. psidii*, which limits the in vitro manipulation. To overcome the defense mechanisms of plants, fungi can release effectors during the infection. In general, effectors are molecules secreted by the pathogen that may alter the host's physiology for successful infection and colonization. Thus, the characterization of secreted effectors is a crucial strategy to understand the mechanisms involved in the host infection by the pathogen. Chapter 1 shows the first study on effector candidates of *A. psidii* biotype MF-1. First, 255 effector candidates were identified, and in silico prediction of localization and functions was performed, the most effector candidates were predicted as apoplastic and as hypothetical proteins with unknown functions. By RT-qPCR, we performed in vitro expression validation of seven randomly selected effector candidates, using as stimulus cuticular waxes extracted from leaves of resistant and susceptible Eucalyptus species to the pathogen, *E. urophylla* and *E. grandis*, respectively. The seven effector candidate's expression was modulated according to cuticular waxes. Two effector candidates, Ap28303 and Ap30385, were cloned into binary vectors containing the G3GFP (Green Fluorescent Protein) protein, and agroinfiltrated in leaves of *Nicotiana benthamiana*. Agroinfiltration was performed to observe the subcellular localization of the effector candidates, however the effector candidate Ap30385 was not observed in any compartment, and the effector candidate Ap28303 was observed accumulating in the nucleus. For the first time, *A. psidii* effector candidates were identified, as well as the subcellular localization of one effector candidate. In Chapter 2, the identification and comparison of effectors from three *A. psidii* biotypes, a pandemic biotype from Australia, a biotype from South Africa, and the MF-1 biotype from Brazil were carried out. It was observed a greater number of effectors from pandemic biotype compared with the others, however, it was not found differences in the predicted localization of effector candidates. By homology analysis, it was observed that the Australian biotype was more distant from the other two, regarding the effector candidates, showing the highest number of exclusive proteins. From PCR validation, the most effector candidates showed conserved among the tested biotypes, and polymorphisms were found. Therefore, deep studies are required for a better understanding of variation importance on host range. Certainly, this pioneering study will enable new studies about effector candidates from *A. psidii*, improving the comprehension of effector evolution and host relationship, as well offering a profile to further detailed characterization of other effector candidates.

Keywords: Effectoromic, Agroinfiltration, Myrtle rust, Biotypes

1. INTRODUCTION

Austropuccinia psidii (G. Winter) Beenken comb. nov. is a biotrophic fungus, the causal agent of rust in a great number of Myrtaceae species, known as myrtle rust (Beenken, 2017), guava rust, eucalyptus rust, or ‘ohi‘a rust, usually named after the host (Carnegie & Pegg, 2018). *A. psidii* is considered native from South America (Glen et al., 2007), being first described in Brazil infecting guava (*Psidium guajava* (Winter, 1884)) and in 1912 was reported in *Eucalyptus* spp. (Joffily, 1944). From the first outbreak of rust in *Eucalyptus* plantations it was recognized the importance of this pathogen in Brazil (Carnegie & Pegg, 2018; Ferreira, 1983) and more recently around the world (Carnegie & Pegg, 2018).

Brazil is one of the most important *Eucalyptus* producers in the world, and eucalyptus rust impacts wood productivity, which affects seedlings, nurseries, and young trees in the field, resulting in economic losses (Coutinho et al., 1998; Nóia Júnior et al., 2019). However, in 2019, it was described 480 Myrtaceous species globally affected by *A. psidii* (Soewarto et al., 2019). To date, this pathogen is spread worldwide, including Australia, where it is serious a threat to the country’s biodiversity since it hosts around 2,280 myrtaceous species (Berthon et al., 2018). Myrtaceous species from Australia have been decreased or led to the near of extinction, for continuous infections causing death (Makinson, 2018; Pegg et al., 2017). In this country, myrtle rust also affects the commercial production of tea-tree (*Melaleuca alternifolia*) and lemon myrtle (*Backhousia citriodora*) (Carnegie & Pegg, 2018).

The symptoms caused by *A. psidii* in susceptible species are lesions on young and growing leaves, shoots, fruits, and sepals. These lesions are brown to grey with urediniospores yellow or orange-yellow (Glen et al., 2007). In resistant species, no symptoms are observed or a hypersensitive reaction forming lesions without fungal sporulation (Junghans et al., 2003). McTaggart et al. (2018) showed that *A. psidii* is autoecious, that completed its sexual and asexual lifecycle in a single host, and the meiotic recombination produced basidiospores, which were capable to infect species under controlled conditions. McTaggart et al. (2020) endorsed the hypothesis that sexual reproduction occurs in populations of *A. psidii* and might be responsible for the adaptation to environmental change.

Several studies investigating *A. psidii* genetic and physiologic variability have been performed in order to understand the high host diversity of *A. psidii* (Graça et al., 2013; Machado et al., 2015; Quecine et al., 2014; Stewart et al., 2018). For instance, Stewart et al. (2018) grouped the *A. psidii* biotypes in clusters, the pandemic biotype was grouped separately from the Brazilian biotypes, associated with rose apple, eucalypt, and guava. The authors concluded that the origin source of the Pandemic biotype is different from the others and still unknown. Quecine et al. (2014) showed the genetic diversity among different populations of *A. psidii* from Brazil. Despite the myrtle rust impacts on biodiversity and the economy around the world, little is known about this interaction with the host due to the complexity of co-evolution between biotrophic fungi and plant hosts.

A. psidii MF-1 (Max Feffer 1) biotype was isolated from one single pustule from *Eucalyptus grandis* leaves in São Paulo State, Brazil (Leite, 2012). Since isolated, several studies about it and its host interaction have been performed. Leite et al. (2013) developed a protocol to increase the urediniospores in *Eucalyptus* species. Bini (2016) developed a protocol to induce the germination of *A. psidii* MF-1 *in vitro*, using different stimuli and performed the transcriptome study from the early stages of infection. Lopes (2017) identified effector candidates from the MF-1 biotype and validated the expression of these effector candidates from *A. psidii* MF-1 and another biotype from *Syzigium jambos in vitro* conditions, showing a modulation by the host. Santos (2019) performed a transcriptome analysis of the *A. psidii* MF-1 under cuticular wax stimuli from leaves of *E. grandis*, *E. urograndis*, and *E. urophylla*, at 18 hours post-inoculation. The authors supposed that *Eucalyptus* spp. cuticular waxes modulated the expression of *A. psidii* MF-1 genes. Almeida et al. (2021) sequenced and assembled the mitochondrial genome of *A. psidii* MF-1 and performed a phylogenomic analysis using other mitochondrial genome rusts. It was found evidence of three proteins exclusive of *A. psidii* MF-1 mitochondrial genome. Regarding the *A. psidii* MF-1 host, Sekiya et al. (2021) observed differences in the metabolomic profile during the early stages of infection of *A. psidii* MF-1, between resistant and susceptible *E. grandis* species. The MF-1 genome was recently deposited at NCBI (National Center for Biotechnology Information, Accession Number: AVOT00000000). From genome information, studies about the infection process and proteins involved in the process have been possible. Moreover, as a result of the efforts to sequence a high-quality *A. psidii* genome, two genomes from Australian pandemic biotype and South-African biotype became available in the last few years (McTaggart et al., 2018; Tobias et al., 2020).

The study of effector proteins from rusts pathogens has become an approach very useful and popular to investigate the pathogen and its host interaction (Lorrain et al., 2018). In general, effectors are molecules secreted by one organism that manipulate the physiology of another to succeed in the infection (Dalio et al., 2017). They are proteins generally specific to the individual pathogens and non-conserved among the fungal groups above the family level (Boller & Felix, 2009). Effectors are delivered in the apoplast or cytoplasm. Apoplastic effectors are secreted to the apoplast, the extracellular space, and cytoplasmic effectors are delivered inside the host cell, and traffic to different subcellular compartments (Win et al., 2012). The effectors may have distinct functions during the host infection, for instance, they can suppress defense-related genes, interfere in RNAi silencing, and cause cell death hijacking (Jaswal et al., 2020). The effectors must be at the right place and time to achieve an optimal result, especially for biotrophs that the host viability must be preserved (Uhse & Djamei, 2018). Effectors are under constant evolution, they may present positive or negative effects on the plant fitness, and they depend on the resistance or susceptibility of the plant, in order to avoid recognition (Jones & Dangl, 2006; Win et al., 2012), hence, the effector genes evolve quickly compared to other genes (Win et al., 2012).

Plants use resistance genes, called R genes, to recognized effectors and avoid infection (Jones & Dangl, 2006), the recognition may be through binding to the effector or recognizing the alterations in their cellular molecules. The majority of R proteins encode intracellular nucleotide binding-site leucine-rich repeat, NBS-LRR (Han, 2019). In *Eucalyptus* species it was described the presence of R genes, being that *Ppr1* may be a major gene, with incomplete penetrance and/or expressivity (Junghans et al., 2003; Mamani et al., 2010). Santos et al. (2020) showed genes from *E. grandis*, associated with resistance, presenting different expressions between resistant and susceptible species. Among those genes, it was found genes associated with response to salicylic acid and protein kinase leucine-rich receptors (PK-LRR), which are known to be involved in resistance against biotrophic fungi. Although several studies have been made on *Eucalyptus* resistance to *A. psidii*, to date no work on effectors from *A. psidii* was reported. The study of effectors is crucial to understand how the pathogens can establish the infection, and also to the development of disease control strategies and resistant plants (Lorrain et al., 2018; Vleeshouwers & Oliver, 2014).

Therefore, due to *A. psidii* economic and environmental importance, and the role of effectors in plant interactions, this unprecedented work focuses on the investigation of effector candidates from *A. psidii*. The first chapter describes the identification of effector candidates from the MF-1 biotype, the validation by RT-qPCR of 7 selected effector candidates under the stimuli of cuticular wax extracts from *E. grandis* and *E. urophylla*. Also, subcellular localization validation from effector candidates by the heterologous expression using the model plant *Nicotiana benthamiana*. The second chapter approaches the identification and genomic comparison of effector candidates from three biotypes of *A. psidii*, the MF-1 from Brazil, the Australian pandemic, and South African biotypes.

References

Almeida, J. R., Pachón, D. M. R., Franceschini, L. M., dos Santos, I. B., Ferrarezi, J. A., de Andrade, P. A. M., Monteiro-Vitorello, C. B., Labate, C. A., & Quecine, M. C. (2021). Revealing the high variability on nonconserved core and mobile elements of *Austropuccinia psidii* and other rust mitochondrial genomes. *PLoS ONE*, *16* (3 March), 1–20. https://doi.org/10.1371/journal.pone.0248054

Beenken, L. (2017). Austropuccinia: A new genus name for the myrtle rust *Puccinia psidii* placed within the redefined family Sphaerophragmiaceae (Pucciniales). *Phytotaxa*, *297*(1), 53–61. https://doi.org/10.11646/phytotaxa.297.1.5

Berthon, K., Esperon-Rodriguez, M., Beaumont, L. J., Carnegie, A. J., & Leishman, M. R. (2018). Assessment and prioritisation of plant species at risk from myrtle rust (*Austropuccinia psidii*) under current and future climates in Australia. *Biological Conservation*, *218*(May 2017), 154–162. https://doi.org/10.1016/j.biocon.2017.11.035

Bini, A. P. (2016). Estudo molecular do desenvolvimento de *Puccinia psidii* Winter *in vitro* e no processo de infecção em Eucalyptus grandis. In *Thesis*. University of São Paulo.

Boller, T., & Felix, G. (2009). A renaissance of elicitors: Perception of microbe-associated molecular patterns and danger signals by pattern-recognition receptors. *Annual Review of Plant Biology*, *60*, 379–407. https://doi.org/10.1146/annurev.arplant.57.032905.105346

Carnegie, A. J., & Pegg, G. S. (2018). Lessons from the incursion of myrtle rust in Australia. *Annual Review of Phytopathology*, *56*, 457–478. https://doi.org/10.1146/annurev-phyto-080516-035256

Coutinho, T. A., Wingfield, M. J., Alfenas, A. C., & Crous, P. W. (1998). Eucalyptus rust: A disease with the potential for serious international implications. *Plant Disease*, *82*(7), 819–825. https://doi.org/10.1094/PDIS.1998.82.7.819

Dalio, R. J. D., Magalhaes, D. M., Rodrigues, C. M., Arena, G. D., Oliveira, T. S., Souza-Neto, R. R., Picchi, S. C., Martins, P. M. M., Santos, P. J. C., Maximo, H. J., Pacheco, I. S., De Souza, A. A., & Machado, M. A. (2017). PAMPs, PRRs, effectors and R-genes associated with citrus-pathogen interactions. *Annals of Botany*, *119*(5), 749–774. https://doi.org/10.1093/aob/mcw238

Ferreira, F. (1983). Ferrugem do Eucalipto. *Revista Árvore*, *7*, 92–109.

Glen, M., Alfenas, A. C., Zauza, E. A. V., Wingfield, M. J., & Mohammed, C. (2007). *Puccinia psidii*: A threat to the Australian environment and economy - A review. *Australasian Plant Pathology*, *36*(1), 1–16. https://doi.org/10.1071/AP06088

Graça, R. N., Ross-Davis, A. L., Klopfenstein, N. B., Kim, M. S., Peever, T. L., Cannon, P. G., Aun, C. P., Mizubuti, E. S. G., & Alfenas, A. C. (2013). Rust disease of eucalypts, caused by *Puccinia psidii*, did not originate via host jump from guava in Brazil. *Molecular Ecology*, *22*(24), 6033–6047. https://doi.org/10.1111/mec.12545

Han, G. Z. (2019). Origin and evolution of the plant immune system. *New Phytologist*, *222*(1), 70–83. https://doi.org/10.1111/nph.15596

Jaswal, R., Kiran, K., Rajarammohan, S., Dubey, H., Singh, P. K., Sharma, Y., Deshmukh, R., Sonah, H., Gupta, N., & Sharma, T. R. (2020). Effector Biology of Biotrophic Plant Fungal Pathogens: Current Advances and Future Prospects. *Microbiological Research*, *241*(December 2019), 126567. https://doi.org/10.1016/j.micres.2020.126567

Joffily, J. (1944). Ferrugem do eucalipto. *Bragantia*, *4*(8), 475–487. https://doi.org/10.1590/s0006-87051944000300001

Jones, J. D. G., & Dangl, J. L. (2006). The plant immune system. *Nature*, *444*(7117), 323–329.

Junghans, D. T., Alfenas, A. C., Brommonschenkel, S. H., Oda, S., Mello, E. J., & Grattapaglia, D. (2003). Resistance to rust (*Puccinia psidii* Winter) in Eucalyptus: Mode of inheritance and mapping of a major gene with RAPD markers. *Theoretical and Applied Genetics*, *108*(1), 175–180. https://doi.org/10.1007/s00122-003-1415-9

Leite, T. F. (2012). Estabelecimento de um patossistema modelo e análise da interação molecular planta-patógeno entre *Eucalyptus grandis* e *Puccinia psidii* Winter por meio da técnica de RNA-Seq. In *Thesis*. University of São Paulo.

Leite, T. F., Moon, D. H., Lima, A. C. M., Labate, C. A., & Tanaka, F. A. O. (2013). A simple protocol for whole leaf preparation to investigate the interaction between *Puccinia psidii* and *Eucalyptus grandis*. *Australasian Plant Pathology*, *42*(1), 79–84. https://doi.org/10.1007/s13313-012-0179-6

Lopes, M. da S. (2017). Identificação in silico e perfil transcricional de genes candidatos a efetores de *Austropuccinia psidii*. In *Thesis*. Universidade de São Paulo.

Lorrain, C., Petre, B., & Duplessis, S. (2018). Show me the way: rust effector targets in heterologous plant systems. *Current Opinion in Microbiology*, *46*, 19–25. https://doi.org/10.1016/j.mib.2018.01.016

Machado, P. S., Alfenas, A. C., Alfenas, R. F., Mohammed, C. L., & Glen, M. (2015). Microsatellite analysis indicates that *Puccinia psidii* in Australia is mutating but not recombining. *Australasian Plant Pathology*, *44*(4), 455–462. https://doi.org/10.1007/s13313-015-0364-5

Makinson, B. (2018). *Myrtle rust in Australia*. Acta Horticulturae. https://doi.org/10.17660/actahortic.2014.1055.19

Mamani, E. M. C., Bueno, N. W., Faria, D. A., Guimarães, L. M. S., Lau, D., Alfenas, A. C., & Grattapaglia, D. (2010). Positioning of the major locus for *Puccinia psidii* rust resistance (Ppr1) on the *Eucalyptus* reference map and its validation across unrelated pedigrees. *Tree Genetics and Genomes*, *6*(6), 953–962. https://doi.org/10.1007/s11295-010-0304-z

McTaggart, A. R., Duong, T., Le, V. Q., Shuey, L. S., Smidt, W., Naidoo, S., Wingfield, M. J., & Wingfield, B. D. (2018). Chromium sequencing: The doors open for genomics of obligate plant pathogens. *BioTechniques*, *65*(5), 253–257. https://doi.org/10.2144/BTN-2018-0019

McTaggart, A. R., Shuey, L. S., Granados, G. M., du Plessis, E., Fraser, S., Barnes, I., Naidoo, S., Wingfield, M. J., & Roux, J. (2018). Evidence that *Austropuccinia psidii* may complete its sexual life cycle on Myrtaceae. *Plant Pathology*, *67*(3), 729–734. https://doi.org/10.1111/ppa.12763

McTaggart, Alistair R., du Plessis, E., Roux, J., Barnes, I., Fraser, S., Granados, G. M., Ho, W. W. H., Shuey, L. S., & Drenth, A. (2020). Sexual reproduction in populations of *Austropuccinia psidii*. *European Journal of Plant Pathology*, *156*(2), 537–545. https://doi.org/10.1007/s10658-019-01903-y

Nóia Júnior, R. S., Schwerz, F., Safanelli, J. L., Rodrigues, J. C., & Sentelhas, P. C. (2019). *Eucalyptus* rust climatic risk as affected by topography and ENSO phenomenon. *Australasian Plant Pathology*, *48*(2), 131–141. https://doi.org/10.1007/s13313-018-0608-2

Pegg, G., Taylor, T., Entwistle, P., Guymer, G., Giblin, F., & Carnegie, A. (2017). Impact of *Austropuccinia psidii* (myrtle rust) on Myrtaceae-rich wet sclerophyll forests in south east Queensland. *PLoS ONE*, *12*(11). https://doi.org/10.1371/journal.pone.0188058

Quecine, M. C., Bini, A. P., Romagnoli, E. R., Andreote, F. D., Moon, D. H., & Labate, C. A. (2014). Genetic variability in *Puccinia psidii* populations as revealed by PCR-DGGE and T-RFLP markers. *Plant Disease*, *98*(1), 16–23. https://doi.org/10.1094/PDIS-03-13-0332-RE

Santos, I. B. (2019). Deciphering the role of early molecular interactions between *Eucalyptus* spp. x *Austropuccinia psidii* and its pathogenesis. In Thesis. University of São Paulo.

Santos, S. A., Vidigal, P. M. P., Guimarães, L. M. S., Mafia, R. G., Templeton, M. D., & Alfenas, A. C. (2020). Transcriptome analysis of *Eucalyptus grandis* genotypes reveals constitutive overexpression of genes related to rust (*Austropuccinia psidii*) resistance. *Plant Molecular Biology*, *104*(4–5), 339–357. https://doi.org/10.1007/s11103-020-01030-x

Sekiya, A., Marques, F. G., Leite, T. F., Cataldi, T. R., de Moraes, F. E., Pinheiro, A. L. M., Labate, M. T. V., & Labate, C. A. (2021). Network Analysis Combining Proteomics and Metabolomics Reveals New Insights Into Early Responses of *Eucalyptus grandis* During Rust Infection. *Frontiers in Plant Science*, *11*(January), 1–21. https://doi.org/10.3389/fpls.2020.604849

Soewarto, J., Giblin, F., & Carnegie, A. J. (2019). *Austropuccinia psidii* (myrtle rust) global host list. Version 2. *Australian Network for Plant Conservation*. http://www.anpc.asn.au/myrtle-rust

Stewart, J. E., Ross-Davis, A. L., Graça, R. N., Alfenas, A. C., Peever, T. L., Hanna, J. W., Uchida, J. Y., Hauff, R. D., Kadooka, C. Y., Kim, M. S., Cannon, P. G., Namba, S., Simeto, S., Pérez, C. A., Rayamajhi, M. B., Lodge, D. J., Arguedas, M., Medel-Ortiz, R., López-Ramirez, M. A., … Klopfenstein, N. B. (2018). Genetic diversity of the myrtle rust pathogen (*Austropuccinia psidii*) in the Americas and Hawaii: Global implications for invasive threat assessments. *Forest Pathology*, *48*(1), 1–13. https://doi.org/10.1111/efp.12378

Tobias, P. A., Schwessinger, B., Deng, C. H., Wu, C., Dong, C., Sperschneider, J., Jones, A., Smith, G. R., Tibbits, J., Chagné, D., & Park, R. F. (2020). Long read assembly of the pandemic strain of *Austropuccinia psidii* (myrtle rust) reveals an unusually large (gigabase sized) and repetitive fungal genome. *BioRxiv*, 1–44. http://biorxiv.org/content/early/2020/03/20/2020.03.18.996108.abstract

Uhse, S., & Djamei, A. (2018). Effectors of plant-colonizing fungi and beyond. *PLoS Pathogens*, *14*(6), 1–8. https://doi.org/10.1371/journal.ppat.1006992

Vleeshouwers, V. G. A. A., & Oliver, R. P. (2014). Effectors as tools in disease resistance breeding against biotrophic, hemibiotrophic, and necrotrophic plant pathogens. *Molecular Plant-Microbe Interactions*, *27*(3), 196–206. https://doi.org/10.1094/MPMI-10-13-0313-IA

Win, J., Chaparro-Garcia, A., Belhaj, K., Saunders, D. G. O., Yoshida, K., Dong, S., Schornack, S., Zipfel, C., Robatzek, S., Hogenhout, S. A., & Kamoun, S. (2012). Effector biology of plant-associated organisms: Concepts and perspectives. *Cold Spring Harbor Symposia on Quantitative Biology*, *77*, 235–247. https://doi.org/10.1101/sqb.2012.77.015933

Winter, G. (1884). Repertorium. Rabenhorstii fungi europaei et extraeuraopaei Cent. XXXI et XXXII. *Hedwigia*, *23*, 164–172.

2 CHAPTER 1 - FUNCTIONAL STUDY OF EFFECTOR CANDIDATE PROTEINS FROM *Austropuccinia psidii*

ABSTRACT

Austropuccinia psidii is a biotrophic fungus and the causal agent of myrtle rust, first described in Brazil and spread quickly around the world. Besides its economic importance to Brazil and around the world, studies that approach its interaction with its hosts are a challenge due to its biotrophic lifestyle. Regarding *A. psidii – Eucalyptus* spp. interaction, the study of effector highlights, in general, effectors are molecules secreted by the pathogen that modulates the host's physiology to allow the pathogen infection. The identification of effector candidates may support the understanding of the mechanisms involved during the host infection. In our research, we identified and characterized *in silico* effector candidates of *A. psidii* MF-1 biotype, isolated from *E. grandis* in Brazil. We obtained a profile of 255 effector candidates predicted by two methods: a manual pipeline based on effector features, and by the software EffectorP 2.0. The effector expression validation was performed under cuticular wax extracts of eucalypt leaves due to the challenge to deal with *A. psidii* biotrophic lifestyle. Seven effector candidates selected and validated showed different patterns of expression under the stimulus of cuticular species resistant and susceptible, which may indicate that the host influences the gene expression of effector candidates during the infection. To investigate the subcellular localization of effector candidates, we transiently expressed two effector candidates tagged with GFP proteins in leaves of *Nicotiana benthamiana*. We observed the accumulation of the effector candidate Ap28303, described as inhibitor I9 domain-containing protein, in the nucleus by microscopy. To the best of our knowledge, Ap28303 is the first effector candidate from *A. psidii* that was identified, validated its expression, and had its subcellular localization characterized. Our findings open new perspectives to the study of effector and interaction of *A. psidii* – host, as the validation of other effector candidates. A deep investigation about the effector candidate Ap28303 and the comparison to other biotypes of *A. psidii* may be performed in the future.

Keywords: Myrtle rust; Agroinfiltration; Plant-pathogen interaction; Effectoromic; EffectorP

2.1 Introduction

Austropuccinia psidii is a biotrophic fungus, the causal agent of the myrtle rust (Beenken, 2017), that was described infecting approximately 480 species of Myrtaceae (Soewarto et al., 2019). Currently, the myrtle rust is spread out around the world, including Australia, a country that hosts around 2250 Myrtaceae species, being a threat to the ecosystem (Berthon et al., 2018; Pegg et al., 2017). *A. psidii* is native from South America (Coutinho et al., 1998; Glen et al., 2007) since first reported infecting guava (*Psidium guajava* L.) in Brazil (Winter, 1884). Then, it was reported infecting *Eucalyptus* species also in Brazil in 1912 (Joffily, 1944). The disease causes economic losses in the forestry industry, causing damages in nurseries and young plants, hence reducing productivity and sometimes causing death of susceptible plants (Dianese et al., 1984; Masson et al., 2013). Despite the wide range of myrtle species infected by *A. psidii* and its economic and ecological importance, little is known about the molecular mechanisms involved in the host infection, including the role of effector proteins on the *A. psidii* pathogenesis.

Dalio et al. (2017) defined effectors as secreted molecules associated with an organism that may modify the physiology, structure, and function of another organism. During the plant infection, pathogenic fungi use these molecules to modulate the plant physiology and colonize the host (Dodds & Rathjen, 2010). The plants also use their mechanisms to counteract the fungi infection, as described in the *zig-zag* model proposed by Jones & Dangl (2006). Briefly, after the pathogen contact with the plant, Pathogen-Associated Molecular Pattern (PAMP) or Microbe-Associated Molecular Pattern (MAMP) can be recognized by Pattern Recognition Receptors (PRRs), which trigger PAMP Triggered Immunity (PTI). The non-recognized pathogens use effector proteins to infect the plant, resulting in Effector Triggered Susceptibility (ETS). The effectors can be recognized by *R* genes, it may lead to Effector Triggered Immunity (ETI). In last phase, the pathogen evolves to avoid ETI, and successfully infects the host, as well the pathogen and host are under co-evolution (Jones & Dangl, 2006).

The study of effectors is crucial to comprehend the mechanisms involved in plant-pathogen interactions (Hogenhout et al., 2009). To identify and characterize effectors, several methods have been used, as computational tools to predict candidate effectors from genome or transcriptome (Kunjeti et al., 2016; Petre et al., 2015) and RT-qPCR to effector expression validation (Duplessis et al., 2011; Zhang et al., 2017). It is also common to employ transient expression mediated by *Agrobacterium tumefaciens* to functionally characterize effectors from obligate pathogens, since they are not liable to genetic transformation (Caillaud et al., 2012; Lorrain, Petre, et al., 2018), as the case of *A. psidii*.

A. psidii MF-1 biotype was isolated from a single pustule of *Eucalyptus grandis* (Leite, 2012) and successfully infects *Eucalyptus* species (personal communication). Bini (2016) described the viability to cultivate *A. psidii* MF-1 *in vitro* until 48 hours after inoculation, using culture medium agar-water amended with olive oil and dialysis membrane, which offered the necessary stimulus to the development of penetration hyphae and appressorium. From this method it was performed an RNA-seq to obtain the *A. psidii* transcripts during its germination *in vitro* conditions. The author found transcripts differentially expressed which probably codified to effector proteins. Lopes (2017) identified and validated by RT-qPCR the expression of effector candidates during the early pathogen infections *in vitro*, based on the method proposed by Bini (2016). The experiment was performed using urediniospores from two biotypes, one isolated from *Eucalyptus* (MF-1) and another from *Syzigium jambos* (GM-J1). The results suggested a modulation from the host in the effector candidate's expression. Moreover, Santos et al. (2019) described the use of cuticular wax extract from *Eucalyptus* leaves *in vitro* conditions as an important pre-formed mechanism against the pathogen. It was showed a relationship between the cuticular wax composition of resistant and susceptible species and the *in vitro* germination pattern of *A. psidii*, thus the cuticular wax may influence the effectors expression.

Based on these previous studies, we used the genome of *A. psidii* MF-1 biotype, deposited at NCBI (National Center for Biotechnology Information, Accession Number: AVOT00000000), to identify effector candidates. Among the *in silico* predicted effector candidates, 7 were selected to further investigation. We used cuticular wax from *E. grandis* (susceptible species) and *E. urophylla* (resistant

species) leaves to validated *in vitro* the expression of effector candidates along the early stages of *A. psidii* MF-1 infection. Our results suggested that the effector candidate's expression was modulated by the cuticular wax extract source. We observed the candidate G3GFP-tagged Ap28303 accumulated in the nucleus by *A. tumefaciens* transient expression using binary plasmid, the protein was detected by Western blot, probing with an anti-HA antibody. In summary, we obtained a profile of effector candidates from *A. psidii* and the expression profile of effector candidates *in vitro* conditions according to cuticular wax host source. We also confirmed the nuclear localization of Ap28303, firstly described as inhibitor I9 domain-containing protein. For the first time, it was carried out an investigation and characterization of effector candidates of *A. psidii*.

2.2 Materials and Methods

2.2.1 Biological material

Urediniospores from monospostular MF-1 biotype, isolated from *Eucalyptus grandis* (Leite 2012), was used to perform the assays of candidate effectors expression in cuticular wax extract from *E. grandis* and *E. urophylla* leaves. The urediniospores multiplication was realized in the susceptible *E. grandis* M09D1, as detailed in Leite et al. (2013). Urediniospores were desiccated with silica gel and stored in microcentrifuge tubes at -80ºC.

The susceptibility of *Eucalyptus* genotypes was evaluated by Santos et al. (2019) in a field assessment by natural infection. The species *E. grandis* were considered susceptible and the *E. urophylla*, resistant. The eucalypt plants from these two species were kept at "Luiz de Queiroz" College of Agriculture, University of São Paulo (ESALQ/USP), Department of Forestry Sciences, Piracicaba, São Paulo, Brazil, until the experiment installation.

For the cloning experiments *Escherichia coli* DB3.1 and *E. coli* DH5α were used to maintenance and propagation of the plasmids. *A. tumefaciens* GV3101 was used to transiently expression in *N. benthamiana* leaves. The *E. coli* and *A. tumefaciens* strains were routinely grown on Luria-Bertani (LB) medium (Sambrook et al. 1998) at 37 ºC and 28 ºC, respectively. All strains included the transformants were stored in 60% glycerol at -80 ºC. The antibiotics were used in the following concentrations: kanamycin (50 µg/mL and 100 µg/mL), spectinomycin (50 µg/mL), gentamycin (25 µg/mL and 50 µg/mL), rifampicin (100 µg/mL) and ampicillin (50 µg/mL).

The plants of *N. benthamiana* were kept in room temperature (RT) with photoperiod of 16/8 hours (light/dark), in the Laboratory of Genetics of Microorganisms "Professor João Lúcio de Azevedo" at ESALQ/USP.

2.2.2 Prediction of effector candidates

The effector candidates were predicted from *A. psidii* MF-1 draft genome (Accession Number: AVOT00000000). Two methods were used: a manual pipeline and the EffectorP 2.0 software (Sperschneider et al., 2018) (Figure 1). First, the 47,121 predicted protein sequences were submitted to SignalP 4.1 (Nielsen, 2017) to check the presence of signal peptide. All predicted proteins with peptide signal were submitted to these two methods. To the manual pipeline, after selected the proteins with signal peptide, protein sequences were submitted to TMHMM V2.0 (Krogh et al., 2001) and GPISom (Fankhauser & Mäser, 2005), to checked for transmembrane domain and glycophosphatidylinositol (GPI)-anchors, respectively, using default parameters. Then, the proteins with no transmembrane domain, no GPI-anchors, and with less than 300 residues were selected, as described by Duplessis et al. (2011) and Germain et al. (2018). To EffectorP 2.0 all predicted proteins with peptide signal were submitted to the software using the default parameters.

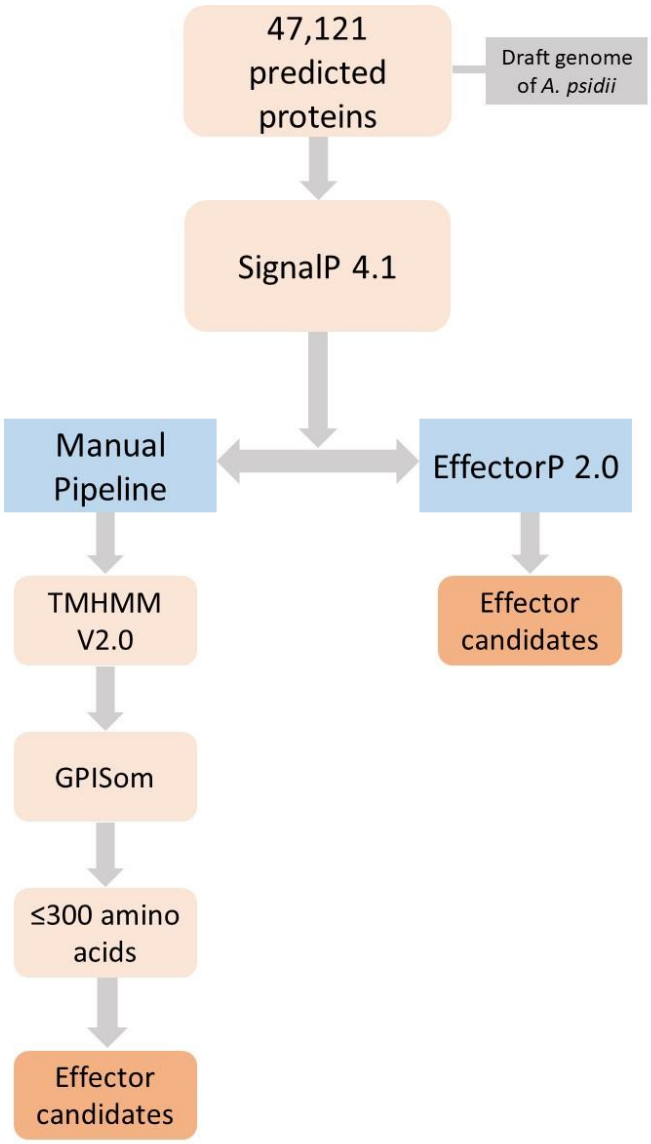

Figure 1. *In silico* prediction workflow for the prediction of effector candidates of *A. psidii*

The subcellular localization of the predicted effector candidates was obtained by LocTree3 (Goldberg et al., 2014). The functional categorization was obtained by the Gene Ontology Consortium (GO) (Ashburner et al., 2000), the terms were derived from the Blast2GO software (Conesa et al., 2005), using the default parameters. The obtained annotations were previously simplified by GO Slim. The annotation was manually verified using the UniProtKB reference proteomes Swiss-Prot database (The UniProt Consortium, 2021).

2.2.3 Effector candidates expression validation

We randomly selected 7 effector candidates that were predicted by both strategies to analyse their expression *in vitro* (Table 1). The gene expressions of these effector candidates were evaluated

under different source of cuticular wax extracts from *Eucalyptus* spp. as stimuli to *A. psidii* germination. The oil mineral and cuticular wax extracts from leaves provided the chemical stimulus, whereas the dialysis membrane provided the physical stimulus.

Table 1. Effector candidate genes selected to be validated by RT-qPCR

Abbreviation	Gene ID in the *A. psidii* genome
Ap15054	evm.model.NODE_15054_length_8284_cov_1.25043.1
Ap30385	evm.model.NODE_30385_length_5682_cov_0.453105.1
Ap28303	evm.model.NODE_28303_length_5903_cov_0.666551.1
Ap11108	evm.model.NODE_11108_length_9646_cov_0.920475.1
Ap12491	evm.model.NODE_12491_length_9093_cov_0.505688.1
Ap23389	evm.model.NODE_23389_length_6527_cov_0.825156.1
Ap2160	evm.model.NODE_2160_length_20942_cov_0.93375.2

Four plants of each species, *E. grandis* (rust susceptible) and *E. urophylla* (rust resistant) were used to extract cuticular wax from the leaves. The youngest leaves were collected and extracted the cuticular wax as described by Viana et al. (2010) and adapted by Santos et al. (2019). The treatments were composed by Petri dishes with agar water (0.8%), amended with 50 µl of mineral oil (Sigma Aldrich), dialysis membrane, 50 µl of cuticular wax extract and 7 mg of *A. psidii* urediniospores. The plates were kept in the dark at room temperature. For each collection interval 0, 6, 12 and 24 hours post-inoculation (h.p.i.) we used 5 biological replicates, composed by 1 (one) Petri dish for each species cuticular wax. The time course was chosen based on the fungi structure formation *in vitro*, 6 h.p.i. it is observed the germination tube formation,12 h.p.i., appressorium formation and 24 h.p.i. appressorium presence and a considerable germination tube (Lopes, 2017).

In each interval the dialysis membrane with the urediniospores were collected and ground in liquid nitrogen immediately. RNA was extracted using RNeasy Mini Kit® (Qiagen), following the manufacturer's protocol. The cDNA synthesis was performed with RevertAid First Strand cDNA Synthesis Kit® (ThermoFisher Scientific) following the manufacturer's protocol.

2.2.3.1 RT-qPCR

The coding sequence from the 7 selected effector candidates were used to design the primers using the OligoPerfect tool (https://apps.thermofisher.com/apps/oligoperfect/#!/design) (Table 2). The primer set was optimized for annealing temperature by conventional PCR (cPCR). The reactions were prepared with a volume of 25 µl containing: 10 X PCR Buffer (1mM $MgCl_2$), dNTP (0.2 mM), primer set (5 pmol), BSA (10 mg mL^{-1}), Taq DNA Polymerase (5 U μL^{-1}), 20 ng DNA template (*A. psidii* MF-1) and ultrapure water to complete the volume. PCR was performed in thermocycler with initial denaturation of 95 ºC for 4 min; followed by 35 cycles of 95 °C for 30 sec, 52-62 °C for 30 sec, 72 °C

for 30 sec, and final extension of 72 °C for 10 min. PCR products were revealed by electrophoresis in agarose gel (1.2%).

After the primer set validation, the RT-qPCR was performed following the parameters: initial denaturation 95 °C for 5 min, 95 °C for 30 sec and 58 °C for 45 sec for 35 cycles, and the dissociation curve (95 °C - 15sec; 60 °C - 30sec; 95 °C - 15sec) in the Applied Biosystem 7300. The reaction of 12.5 µl was performed with the GoTaq® qPCR Master Mix (Promega) composed by GoTaq mix (1X), CXR Reference Dye (300 nM), Forward and Reverse (200 nM), cDNA sample (160 ng) and RNA-free Water to complete the volume. The primers from the genes beta-tubulin (BTub) and elongation factor (EF) were used as reference genes (Bini et al., 2018). All treatments were composed by five biological replicates and two technical replicates.

The RT-qPCR amplification specificity was checked by dissociation curve analysis (melting curve). The fluorescence-per-cycle data were submitted in LinRegPCR v.11.0 (Ramakers et al., 2003) to calculate the average amplification efficiency of each primer set. The ratio expressions were calculated by the PFAFFL method, using the REST software (Relative Expression Software Tool) using default parameters (Pfaffl et al., 2002). The expression graphics were design in the R software (RStudio Team, 2019).

Table 2. Primer set of effector candidates validated by RT-qPCR and the reference genes

Gene	Forward (5'-3')	Reverse (5'-3')	Reference
Effector candidates			
Ap15054	GACAGCGAGGAAAATTGCAC	TACGCCCGAAGTTTTACCTG	This study
Ap30385	TCATCCACCATCCTTCAACG	ACTCTCTCACATGCTTCCCAAG	This study
Ap28303	CCTCAGTTGAACTCGGTGATTC	ATTTGGGGGTTCTGTTGGAG	This study
Ap11108	AAGCATCCAAGCAAGAGGTC	TTCTTGGCAACGTCTTCGTC	This study
Ap12491	TAGCGCCTACTCTGGTGGTT	GCGGATTTTGACGTTT	This study
Ap23389	CGTCGATAGAGCTGCAAACA	GTCCTGGACTAGGTGGTGGA	This study
Ap2160	CTCGAGTGTCCAGGTCCAAT	TTAGCGCCTACTCTGGTGCT	This study
Reference genes			
Btub*	GGACTCTGTTTTAGATGTCGTC	TTGATGGACTGATAGGGTAGCG	(Bini et al., 2018)
EF**	CAGTTATGGAAGTTTGAAACTCC	GACAATAAGCTGTCGAACACCAAGG	(Bini et al., 2018)

*Btub: beta-tubulin gene of *A. psidii* MF-1
**EF: elongation factor gene of *A. psidii* MF-1

2.2.4 Transient expression and subcellular localization

2.2.4.1 Plasmids and cloning procedures

The coding sequences of 5 effector candidates Ap28303, Ap12491, Ap30385, Ap23389, and Ap15054 were used to design the primers manually. These effector candidates were selected due to their interestingly differential expression under cuticular wax stimuli. The Gateway System was used to plasmids constructions. First, we removed the signal peptide from the sequences. Then, to design the primers for the recombination using plasmid C-terminal tag, we added the *attb1* sequence, the *Kozak* sequence, an artificial methionine, and around 20 bases pair of the gene from 5', for the forward primer. The reverse primer was designed with *attb2* sequence and around 22 bases pair of the gene from 3' and the stop codon was removed (Appendix A and B). For the plasmids N-terminal tag, in the forward primer we added the *attb1* sequence, and for the reverse primer we added the *attb2* sequence (Appendix A and B).

All PCRs for the cloning procedures were performed with Phusion™ High-Fidelity DNA Polymerase (ThermoFisher Scientific). The reactions were prepared with a final volume of 50 µl containing: 5X Phusion HF Buffer (1.5 mM $MgCl_2$), dNTP (200 µM), primer Forward and Reverse (0.5 µM each), DMSO (3%), Phusion DNA Polymerase (0.02 U/µL), 2 µl cDNA template and water to complete the volume. PCR was performed with initial denaturation of 98 ºC for 30 sec; followed by 35 cycles of 98 °C for 5 sec, 62 °C for 30 sec, 72 °C for 15 sec, and final extension of 72 °C for 5 min. The PCRs products were purified using Illustra GFX PCR DNA and Gel Band Purification Kit (GE Healthcare) following the manufacture instructions.

The first round of PCR was performed using the primers listed in the Appendix B. Just two effector candidate's primers were amplified by PCR, so we proceeded with two effector candidates (Ap30385 and Ap28303). After, PCR products were purified and used as template for the second round of PCR using the *attb* primers (Appendix B), then checked by electrophoresis in agarose gel (1.2%), and purified prior to recombination in the plasmid pDNOR221.

The next step was generating an Entry plasmid, using the pDNOR221 plasmid and the PCR products. To that, the purified PCR products from Ap28303 and Ap30385 candidates containing the *attb* sites were recombined in the pDONR221 plasmid (Table 3) using the Gateway BP® Clonase® II Enzyme Mix (Invitrogen). The 10 µl of plasmid reactions were performed with PCR purified products (50 fmol), pDNOR221 (150 ng/µl), TE to complete the volume and 2 µl of Gateway BP® Clonase® II Enzyme Mix, the reactions were incubated overnight at 25 °C. After the incubation, it was added 1 µl of Proteinase K solution (2 µg/µl) in the reactions and incubated for 10 minutes, at 37 °C. It was electroporated 2 µl of the reaction's products in *E. coli* DH5α, then diluted into 1 (one) mL of LB and incubated for 2 h at 37°C under agitation (150 rpm). Subsequently, the bacterial suspension was spread onto LB plates amended with kanamycin (100 µg/mL) at 37 ºC. Single colonies that grown onto LB

plates were selected as transformants and grown again onto Petri dishes containing LB solid media supplemented with kanamycin (100 µg/mL) at 37 ºC to double check the transformants. Later, single colonies were grown overnight into LB liquid medium supplemented with kanamycin (100 µg/mL) at 37 ºC, 180 rpm and stored in 60% glycerol at -80 ºC. The plasmids pENTRY::Ap28303 and pENTRY::Ap30385 from the bacteria transformants were extracted using the QIAprep Spin Miniprep Kit (Qiagen) according to the manufacturer's instructions. Constructs were confirmed by PCR using the M13 primers (Appendix B).

The last step for plasmids construction was the recombination of pENTRY::Ap28303 and pENTRY::Ap30385 plasmids to the destination plasmids containing the green fluorescence protein (G3GFP), pGWB651 and pGWB652 (Table 3) (Nakagawa at al. 2007). Recombinations were performed using LR Gateway BP Clonase II Enzyme Mix (Invitrogen). The 10 µl reactions were performed with pENTRY plasmids (126 ng/µl), pGWB651 or pGWB652 (150 ng/µl), TE to complete the volume and 2 µl of Gateway LR® Clonase® II Enzyme Mix, the reactions were incubated overnight at 25 °C. After, it was added 1 (one) µl of Proteinase K solution (2 µg/µl) in the reactions and incubated for 10 minutes, at 37 °C. It was electroporated 3 µl in *E. coli* DH5α, after diluted into 1 (one) mL LB liquid media and incubated for 2 h at 37°C under agitation (150 rpm). The bacterial suspension was spread onto Petri dishes containing LB solid media containing spectinomycin (50 µg/mL) at 37 ºC to select the transformants. A single colony was growth into LB liquid with spectinomycin (50 µg/mL) at 37 ºC, 180 rpm overnight. The bacterial culture was stoked in glycerol 60% and stored in -80 ºC. The plasmids generated 35S::Ap28303-G3GFP, 35S::Ap30385-G3GFP, 35S::G3GFP-28303 and 35S::G3GFP-Ap30385 were extracted from the transformants bacteria using the QIAprep Spin Miniprep Kit (Qiagen) according to the manufacturer's instructions. Constructs were confirmed by PCR using M13 primers and sequenced by Sanger method in Genetic Analyzer 3500 (Applied Biosystems) at Laboratory of Plant Breeding in CENA/ USP.

2.2.4.2 Transient expression and confocal microscopy

The obtained plasmids (35S::Ap28303-G3GFP, 35S::Ap30385-G3GFP, 35S::G3GFP-28303 and 35S::G3GFP-Ap30385) were electroporated in the *A. tumefaciens* strain GV3101, according to Win et al. (2011) this strain has the ability to transfer its plasmid to *N. benhamiana* and high efficiency for transformation. Transformants were selected onto Petri dishes containing LB solid medium supplemented with gentamycin (100 µg/mL) and spectinomycin (50 µg/mL). Single colony transformants were grown into LB liquid medium supplemented with the respective antibiotics, overnight, at 28 ºC, 180 rpm. 1 (one) mL of bacteria suspension were stored in glycerol 60% at -80 ºC.

A. tumefaciens containing the plasmid nuclear marker fused to mCherry (Table 3) was growth into 12 mL of LB liquid supplement with rifampicin (100 µg/mL), kanamycin (50 µg/mL) and

gentamycin (25 µg/mL). *A. tumefaciens* containing the plasmid plasma membrane marker fused to mCherry and *A. tumefaciens* containing the plasmid p19 (silencing suppressor) (Table 3) were growth into 12 mL of LB liquid supplement with ampicillin (50 µg/mL) and gentamycin (25 µg/mL). The *A. tumefaciens* containing the constructed plasmids were grown into 12 mL of LB liquid supplement with spectinomycin (50 µg/mL) and gentamycin (100 µg/mL). All tubes (50 mL) containing the bacteria were incubated overnight at 28 ºC under agitation of 180 rpm. After this period, we measured the $OD_{600,}$ and centrifugated the bacteria suspensions at 4000g for 10 minutes. The pellets were resuspended with Infiltration Buffer (10 mM $MgCl_2$, 10 mM MES, 150 µM acetosyringone) to remove the antibiotic excess. After, the bacterial suspensions were centrifugated again, and the pellets were resuspended in Infiltration Buffer to adjust optical density to OD_{600}=0.8, except p19, and sat at room temperature for 3 hours.

The constructed plasmids (OD_{600}=0.8) were co-infiltrated with *A. tumefaciens* containing the plasmid p19 (silencing suppressor), to OD_{600}=0.1, and the organelles markers plasmids (OD_{600}=0.8) (nucleus and plasmatic membrane). *A. tumefaciens* containing the plasmids pGWB651 and pGWB652 (OD_{600}=0.8) were infiltrated for free G3GFP delivery, as mock. The infiltrations were performed *in N. benthamiana* leaves using a syringe without needle. All plasmids used in the present study are listed in Table 3.

The transient expression was evaluated 2 days after infiltration, the agroinfiltrated leaves were collected, cut approximately 10 mm by 10 mm, and placed in PBS (Phosphate Buffered Saline: 8g NaCl, 0.2g KCl, 1.44g Na_2HPO_4, 0.24g KH_2PO_4, distilled water to complete the volume of 1000 mL, pH 7.4) between slide and cover glass. The compartments with proteins accumulation were verified by laser-scanning microscopy (Nikon Eclipse Ti/C2si) in the Laboratory of Plant Breeding at CENA/USP.

Table 3. Plasmid's description used in this work

Plasmid name	Description	Reference
pDONR221	Gateway donor plasmid	Thermo Fisher Scientific
pGWB651	Binary plasmid for C-terminal G3GFP (green fluorescence protein) fusions	(Nakagawa et al., 2007)
pGWB652	Binary plasmid for N-terminal G3GFP (green fluorescence protein) fusions	(Nakagawa et al., 2007)
p19	Binary plasmid containing the p19 protein from tomato bushy stunt virus, silencing suppressor of gene expression in tobacco	Provided by the Laboratory of Genetics and Immunology of Plants - ESALQ/USP
pUFV2224	Nuclear marker *Arabidopsis thaliana* AtWWP1 fused to mCherry	(Silva et al., 2015)
pCMU-PMr; pCMB-PMr	Plasma membrane marker, PIP2a-mcherry; AtPIP2a, plasma membrane aquaporin	(Cutler et al., 2000)
pENTRY::Ap28303	PCR purified product from the effector candidate Ap28303 recombined in pDNOR221 plasmid	This study
pENTRY::Ap30385	PCR purified product from the effector candidate Ap30385 recombined in pDNOR221 plasmid	This study
35S::Ap30385-G3GFP	pGWB651, binary plasmid for C-terminal G3GFP (green fluorescence protein) fused to the effector candidate Ap30385	This study
35S::G3GFP-Ap30385	pGWB652, binary plasmid for N-terminal G3GFP (green fluorescence protein) fused to the effector candidate Ap30385	This study
35S::Ap28303-G3GFP	pGWB651, binary plasmid for C-terminal G3GFP (green fluorescence protein) fused to the effector candidate Ap28303	This study
35S::G3GFP-Ap28303	pGWB652, binary plasmid for N-terminal G3GFP (green fluorescence protein) fused to the effector candidate Ap28303	This study

2.2.4.3 Protein extraction and Western blot analysis

Two days after the agroinfiltration, *N. benthamiana* leaves were harvested, and 3 discs (diameter: 0.9 cm) were kept at -80 ºC until the protein extraction. The leaf samples were ground (3 times of 30 Hz for 30 seconds each) in a TissueLyser II bead beater using three 3mm glass beads. After the addition of, 60 µl Protein Extraction Buffer (50 mM Tris-HCl, pH 8.0; 1% SDS; 1mM EDTA, pH 8.0; Beta-mercaptoethanol; Protease inhibitor; Ultrapure water), the samples were incubated on ice for 5 minutes. Next, the samples were centrifugated twice at 14,000 rpm for 10 minutes at 4 ºC. Sixty microliters of the supernatant were collected after each centrifugation. Finally, 12 µl of 6X Loading Buffer (375 mM Tris-HCl, pH 6.8; 60% Glycerol; 12% SDS; 0.6M DTT; 0.06% Bromophenol blue; Ultrapure water) were added to the samples and incubated at 95 ºC for 5 minutes. A total of 20 µl of each sample was separated in a 12% SDS-PAGE gel.

Proteins from the SDS-PAGE gel were transferred to a nitrocellulose membrane using a semi-dry system (Owl, ThermoScientific). Membrane blocking was performed using 5% skimmed milk powder in 1X TBS-T buffer (10X TBS; Ultrapure water; Tween 20) for 1 hour at room temperature.

Then, the membrane was washed three times in TBS-T for 5 minutes. The membrane was then incubated with the rabbit anti-GFP antibody (GFP Polyclonal Antibody, Invitrogen) at a dilution of 1:1000 in 10 mL of 1% skimmed milk powder overnight, at 4 ºC in a hybridizer. The membrane was then washed three times with TBS-T and incubated for 1 hour at room temperature with a 1:5000 dilution of the Goat anti-Rabbit secondary antibody (IgG (H+L) Cross-Adsorbed Secondary Antibody, HRP, Invitrogen). Then, the membrane was washed three times in TBS-T and once in 1X TBS to remove residual Tween 20. The signal was visualised with the Amersham ECL Prime (GE Healthcare) according to the manufacturer's instructions and revealed in ChemiDoc XRS+ Gel Imaging System (Bio-Rad).

2.3 Results

2.3.1 *In silico* analyses

We found 708 effector candidates by the manual pipeline and 282 were predicted by EffectorP 2.0. We performed a Venn Diagram (Heberle et al., 2015) to overlap the effector candidates predicted by both methods, and it was found 255 effector candidates in common (Figure 2). The common sequences of effector candidates predicted by both methods were considered the profile of *A. psidii* effector candidates (Appendix C).

The prediction of subcellular localization of effector candidate's profile by LocTree3 showed that the most abundant localization was apoplastic, 87.45%, followed by cytoplasmatic (6.27%) and by nuclear (3.14%) (Table 4).

The description of effector candidate's profile was mostly non-annotated (65.49%), followed by hypothetical proteins (23.14%) and known function (11.37%). Among the effector candidates with known functions, it was observed secreted proteins, enzymes as hydrolases, lipases, and chitin deacetylases, or domains. The majority of effector candidates with known function were associated to other rusts (*Puccinia* spp. and *M. larici-populina*) (Table 5). The subcellular localization and the functional description of the effector candidate profile were listed in Appendix C. The effector candidates were categorized according to biological process terms using Blast2GO (Figure 3). The most abundant terms were carbohydrate metabolic process, catabolic process and biosynthetic process.

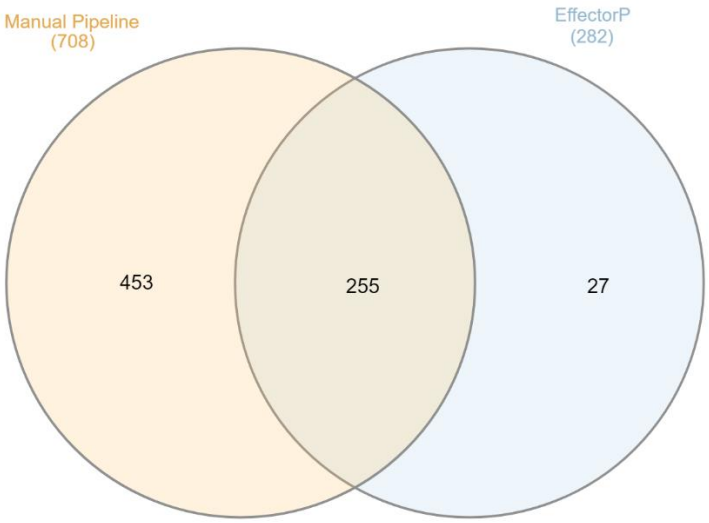

Figure 2. Venn Diagram from the effector candidates predicted by manual Pipeline (right) and EffectorP (left) and common to both methods (center) from *A. psidii*

Table 4. Percentage of the effector candidates localization in the host predicted by LocTree3*

Localization	Percentage of hits (%)
Apoplast/secreted	87.45
Cytoplasm	6.27
Nucleus	3.14
Endoplasmatic reticulum	0.78
Mitochondria	0.78
Vacuole	0.78
Chloroplast	0.39
Plasma membrane	0.39

* (Goldberg et al., 2014)

Table 5. Description of effector candidates known function

Effector candidates*	Description[a]
evm.model.NODE_10061_length_10145_cov_0.0507087.1	Alpha,alpha-trehalose-phosphate synthase (UDP-forming) *P. coronata* var. *avenae* f. sp. *avenae*
evm.model.NODE_11108_length_9646_cov_0.920475.1	Chorismate mutase domain-containing protein *P. coronata* var. *avenae* f. sp. *avenae*
evm.model.NODE_11786_length_9347_cov_1.30542.1	SCP domain-containing protein *P. coronata* var. *avenae* f. sp. *avenae*
evm.model.NODE_11794_length_9343_cov_0.50255.1	Secreted protein *M. larici-populina*
evm.model.NODE_12507_length_9082_cov_0.159058.2	Protein ROT1 *M. larici-populina*
evm.model.NODE_12743_length_9006_cov_0.699628.1	Tnp4 domain-containing protein *P. striiformis*
evm.model.NODE_13752_length_8677_cov_0.852865.1	SCP domain-containing protein *P. coronata* var. *avenae* f. sp. *avenae*

evm.model.NODE_14121_length_8545_cov_0.464531.1	Secreted protein *M. larici-populina*
evm.model.NODE_15054_length_8284_cov_1.25043.1	Secreted protein *M. larici-populina*
evm.model.NODE_150611_length_1345_cov_0.1	Secreted protein *M. larici-populina*
evm.model.NODE_15688_length_8108_cov_1.01428.1	Chitin deacetylase *P. graminis* f. sp. *tritici*
evm.model.NODE_17047_length_7793_cov_0.273379.1	SCP domain-containing protein *P. striiformis*
evm.model.NODE_17596_length_7670_cov_0.351982.1	Carboxylic ester hydrolase *Helicocarpus griseus*
evm.model.NODE_17742_length_7635_cov_0.85895.1	Chitin deacetylase *M. larici-populina*
evm.model.NODE_2638_length_19144_cov_0.79755.1	Sod_Cu domain-containing protein *P. graminis* f. sp. *tritici*
evm.model.NODE_26623_length_6099_cov_0.992802.1	Chitin deacetylase *P. graminis* f. sp. *tritici*
evm.model.NODE_28303_length_5903_cov_0.666551.1	Inhibitor I9 domain-containing protein
evm.model.NODE_28608_length_5870_cov_0.279122.1	Secreted protein *M. larici-populina*
evm.model.NODE_29272_length_5795_cov_1.39132.1	Lipase_3 domain-containing protein *P. striiformis* f. sp. *tritici*
evm.model.NODE_30484_length_5672_cov_0.655005.1	Sod_Cu domain-containing protein *P. graminis* f. sp. *tritici*
evm.model.NODE_31345_length_5584_cov_0.223016.1	Dimer_Tnp_hAT domain-containing protein
evm.model.NODE_33603_length_5352_cov_1.82086.2	Alpha-galactosidase *P. graminis* f. sp. *tritici*
evm.model.NODE_36746_length_5068_cov_0.660393.1	Alpha/Beta hydrolase protein *Pseudomassariella vexata*
evm.model.NODE_38089_length_4957_cov_0.561698.1	Thioredoxin domain-containing protein *P. triticina*
evm.model.NODE_42655_length_4604_cov_0.279875.1	Secreted protein *M. larici-populina*
evm.model.NODE_47016_length_4308_cov_0.743902.1	DPBB_1 domain-containing protein *P. striiformis* f. sp. *tritici* PST-78
evm.model.NODE_50324_length_4107_cov_0.0743719.1	Secreted protein *M. larici-populina*
evm.model.NODE_55075_length_3839_cov_0.0344828.1	SurE domain-containing protein *P. graminis* f. sp. *tritici*
evm.model.NODE_55_length_65597_cov_0.286605.1	Phosphatidylglycerol/phosphatidylinositol transfer protein *P. graminis* f. sp. *tritici*

[a] The description was obtained by Blast2GO and validated by UniProt

*Total of effector candidates: 255; Known function: 29; Hypothetical: 59; Unknown function: 167

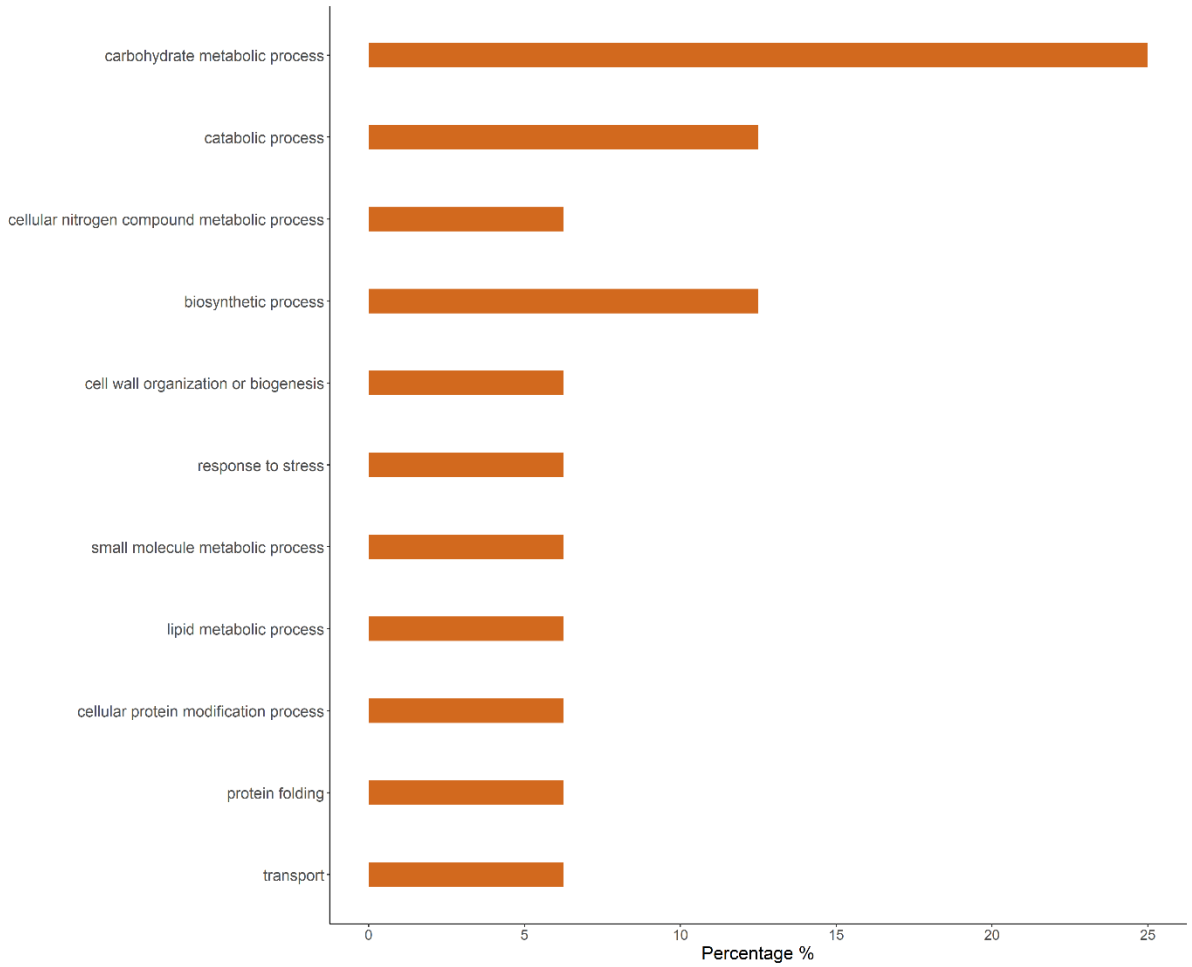

Figure 3. Gene ontology of biological process GO terms from effector candidates. Bar graph represents the ratio of percentage composition of terms in the effector candidates.

2.3.2 Functional characterization

2.3.2.1 Expression validation

Among the effector candidates, 7 genes were selected to have their expression validated under cuticular wax stimulus from different *Eucalyptus species*. We selected effector candidates with different localizations and functions (Table 6). The unique effector candidate selected that was not predicted by both methods was the Ap23389, it was selected based on a previous work (Lopes, 2017) which showed a differential expression in all times evaluated for the MF-1 biotype. The amino acid sequences of the 7 effector candidates selected are available in Appendix D.

Table 6. Functions and localization predicted to effector candidates selected to validation

Effector candidate	Description[a]	Localization[b]
Ap15054	Secreted protein	Secreted
Ap30385	hypothetical protein	Nucleus
Ap28303	inhibitor I9 domain-containing protein	Nucleus
Ap11108	chorismate mutase domain-containing protein	Cytoplasm
Ap12491	hypothetical protein	Secreted
Ap23389	Hypothetical protein	Nucleus
Ap2160	non-annotated	Secreted

[a] The description was obtained by Blast2GO and validated by UniProt
[b] The localizations were obtained by LocTree3

The effector candidate Ap15054 expression was significantly different and down-regulated in all time for both cuticular wax source (Figure 4a). The effector candidate Ap30385 and Ap28303 (Figure 4b, c) were differentially expressed only in one interval under the cuticular wax stimulus of *E. grandis.* The effector candidate Ap1108 (Figure 4d) did not shown significantly expression under cuticular wax stimulus to all sampled time. The only effector candidate differentially expressed and up-regulated in all intervals was the Ap12491, under the stimulus of cuticular wax from *E. grandis* (Figure 4e). The Ap23389 under the cuticular wax stimulus of *E. urophylla* was differentially expressed in 24 h.p.i (Figure 4f). The effector candidate Ap2160 did not have its expression detected under the stimulus of *E. urophylla* cuticular waxes (Figure 4g), just under the stimulus of *E. grandis* cuticular waxes.

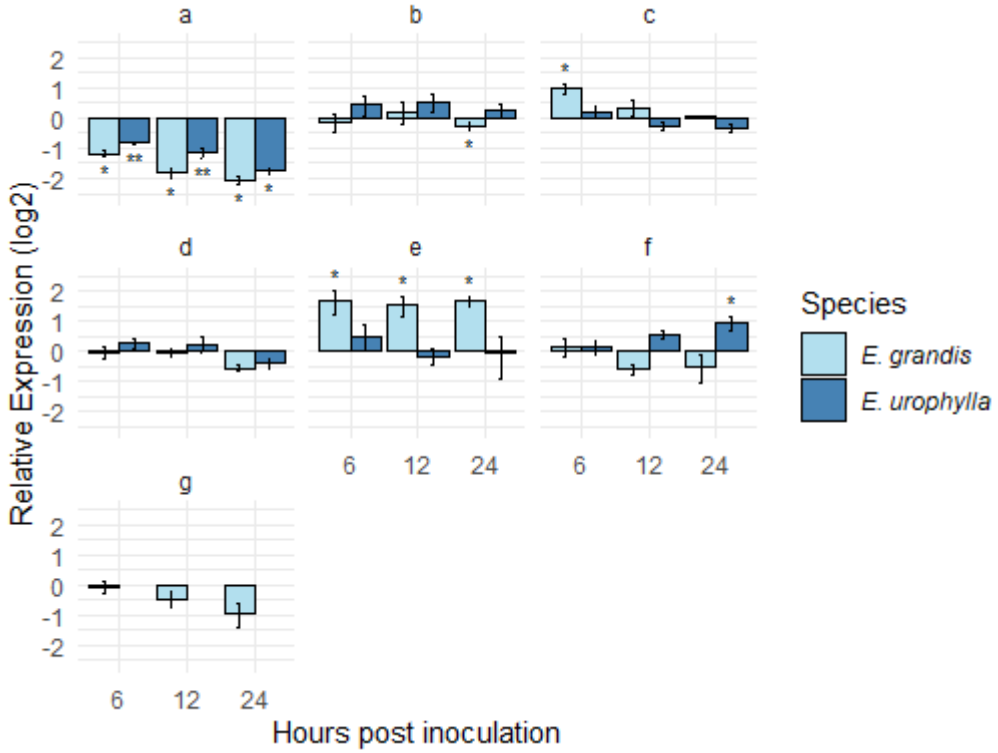

Figure 4. Expression of effector candidates under cuticular wax extracts from *E. grandis* and *E. urophylla* at 6, 12 and 24 hours post-inoculation; The time 0 hour post-inoculation was considered as control and the transcript levels of effector candidates were normalized to the levels of the reference gene beta -tubulin (Btub) and effector elongation (EF) to performed the analyses in REST; a: effector candidate Ap15054; b: effector candidate Ap30385; c: effector candidate Ap28303; d: effector candidate Ap11108; e: effector candidate Ap12491; f: effector candidate Ap23389; g: effector candidate Ap2160. *p<0.05; **p<0.001

2.3.2.2 Subcellular localization

Nuclear accumulation of the Ap28303 effector candidate was observed in *N. benthamiana* leaves transiently expressing the 35S::G3GFP-Ap28303 construct (Figure 5a). No fluorescence was detected when a C-terminal GFP tag was used (35S::Ap28303-G3GFP) (Figure 5b). On the other hand, accumulation of Ap30385 could not be observed by confocal microscopy regardless of the fusion tag used (35S::Ap30385-G3GFP, and 35S::G3GFP-Ap30385) (Figure 5c, d). Consistent with these results, protein accumulation could only be detected by Blot in plants expressing the GFP-Ap28303 construct (Figure 5e).

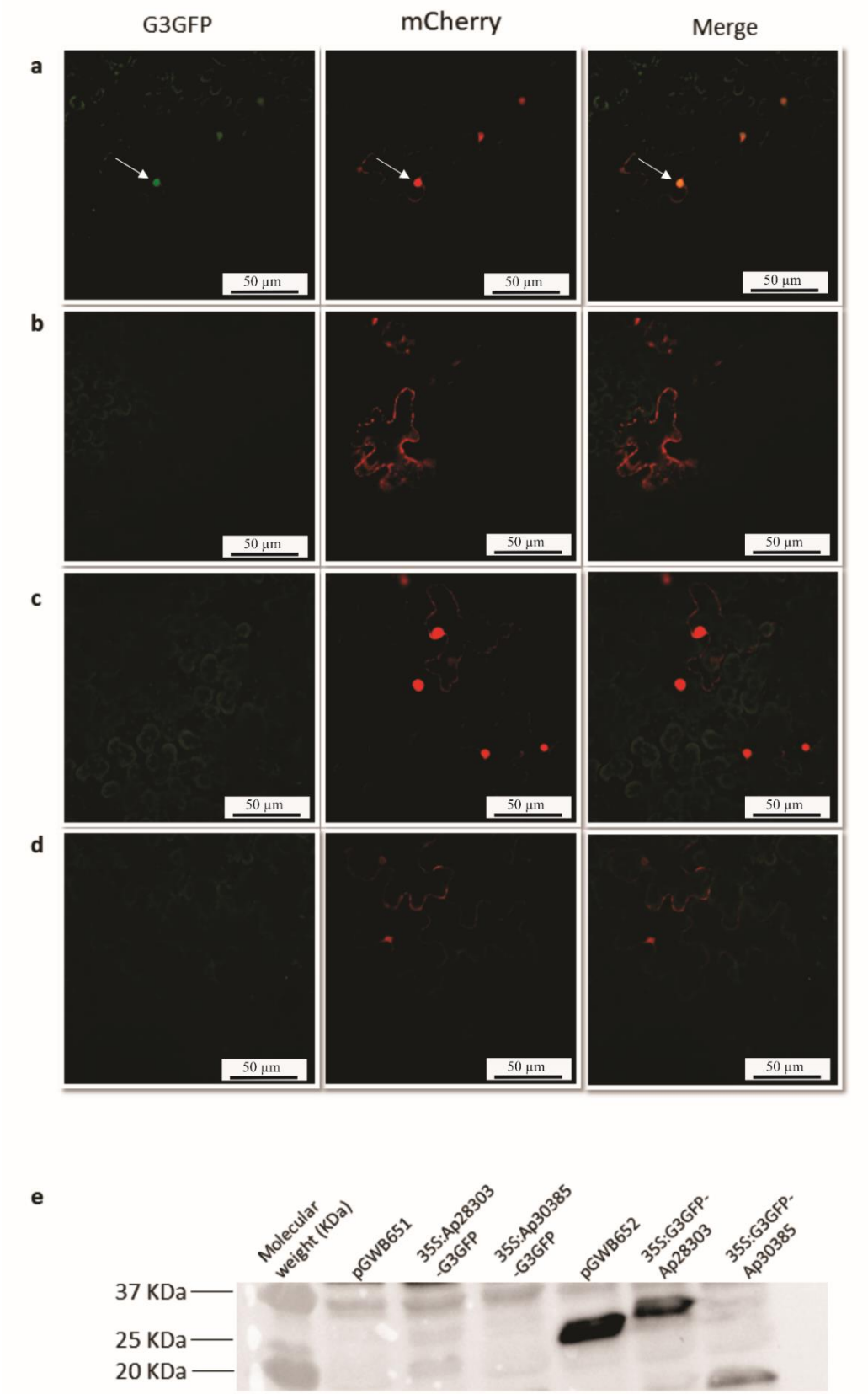

Figure 5. Confocal microscopy of the effector candidates, white arrows indicate nuclei; (a) 35S::G3GFP-Ap28303 construct accumulated in the nucleus. (b) no accumulation of 35S::Ap28303-G3GFP; (c) no accumulation of 35S::G3GFP-Ap30385; (d) no accumulation of 35S::Ap30385-G3GFP; (e) a band of the expected size for the 35S::G3GFP-Ap28303 fusion (40 KDa: 13 kDa of Ap28303 protein + 27 kDa of GFP protein). As expected, expression of the empty pGWB652 vector resulted in a band compatible with the G3GFP tag (~27 kDa)

2.4 Discussion

Plant pathogens use different strategies to avoid to be recognized by the plant immune system and overcome its defense, including the secretion of effector proteins, which is able to supress the immune responses facilitating the pathogen penetration and its survival inside the host (Göhre & Robatzek, 2008; Han, 2019; Jones & Dangl, 2006). Therefore, the study of effectors highlights in plant-pathogen interaction comprehension.

We performed the prediction of effector candidates using two methods, a manual pipeline and the software EffectorP 2.0. Both methods have been used to predict effector candidates from other phytopathogen genomes, they are based on common effector features: presence of peptide signal, absence of transmembrane domain and anchorage surface and/or protein size (Dalio et al., 2017; Petre et al., 2015; Tsushima et al., 2019). Manual pipelines are established by authors and based on the effector features mentioned. The EffectorP was the first software described to predict effectors of fungi from secretomes and to dispose the manual prediction (Sperschneider et al., 2016; Sperschneider et al., 2018). The number of effectors predicted varies according to criteria and/or method selected. For instance, to *P. striiformis* f.sp. *tritici* (wheat strip rust) it was predicted 969 effector candidates for Pst-104E strain (Schwessinger et al., 2018) by EffectorP 1.0, and 557 effector candidates for Pst-DK0911 strain (Schwessinger et al., 2020) using EffectorP 2.0. On the other hand, Garnica et al. (2013) found 437 haustorial secreted proteins using a manual pipeline, unlike our results that showed a higher number of effector candidates predicted by manual pipeline than by the software.

The number of effector candidates found in the rust pathogens is variable, these variations may be associated with the genome size of the fungi, the host-pathogen interaction, but mainly by the method used to predict the effector candidates. By manual pipeline, it was found 1,184 small proteins in the genome of *M. larici-populina*, causal agent of leaf rust on cultivated poplars. To *P. graminis* f. sp. *tritici*, wheat steam rust, it was predicted 1,186 small proteins (Duplessis et al., 2011) and 520 haustorial secreted proteins (Upadhyaya et al., 2015) using distinct pipelines. Link et al. (2014) investigating the transcriptome of *Uromyces appendiculatus* and *Phakopsora pachyrhizi*, the common bean and soybean rust, identified 385 and 156 secreted proteins, respectively. Other works used the EffectorP to perform the predictions from fungi species, as *U. appendiculatus*, *C. higginsianum* and *P. striiformis* f.sp. *tritici* (Qi et al., 2019; Schwessinger et al., 2020; Tsushima et al., 2019). Thus, the difference in the number of effector candidates predicted in this work is associated with the method used, using a manual pipeline other features could be considered to achieve a restrict number of effectors, as percentage of cysteine or also proteins exclusively or not to the order Pucciniales. Nevertheless, to double check the effector candidates predicted we used the effector candidates selected by two predictions, in this way, we identified 255 effector candidates for *A. psidii* MF-1 biotype. To date there is no information about effector candidates from *A. psidii* previously.

It was observed that the major effector candidates (65.49%) of *A. psidii* MF-1 with unknown function, and just 11.37% with annotated function. Tsushima et al. (2019) found around 70% of the effector candidates with unknown function for *C. higginsianum*, as well Duplessis et al. (2011) found 84% for *P. graminis* and 74% for *M. larici-populina*. This fact may be associated to low number of effectors from fungi characterized, which have been increasing with the advances in genome tools for the last years (Arroyo-Velez et al., 2020).

The host subcellular target localization by effectors is fundamental to understand its function (Alfano, 2009). Apoplastic effectors act in the host extracellular space and can be recognized by PRRs. Cytoplasmic effectors act inside the host cell and traffic to several subcellular compartments to play their function (Win et al., 2012). In the cytoplasm, the effectors target different organelles, and a great number of effectors accumulate in the plant nucleus (Caillaud et al., 2012). Thus, we first predicted *in silico* the subcellular localization of effector candidates from *A. psidii* MF-1, and transiently expressed to confirm their localization.

Based on the prediction *in silico* using LocTree3, we found a higher number of apoplastic effector candidates. We observed 87% of apoplastic effectors, whereas Sperschneider et al. (2018) observed lower percentage of apoplatic effectors to *P. striiformis* f. sp. *tritici* PST-130 (61.2%), *P. graminis* f. sp. *tritici* (61.6%), *M. larici-populina* (58.7%) and *P. triticina* (53.51%). To predict the subcellular localization, Sperschneider et al., (2017) used the LOCALIZER software and found effector candidates of rust fungi targeting chloroplast, nucleus and mitochondria. The percentage average of proteins secreted for rust fungi (5 genomes analysed) was 3.35% targeting chloroplast, 0.93% mitochondria and 4.5% nucleus. The proportion of effector candidates targeting the nucleus was the highest, as to *P. graminis* f. sp. *tritici* 5.61% and *P. triticina* 5.44%. In this work, we found 3.14% of effector candidates targeting the nucleus, 0.39% chloroplast and 0.78% mitochondria, using LocTree3. Our results showed that *A. psidii* MF-1 present a higher number of apoplastic effectors compared to other rusts, whereas concerning cytoplasmic effectors, we found similar results to Sperschneider et al. (2017), which the nucleus was the main target of cytoplasmic effectors. However, rust fungi present a low number of apoplastic effector compared to other fungi as *Cladosporium fulvum, Zymoseptoria tritici*, *Leptosphaeria maculans* and *Venturia inaequalis* (Sperschneider et al., 2018). Caillaud et al. (2012) observed that the prediction *in silico* and *in vivo* may be contradictory, just 20% were found in the same location *in vivo* and *in silico.* Therefore, the validation of prediction *in silico* is an essential step to characterize the effector candidates prior to the transient expression.

The validation of effector candidate's expression is essential to elucidate its expression during the host infection. The interaction *A. psidii* x *Eucalyptus* is a complex system to explore, the obligate biotrophic lifestyle from the fungus turns the *in vitro* cultivation limited to a 24-48 hours in specific culture medium (Bini, 2016). The use of cuticular waxes from *Eucalyptus* species as stimulus to decipher the mechanisms involved during the infection of *A. psidii* in different species was a feasible alternative (Santos et al., 2019). In this way, we performed our expression analysis under the stimulus of cuticular

wax. In general, we observed a changing expression amongst effector candidates, although it was not observed an expression pattern. Our findings indicate that the cuticular wax source modulate the effector candidate's expression.

The effector candidate Ap11108 was found in database described as chorismate mutase domain-containing protein of *P. coronata* var. *avenae* f. sp. *avenae*. An effector, named Cmu1, was described in *Ustilago maydis* as secreted chorismate mutase. It is suggested that this effector consume the chorismate to supress the SA (salicylic acid), hence playing a role in virulence (Djamei et al., 2011). The expression of effector candidate Ap11108 under stimulus of cuticular wax did not shown differential expression. Probably it plays a role in a different infection stage, where it may be differentially expressed.

Under the stimuli of cuticular wax from *E. urophylla*, the resistant genotype, it was observed at 24 h.p.i. an up-regulated expression of Ap23389 effector candidate, indicating that this effector might have a role in later stages in resistant genotypes. The hypothetical protein, Ap12491, was up-regulated and differentially expressed at all intervals under stimulus of cuticular wax from the susceptible species, *E. grandis*. In *in vitro* conditions, at 12 h.p.i. is observed the germinative tube formation (Bini, 2016), the up-regulated expression of the effector candidate Ap12491 showed that it might develop a role since the beginning of infection under cuticular wax stimulus of susceptible species, which might play an important role in the successful infection in these species. Meanwhile, the effector candidate Ap30385 was functionally described as hypothetical protein and predicted as nuclear by LocTree3. This effector candidate was differentially expressed just at 24 h.p.i. under stimulus of cuticular wax of susceptible species, which suggest that this effector candidates are involved during later stages of infection.

For both cuticular wax species stimuli, the effector candidate Ap15054 was down-regulated and differentially expressed in all intervals. This effector candidate was described as a secreted protein of *M. larici-populina*, a causal agent of poplar rust. The down-regulation of an effector gene may be tied to avoid the plant recognition as in *C. graminicola* (Oliveira-Garcia & Deising, 2016). The down-regulation did not exclude Ap15054 as an effector. It is known that the up-regulation of an effector candidate *in planta* may not be an evidence that whether the protein is an effector or not. Even effectors predicted as expressed in haustoria were down-regulated, moreover the mechanisms of posttranscriptional regulation may control effector expression (Qi et al., 2019).

The validation of the subcellular localization computational prediction is also fundamental. It is commonly used the *in planta* characterization method by agroinfiltration, an assay to express candidate effectors in plant cells using the non-host *N. benthamiana* to identify the subcellular localization of effector candidates (Du et al., 2014; Petre et al., 2015). The effectors tagged with a fluorescent protein are visualized in a confocal microscopy (Caillaud et al., 2012). Effector candidates from *M. larici-populina* were identified present in nuclei, nuclear bodies, chloroplasts, and mitochondria (Germain et al., 2018; Petre et al., 2015). Qi et al. (2018) by transient expression found effector candidates from the pathogen *P. pachyrhizi* accumulating in the nucleus and cytoplasm. Also, there are

reports of effector candidates rust targeting the chloroplasts (Carvalho et al., 2017; Petre et al., 2016). Most works investigating subcellular localization of effector candidates using heterologous system assays, this methodology was performed to rusts species as *M. larici-populina*, *M. lini*, *P. pachyrhizi*, *P. graminis* f. sp. *tritici*, *P. striiformis* f. sp. *tritici* due to limitation of obligate pathogens manipulation (Lorrain, Petre, et al., 2018). Similarly, we aimed to investigate the subcellular localization of effector candidates of *A. psidii* MF-1 using the heterologous system. We started the cloning procedures with 5 effector candidates, however just 2 effector candidates, Ap30385 and Ap28303 proceeded to agroinfiltration. It was not possible to proceed with the cloning procedures to the other three effector candidates due to unsuccessfully PCR amplification primers. We cloned the effector candidate Ap30385 to an *A. tumefaciens* binary plasmid, however, it was not observed the constructions accumulating in any subcellular compartment. We did not observe any green fluorescence either N- or C-terminal fusions, only the autofluorescence, although the mCherry plasmids were expressed in the membrane and nucleus, which proves that agroinfiltration was not the issue, probably there is a limitation using a heterologous system (Petre et al., 2015). We also did not recover by Western blot the G3GFP protein.

Plants use proteases in the apoplast to defend themselves, whereas the pathogens effectors target these proteins to protect against degradation (Doehlemann & Hemetsberger, 2013). Rawlings et al. (2004) classified peptidases in 48 families based on similarities among them, and the family I9 was classified as protease inhibitor. We selected the effector candidate Ap28303, described as inhibitor I9 domain-containing protein to validate its expression. It was observed a significantly expression at 6 h.p.i. just under the cuticular wax stimulus of the susceptible species, *E. grandis*. In the other hand, Lopes (2017) observed a differentially up-regulated expression of Ap28303 for MF-1 biotype and GM-J1 biotype from *S. jambos* at 6, 12 and 24 h.p.i.. Thus, this effector candidate might play a role in the early stages of infection, and in distinct hosts. Studies have been describing effectors that attack the proteases proteins from the plant (Mueller et al., 2013; Van Esse et al., 2008), to rust fungi the protein RTP1p from *U. fabae* and *U. striatus* was found in cytoplasm and described with protease inhibitor activity. It was supposed that the homologues of RTP1p may be spread in the order Pucciniales, and possibly it is fundamental to biotrophic lifestyle (Kemen et al., 2005).

The prediction by LocTree3 showed nuclear localization of Ap28303, which is a divergence of its function as protease inhibitor. We transiently expressed this effector candidate in a binary system in *N. benthamiana* leaves, and by confocal microscopy we observed its accumulation in the epidermal cell nucleus using the protein fused in N-terminal. This result confirmed the prediction *in silico*. Qi et al. (2019) also used N-terminal fusions based on the supposition that the tag is replacing the signal peptide. The authors observed that the candidate protein Uf-RTP1p with protease inhibitor activity did not suppress plant defenses, which was expected in the assays, and the GFP protein fusions for Uf-RTP1p proteins were observed in the nucleus, but also in the cytoplasm. Effectors targeting the host nucleus have been reported (Lorrain, Petre, et al., 2018; Zhang et al., 2017), including in rust pathogens as *M. larici-populina* (Petre et al., 2015) and *U. fabae* (Qi et al., 2019). Proteins localized at the nuclei

target host transcriptional factors (Cui et al., 2015), RNAi components (Qiao et al., 2013) or associates with TOPLESS-related proteins, that are involved in plant immune responses (Petre et al., 2015).

This pioneer study of effector candidates from *A. psidii* identified 255 effector candidates from *A. psidii* MF-1 biotype. We observed that cuticular wax from susceptible and resistant host modulated the expression of 7 effector candidates selected, and the effector candidate Ap28303 showed nuclear localization by heterologous plant systems. It is necessary further studies about the candidate effector Ap28303 to figure out its function and role in the host infection. Besides its annotation as protease inhibitor, it targeted the host nucleus, which might imply more than one function or different function and localization for this effector candidate.

References

Alfano, J. R. (2009). Roadmap for future research on plant pathogen effectors: Micro-Review. *Molecular Plant Pathology*, *10*(6), 805–813. https://doi.org/10.1111/j.1364-3703.2009.00588.x

Arroyo-Velez, N., González-Fuente, M., Peeters, N., Lauber, E., & Noël, L. D. (2020). From effectors to effectomes: Are functional studies of individual effectors enough to decipher plant pathogen infectious strategies? *PLoS Pathogens*, *16*(12), 1–8. https://doi.org/10.1371/journal.ppat.1009059

Ashburner, M., Ball, C. A., Blake, J. A., Botstein, D., Butler, H., Cherry, M. J., Davis, A. P., Dolinski, K., Dwight, S. S., Eppig, J. T., Harris, Mi. A., Hill, D. P., Issel-Tarver, L., Kasarskis, A., Lewis, S., Matese, J. C., Richardson, J. E., Ringwald, M., Rubin, G., & Sherlock, Ga. (2000). Gene Ontology: tool for the unification of biology The. *Nature Genetics*, *25*(1), 25–29. https://doi.org/10.1038/75556.Gene

Beenken, L. (2017). Austropuccinia: A new genus name for the myrtle rust *Puccinia psidii* placed within the redefined family sphaerophragmiaceae (pucciniales). *Phytotaxa*, *297*(1), 53–61. https://doi.org/10.11646/phytotaxa.297.1.5

Berthon, K., Esperon-Rodriguez, M., Beaumont, L. J., Carnegie, A. J., & Leishman, M. R. (2018). Assessment and prioritisation of plant species at risk from myrtle rust (*Austropuccinia psidii*) under current and future climates in Australia. *Biological Conservation*, *218*(May 2017), 154–162. https://doi.org/10.1016/j.biocon.2017.11.035

Bini, A. P. (2016). Estudo molecular do desenvolvimento de *Puccinia psidii* Winter in vitro e no processo de infecção em Eucalyptus grandis. In *Thesis*. University of São Paulo.

Bini, A. P., Quecine, M. C., da Silva, T. M., Silva, L. D., & Labate, C. A. (2018). Development of a quantitative real-time PCR assay using SYBR Green for early detection and quantification of *Austropuccinia psidii* in *Eucalyptus grandis*. *European Journal of Plant Pathology*, *150*(3), 735–746. https://doi.org/10.1007/s10658-017-1321-7

Caillaud, M. C., Piquerez, S. J. M., Fabro, G., Steinbrenner, J., Ishaque, N., Beynon, J., & Jones, J. D. G. (2012). Subcellular localization of the Hpa RxLR effector repertoire identifies a tonoplast-associated protein HaRxL17 that confers enhanced plant susceptibility. *Plant Journal*, *69*(2), 252–265. https://doi.org/10.1111/j.1365-313X.2011.04787.x

Carvalho, M. C. d. C. G., Costa Nascimento, L., Darben, L. M., Polizel-Podanosqui, A. M., Lopes-Caitar, V. S., Qi, M., Rocha, C. S., Carazzolle, M. F., Kuwahara, M. K., Pereira, G. A. G., Abdelnoor, R. V., Whitham, S. A., & Marcelino-Guimarães, F. C. (2017). Prediction of the in planta *Phakopsora pachyrhizi* secretome and potential effector families. *Molecular Plant Pathology*, *18*(3), 363–377. https://doi.org/10.1111/mpp.12405

Conesa, A., Götz, S., García-Gómez, J. M., Terol, J., Talón, M., & Robles, M. (2005). Blast2GO: A universal tool for annotation, visualization and analysis in functional genomics research. *Bioinformatics*, *21*(18), 3674–3676. https://doi.org/10.1093/bioinformatics/bti610

Consortium, T. U. (2021). UniProt: The universal protein knowledgebase in 2021. *Nucleic Acids Research*, *49*(D1), D480–D489. https://doi.org/10.1093/nar/gkaa1100

Coutinho, T. A., Wingfield, M. J., Alfenas, A. C., & Crous, P. W. (1998). *Eucalyptus* rust: A disease with the potential for serious international implications. *Plant Disease*, *82*(7), 819–825. https://doi.org/10.1094/PDIS.1998.82.7.819

Cui, H., Tsuda, K., & Parker, J. E. (2015). Effector-triggered immunity: From pathogen perception to robust defense. *Annual Review of Plant Biology*, *66*, 487–511. https://doi.org/10.1146/annurev-arplant-050213-040012

Cutler, S. R., Ehrhardt, D. W., Griffitts, J. S., & Somerville, C. R. (2000). Random GFP::cDNA fusions enable visualization of subcellular structures in cells of Arabidopsis at a high frequency. *Proceedings of the National Academy of Sciences of the United States of America*, *97*(7), 3718–3723. https://doi.org/10.1073/pnas.97.7.3718

Dalio, R. J. D., Magalhaes, D. M., Rodrigues, C. M., Arena, G. D., Oliveira, T. S., Souza-Neto, R. R., Picchi, S. C., Martins, P. M. M., Santos, P. J. C., Maximo, H. J., Pacheco, I. S., De Souza, A. A., & Machado, M. A. (2017). PAMPs, PRRs, effectors and R-genes associated with citrus-pathogen interactions. *Annals of Botany*, *119*(5), 749–774. https://doi.org/10.1093/aob/mcw238

Dianese, J. C., Moraes, T. S., & Silva, A. R. (1984). Response of *Eucalyptus* species to field infection by *Puccinia psidii*. *Plant Disease*, *68*(4), 314–316.

Djamei, A., Schipper, K., Rabe, F., Ghosh, A., Vincon, V., Kahnt, J., Osorio, S., Tohge, T., Fernie, A. R., Feussner, I., Feussner, K., Meinicke, P., Stierhof, Y. D., Schwarz, H., MacEk, B., Mann, M., & Kahmann, R. (2011). Metabolic priming by a secreted fungal effector. *Nature*, *478*(7369), 395–398. https://doi.org/10.1038/nature10454

Dodds, P. N., & Rathjen, J. P. (2010). Plant immunity: Towards an integrated view of plant-pathogen interactions. *Nature Reviews Genetics*, *11*(8), 539–548. https://doi.org/10.1038/nrg2812

Doehlemann, G., & Hemetsberger, C. (2013). Apoplastic immunity and its suppression by filamentous plant pathogens. *New Phytologist*, *198*(4), 1001–1016. https://doi.org/10.1111/nph.12277

Du, J., Rietman, H., & Vleeshouwers, V. G. A. A. (2014). Agroinfiltration and PVX agroinfection in potato and *Nicotiana benthamiana*. *Journal of Visualized Experiments*, *83*, 1–7. https://doi.org/10.3791/50971

Duplessis, S., Cuomo, C. A., Lin, Y. C., Aerts, A., Tisserant, E., Veneault-Fourrey, C., Joly, D. L., Hacquard, S., Amselem, J., Cantarel, B. L., Chiu, R., Coutinho, P. M., Feaue, N., Field, M., Frey, P., Gelhaye, E., Goldberg, J., Grabherr, M. G., Kodira, C. D., … Martin, F. (2011). Obligate biotrophy features unraveled by the genomic analysis of rust fungi. *Proceedings of the National Academy of Sciences of the United States of America*, *108*(22), 9166–9171. https://doi.org/10.1073/pnas.1019315108

Fankhauser, N., & Mäser, P. (2005). Identification of GPI anchor attachment signals by a Kohonen self-organizing map. *Bioinformatics*, *21*(9), 1846–1852. https://doi.org/10.1093/bioinformatics/bti299

Garnica, D. P., Upadhyaya, N. M., Dodds, P. N., & Rathjen, J. P. (2013). Strategies for Wheat Stripe Rust Pathogenicity Identified by Transcriptome Sequencing. *PLoS ONE*, *8*(6). https://doi.org/10.1371/journal.pone.0067150

Germain, H., Joly, D. L., Mireault, C., Plourde, M. B., Letanneur, C., Stewart, D., Morency, M. J., Petre, B., Duplessis, S., & Séguin, A. (2018). Infection assays in *Arabidopsis* reveal candidate effectors from the poplar rust fungus that promote susceptibility to bacteria and oomycete pathogens. *Molecular Plant Pathology*, *19*(1), 191–200. https://doi.org/10.1111/mpp.12514

Glen, M., Alfenas, A. C., Zauza, E. A. V., Wingfield, M. J., & Mohammed, C. (2007). *Puccinia psidii*: A threat to the Australian environment and economy - A review. *Australasian Plant Pathology*, *36*(1), 1–16. https://doi.org/10.1071/AP06088

Göhre, V., & Robatzek, S. (2008). Breaking the barriers: Microbial effector molecules subvert plant immunity. *Annual Review of Phytopathology*, *46*, 189–215. https://doi.org/10.1146/annurev.phyto.46.120407.110050

Goldberg, T., Hecht, M., Hamp, T., Karl, T., Yachdav, G., Ahmed, N., Altermann, U., Angerer, P., Ansorge, S., Balasz, K., Bernhofer, M., Betz, A., Cizmadija, L., Do, K. T., Gerke, J., Greil, R., Joerdens, V., Hastreiter, M., Hembach, K., … Rost, B. (2014). LocTree3 prediction of localization. *Nucleic Acids Research*, *42*(W1), 350–355. https://doi.org/10.1093/nar/gku396

Han, G. Z. (2019). Origin and evolution of the plant immune system. *New Phytologist*, *222*(1), 70–83. https://doi.org/10.1111/nph.15596

Heberle, H., Meirelles, V. G., da Silva, F. R., Telles, G. P., & Minghim, R. (2015). InteractiVenn: A web-based tool for the analysis of sets through Venn diagrams. *BMC Bioinformatics*, *16*(1), 1–7. https://doi.org/10.1186/s12859-015-0611-3

Hogenhout, S. A., Van Der Hoorn, R. A. L., Terauchi, R., & Kamoun, S. (2009). Emerging concepts in effector biology of plant-associated organisms. *Molecular Plant-Microbe Interactions*, *22*(2), 115–122. https://doi.org/10.1094/MPMI-22-2-0115

Joffily, J. (1944). Ferrugem do eucalipto. *Bragantia*, *4*(8), 475–487. https://doi.org/10.1590/s0006-87051944000300001

Jones, J. D. G., & Dangl, J. L. (2006). The plant immune system. *Nature*, *444*(7117), 323–329.

Kemen, E., Kemen, A. C., Rafiqi, M., Hempel, U., Mendgen, K., Hahn, M., & Voegele, R. T. (2005). Identification of a protein from rust fungi transferred from haustoria into infected plant cells. *Molecular Plant-Microbe Interactions*, *18*(11), 1130–1139. https://doi.org/10.1094/MPMI-18-1130

Krogh, A., Larsson, B., Von Heijne, G., & Sonnhammer, E. L. L. (2001). Predicting transmembrane protein topology with a hidden Markov model: Application to complete genomes. *Journal of Molecular Biology*, *305*(3), 567–580. https://doi.org/10.1006/jmbi.2000.4315

Kunjeti, S. G., Iyer, G., Johnson, E., Li, E., Broglie, K. E., Rauscher, G., & Rairdan, G. J. (2016). Identification of *Phakopsora pachyrhizi* candidate effectors with virulence activity in a distantly related pathosystem. *Frontiers in Plant Science*, *7*(MAR2016), 1–9. https://doi.org/10.3389/fpls.2016.00269

Leite, T. F. (2012). Estabelecimento de um patossistema modelo e análise da interação molecular planta-patógeno entre Eucalyptus grandis e *Puccinia psidii* Winter por meio da técnica de RNA-Seq. In *Thesis*. University of São Paulo.

Leite, T. F., Moon, D. H., Lima, A. C. M., Labate, C. A., & Tanaka, F. A. O. (2013). A simple protocol for whole leaf preparation to investigate the interaction between *Puccinia psidii* and *Eucalyptus grandis*. *Australasian Plant Pathology*, *42*(1), 79–84. https://doi.org/10.1007/s13313-012-0179-6

Link, T. I., Lang, P., Scheffler, B. E., Duke, M. V., Graham, M. A., Cooper, B., Tucker, M. L., van de Mortel, M., Voegele, R. T., Mendgen, K., Baum, T. J., & Whitham, S. A. (2014). The haustorial transcriptomes of *Uromyces appendiculatus* and *Phakopsora pachyrhizi* and their candidate effector families. *Molecular Plant Pathology*, *15*(4), 379–393. https://doi.org/10.1111/mpp.12099

Lopes, M. da S. (2017). Identificação in silico e perfil transcricional de genes candidatos a efetores de *Austropuccinia psidii*. In *Thesis*. Universidade de São Paulo.

Lorrain, C., Petre, B., & Duplessis, S. (2018). Show me the way: rust effector targets in heterologous plant systems. *Current Opinion in Microbiology*, *46*, 19–25. https://doi.org/10.1016/j.mib.2018.01.016

Masson, M. V., Moraes, W. B., & Furtado, L. (2013). Chemical Control of *Eucalyptus* Rust: Brazilian Experiences. In *Fungicides – Showcases of Integrated Plant Disease Management from Around the World* (Vol. 32, Issue July, pp. 117–134). https://doi.org/http://dx.doi.org/10.5772/56319

Mueller, A. N., Ziemann, S., Treitschke, S., Aßmann, D., & Doehlemann, G. (2013). Compatibility in the *Ustilago maydis*-Maize Interaction Requires Inhibition of Host Cysteine Proteases by the Fungal Effector Pit2. *PLoS Pathogens*, *9*(2). https://doi.org/10.1371/journal.ppat.1003177

Nakagawa, T., Suzuki, T., Murata, S., Nakamura, S., Hino, T., Maeo, K., Tabata, R., Kawai, T., Tanaka, K., Niwa, Y., Watanabe, Y., Nakamura, K., Kimura, T., & Ishiguro, S. (2007). Improved gateway binary vectors: High-performance vectors for creation of fusion constructs in transgenic analysis of plants. *Bioscience, Biotechnology and Biochemistry*, *71*(8), 2095–2100. https://doi.org/10.1271/bbb.70216

Nielsen, H. (2017). Predicting secretory proteins with signalP. In D. Kihara (Ed.), *Protein Function Prediction (Methods in Molecular Biology)* (Vol. 1611, pp. 59–73). Springer. https://doi.org/10.1007/978-1-4939-7015-5_6

Oliveira-Garcia, E., & Deising, H. B. (2016). Attenuation of PAMP-triggered immunity in maize requires down-regulation of the key β-1,6-glucan synthesis genes KRE5 and KRE6 in biotrophic hyphae of Colletotrichum graminicola. *Plant Journal*, *87*(4), 355–375. https://doi.org/10.1111/tpj.13205

Pegg, G., Taylor, T., Entwistle, P., Guymer, G., Giblin, F., & Carnegie, A. (2017). Impact of *Austropuccinia psidii* (myrtle rust) on Myrtaceae-rich wet sclerophyll forests in south east Queensland. *PLoS ONE*, *12*(11). https://doi.org/10.1371/journal.pone.0188058

Petre, B., Saunders, D. G. O., Sklenar, J., Lorrain, C., Krasileva, K. V., Win, J., Duplessis, S., & Kamoun, S. (2016). Heterologous expression screens in *Nicotiana benthamiana* identify a candidate effector of the wheat yellow rust pathogen that associates with processing bodies. *PLoS ONE*, *11*(2), 1–16. https://doi.org/10.1371/journal.pone.0149035

Petre, B., Saunders, D. G. O., Sklenar, J., Lorrain, C., Win, J., Duplessis, S., & Kamoun, S. (2015). Candidate effector proteins of the rust pathogen *Melampsora larici-populina* target diverse plant cell compartments. *Molecular Plant-Microbe Interactions*, *28*(6), 689–700. https://doi.org/10.1094/MPMI-01-15-0003-R

Pfaffl, M. W., Horgan, G. W., & Dempfle, L. (2002). Relative expression software tool (REST) for group-wise comparison and statistical analysis of relative expression results in real-time PCR. *Nucleic Acids Research*, *30*(9). https://doi.org/10.1093/nar/30.9.e36

Qi, M., Grayczyk, J. P., Seitz, J. M., Lee, Y., Link, T. I., Choi, D., Pedley, K. F., Voegele, R. T., Baum, T. J., & Whitham, S. A. (2018). Suppression or activation of immune responses by predicted secreted proteins of the soybean rust pathogen *Phakopsora pachyrhizi*. *Molecular Plant-Microbe Interactions*, *31*(1), 163–174. https://doi.org/10.1094/MPMI-07-17-0173-FI

Qi, M., Mei, Y., Grayczyk, J. P., Darben, L. M., Rieker, M. E. G., Seitz, J. M., Voegele, R. T., Whitham, S. A., & Link, T. I. (2019). Candidate Effectors From *Uromyces appendiculatus*, the Causal Agent of Rust on Common Bean, Can Be Discriminated Based on Suppression of Immune Responses. *Frontiers in Plant Science*, *10*(October). https://doi.org/10.3389/fpls.2019.01182

Qiao, Y., Liu, L., Xiong, Q., Flores, C., Wong, J., Shi, J., Wang, X., Liu, X., Xiang, Q., Jiang, S., Zhang, F., Wang, Y., Judelson, H., Chen, X., & Ma, W. (2013). Oomycete pathogens encode RNA silencing supressors. *Nature Genetics*, *45*(3), 330–333. https://doi.org/10.1038/ng.2525.Oomycete

Ramakers, C., Ruijter, J. M., Lekanne Deprez, R. H., & Moorman, A. F. M. (2003). Assumption-free analysis of quantitative real-time polymerase chain reaction (PCR) data. *Neuroscience Letters*, *339*(1), 62–66. https://doi.org/10.1016/S0304-3940(02)01423-4

Rawlings, N. D., Tolle, D. P., & Barrett, A. J. (2004). Evolutionary families of peptidase inhibitors. *Biochemical Journal*, *378*(3), 705–716. https://doi.org/10.1042/BJ20031825

RStudio Team. (2019). *RStudio: Integrated Development Environment for R* ('1.2.5033'). http://www.rstudio.com/

Sambrook, J., Fritsch, E.F., and Maniatis, T. (1989) Molecular cloning, a laboratory manual, 2nd ed. *Cold Spring Harbor*, NY: Cold Spring Harbor Laboratory.

Santos, I. B. dos, Lopes, M. da S., Bini, A. P., Tschoeke, B. A. P., Verssani, B. A. W., Figueredo, E. F., Cataldi, T. R., Marques, J. P. R., Silva, L. D., Labate, C. A., & Quecine, M. C. (2019). The *Eucalyptus* cuticular Waxes contribute in preformed defense against *Austropuccinia psidii*. *Frontiers in Plant Science*, *9*(January), 1–13. https://doi.org/10.3389/fpls.2018.01978

Schwessinger, B., Chen, Y. J., Tien, R., Vogt, J. K., Sperschneider, J., Nagar, R., McMullan, M., Sicheritz-Ponten, T., Sørensen, C. K., Hovmøller, M. S., Rathjen, J. P., & Justesen, A. F. (2020). Distinct Life Histories Impact Dikaryotic Genome Evolution in the Rust Fungus *Puccinia striiformis* Causing Stripe Rust in Wheat. *Genome Biology and Evolution*, *12*(5), 597–617. https://doi.org/10.1093/gbe/evaa071

Schwessinger, B., Sperschneider, J., Cuddy, W. S., Garnica, D. P., Miller, M. E., Taylor, J. M., Dodds, P. N., Figueroa, M., Park, R. F., & Rathjen, P. (2018). A near-complete haplotype-phased genome of the dikaryotic. *MBio*, *9*, e02275-17.

Silva, P. A., Silva, J. C. F., Caetano, H. D. N., Machado, J. P. B., Mendes, G. C., Reis, P. A. B., Brustolini, O. J. B., Dal-Bianco, M., & Fontes, E. P. B. (2015). Comprehensive analysis of the endoplasmic reticulum stress response in the soybean genome: Conserved and plant-specific features. *BMC Genomics*, *16*(1), 1–20. https://doi.org/10.1186/s12864-015-1952-z

Soewarto, J., Giblin, F., & Carnegie, A. J. (2019). *Austropuccinia psidii* (myrtle rust) global host list. *Version 2. Australian Network for Plant Conservation*. http://www.anpc.asn.au/myrtle-rust

Sperschneider, J., Catanzariti, A. M., Deboer, K., Petre, B., Gardiner, D. M., Singh, K. B., Dodds, P. N., & Taylor, J. M. (2017). LOCALIZER: Subcellular localization prediction of both plant and effector proteins in the plant cell. *Scientific Reports*, *7*(March), 1–14. https://doi.org/10.1038/srep44598

Sperschneider, J., Dodds, P. N., Gardiner, D. M., Singh, K. B., & Taylor, J. M. (2018). Improved prediction of fungal effector proteins from secretomes with EffectorP 2.0. *Molecular Plant Pathology*, *19*(9), 2094–2110. https://doi.org/10.1111/mpp.12682

Sperschneider, J., Dodds, P. N., Singh, K. B., & Taylor, J. M. (2018). ApoplastP: prediction of effectors and plant proteins in the apoplast using machine learning. *New Phytologist*, *217*(4), 1764–1778. https://doi.org/10.1111/nph.14946

Sperschneider, J., Gardiner, D. M., Dodds, P. N., Tini, F., Covarelli, L., Singh, K. B., Manners, J. M., & Taylor, J. M. (2016). EffectorP: Predicting fungal effector proteins from secretomes using machine learning. *New Phytologist*, *210*(2), 743–761. https://doi.org/10.1111/nph.13794

Tsushima, A., Gan, P., Kumakura, N., Narusaka, M., Takano, Y., Narusaka, Y., & Shirasu, K. (2019). Genomic plasticity mediated by transposable elements in the plant pathogenic fungus *Colletotrichum higginsianum*. *Genome Biology and Evolution*, *11*(5), 1487–1500. https://doi.org/10.1093/gbe/evz087

Upadhyaya, N. M., Garnica, D. P., Karaoglu, H., Sperschneider, J., Nemri, A., Xu, B., Mago, R., Cuomo, C. A., Rathjen, J. P., Park, R. F., Ellis, J. G., & Dodds, P. N. (2015). Comparative genomics of australian isolates of the wheat stem rust pathogen *Puccinia graminis* f. sp. *tritici* reveals extensive polymorphism in candidate effector genes. *Frontiers in Plant Science*, *5*(JAN), 1–13. https://doi.org/10.3389/fpls.2014.00759

Van Esse, H. P., Van't Klooster, J. W., Bolton, M. D., Yadeta, K. A., Van Baarlen, P., Boeren, S., Vervoort, J., Dewit, P. J. G. M., & Thomma, B. P. H. J. (2008). The Cl*adosporium fulvum* virulence protein Avr2 inhibits host proteases required for basal defense. *Plant Cell*, *20*(7), 1948–1963. https://doi.org/10.1105/tpc.108.059394

Viana, R. ., Tuffi Santos, L. ., Demuner, A. ., Ferreira, F. ., Ferreira, L. ., Ferreira, E. ., Machado, A. F. ., & Santos, M. . (2010). Quantificação e composição química de cera epicuticular de folhas de eucalipto. *Planta Daninha*, *28*(4), 753–758. https://doi.org/10.1590/s0100-83582010000400007

Win, J., Chaparro-Garcia, A., Belhaj, K., Saunders, D. G. O., Yoshida, K., Dong, S., Schornack, S., Zipfel, C., Robatzek, S., Hogenhout, S. A., & Kamoun, S. (2012). Effector biology of plant-associated organisms: Concepts and perspectives. *Cold Spring Harbor Symposia on Quantitative Biology*, *77*, 235–247. https://doi.org/10.1101/sqb.2012.77.015933

Win, Joe, Kamoun, S., & Jones, A. M. E. (2011). Purification of effector-target protein complexes via transient expression in *Nicotiana benthamiana*. In *Plant Immunity* (Vol. 712, pp. 181–194). Humana Press. https://doi.org/10.1007/978-1-61737-998-7_15

Winter, G. (1884). Repertorium. Rabenhorstii fungi europaei et extraeuraopaei Cent. XXXI et XXXII. *Hedwigia*, *23*, 164–172.

Zhang, L., Ni, H., Du, X., Wang, S., Ma, X. W., Nürnberger, T., Guo, H. S., & Hua, C. (2017). The Verticillium-specific protein VdSCP7 localizes to the plant nucleus and modulates immunity to fungal infections. *New Phytologist*, *215*(1), 368–381. https://doi.org/10.1111/nph.14537

Appendices

APPENDIX A. Construction of primers for cloning experiments (a) construction of the primers to be recombined in the plasmid with the tag in C-terminal (b) construction of the primers to be recombined in the plasmid with the tag in N-terminal

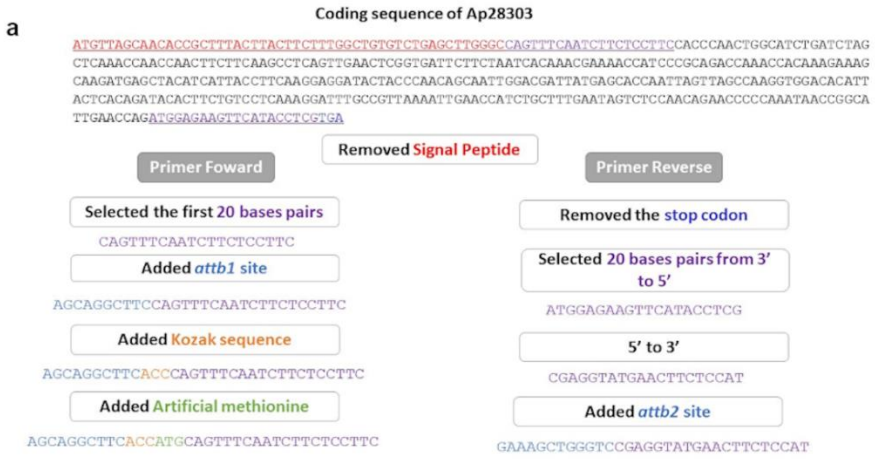

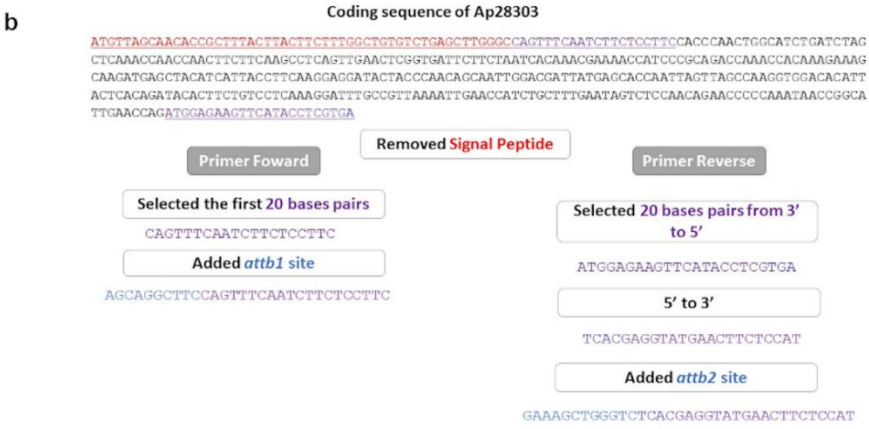

APPENDIX B. List of primers used in cloning experiments

Effector candidate	Primer Forward (5'-3')	Primer Reverse (5'-3')
Ap30385 (C-terminal)	AGCAGGCTTCACCATGATCGATCCAACGATTTTAATCG	GAAAGCTGGGTCGATAAACTCAAAATAGTCCTTTC
Ap28303 (C-terminal)	AGCAGGCTTCACCATGCAGTTTCAATCTTCTCCTTC	GAAAGCTGGGTCCGAGGTATGAACTTCTCCAT
Ap30385 (N-terminal)	AGCAGGCTTCACCATCGATCCAACGATTTTAATCG	GAAAGCTGGGTCTCAGATAAACTCAAAATAGTCCTTTC
Ap28303 (N-terminal)	AGCAGGCTTCCAGTTTCAATCTTCTCCTTC	GAAAGCTGGGTCTCACGAGGTATGAACTTCTCCAT
attb	GGGGACAAGTTTGTACAAAAAAGCAGGCT	GGGGACCACTTTGTACAAGAAAGCTGGGT
M13	GTAAAACGACGGCCAG	CAGGAAACAGCTATGAC

attb site; Kozak sequence; Artificial methionine; Stop codon

APPENDIX C. List of 255 effector candidates, subcellular localization predicted by LocTree3 and their functional description by Blast2GO and validated in UniProt

ID sequence	Localization class	Description
evm.model.NODE_10061_length_10145_cov_0.0507087.1	cytoplasm	Alpha,alpha-trehalose-phosphate synthase (UDP-forming) *P. coronata var. avenae* f. sp. *avenae*
evm.model.NODE_10152_length_10096_cov_0.832481.1	secreted	Hypothetical protein *P. graminis* f. sp. *tritici*
evm.model.NODE_10225_length_10054_cov_0.703536.1	secreted	---NA---
evm.model.NODE_10347_length_9998_cov_1.27474.2	secreted	Hypothetical protein *P. striiformis* f. sp. *tritici* PST-78
evm.model.NODE_10399_length_9973_cov_17.2373.3	secreted	---NA---
evm.model.NODE_104004_length_2112_cov_1.66801.1	secreted	---NA---
evm.model.NODE_10462_length_9942_cov_1.10912.2	secreted	Hypothetical protein *P. sorghi*
evm.model.NODE_10530_length_9908_cov_0.717514.4	secreted	---NA---
evm.model.NODE_10569_length_9889_cov_0.720242.1	secreted	Hypothetical protein *P. graminis* f. sp. *tritici*
evm.model.NODE_105_length_55253_cov_0.45355.1	secreted	---NA---
evm.model.NODE_1060_length_27712_cov_0.666751.1	secreted	---NA---
evm.model.NODE_1074_length_27621_cov_1.26717.2	secreted	---NA---
evm.model.NODE_11108_length_9646_cov_0.920475.1	cytoplasm	Chorismate mutase domain-containing protein *P. coronata* var. *avenae* f. sp. *avenae*
evm.model.NODE_11112_length_9643_cov_0.62768.1	secreted	Hypothetical protein *P. graminis* f. sp. *tritici*
evm.model.NODE_11176_length_9608_cov_0.896003.1	secreted	---NA---
evm.model.NODE_11209_length_9589_cov_0.266751.1	secreted	Hypothetical protein *P. graminis* f. sp. *tritici*
evm.model.NODE_11232_length_9577_cov_1.54677.3	secreted	Hypothetical protein *P. graminis* f. sp. *tritici*

evm.model.NODE_11274_length_9557_cov_0.67561.2	secreted	Hypothetical protein *P. graminis* f. sp. *tritici*
evm.model.NODE_11428_length_9490_cov_0.763695.1	secreted	Hypothetical protein *M. larici-populina*
evm.model.NODE_114746_length_1891_cov_0.502268.1	secreted	---NA---
evm.model.NODE_11687_length_9385_cov_1.54699.2	secreted	---NA---
evm.model.NODE_1172_length_26737_cov_0.188193.1	secreted	Hypothetical protein *P. sorghi*
evm.model.NODE_11786_length_9347_cov_1.30542.1	secreted	SCP domain-containing protein *P. coronata* var. *avenae* f. sp. *avenae*
evm.model.NODE_11794_length_9343_cov_0.50255.1	secreted	Secreted protein *M. larici-populina*
evm.model.NODE_11912_length_9294_cov_0.491655.1	secreted	---NA---
evm.model.NODE_11_length_86909_cov_0.133459.3	secreted	---NA---
evm.model.NODE_12087_length_9232_cov_0.709061.1	secreted	---NA---
evm.model.NODE_12169_length_9205_cov_0.451481.1	secreted	---NA---
evm.model.NODE_12191_length_9196_cov_0.891534.1	secreted	---NA---
evm.model.NODE_12201_length_9196_cov_0.656302.1	secreted	---NA---
evm.model.NODE_123330_length_1735_cov_1.20522.1	secreted	---NA---
evm.model.NODE_12491_length_9093_cov_0.505688.1	secreted	Hypothetical protein *P. sorghi*
evm.model.NODE_12507_length_9082_cov_0.159058.2	secreted	Protein ROT1 *M. larici-populina*
evm.model.NODE_12611_length_9049_cov_0.544945.3	secreted	Hypothetical protein *P. graminis* f. sp. *tritici*
evm.model.NODE_127356_length_1668_cov_0.0661908.1	secreted	---NA---
evm.model.NODE_12741_length_9006_cov_0.176484.1	secreted	---NA---
evm.model.NODE_12743_length_9006_cov_0.699628.1	secreted	Tnp4 domain-containing protein *P. striiformis*

evm.model.NODE_12793_length_8993_cov_0.571622.3	secreted	---NA---
evm.model.NODE_128173_length_1656_cov_0.691302.1	secreted	---NA---
evm.model.NODE_131451_length_1605_cov_1.44655.1	secreted	---NA---
evm.model.NODE_133257_length_1578_cov_1.36527.1	secreted	---NA---
evm.model.NODE_13415_length_8785_cov_0.517672.2	secreted	---NA---
evm.model.NODE_13447_length_8775_cov_0.4493.2	secreted	---NA---
evm.model.NODE_135553_length_1546_cov_1.04299.1	secreted	---NA---
evm.model.NODE_135553_length_1546_cov_1.04299.2	secreted	---NA---
evm.model.NODE_13633_length_8716_cov_0.215275.1	secreted	---NA---
evm.model.NODE_13647_length_8711_cov_0.688956.4	secreted	Hypothetical protein *P. graminis* f. sp. *tritici*
evm.model.NODE_13752_length_8677_cov_0.852865.1	secreted	SCP domain-containing protein *P. coronata* var. *avenae* f. sp. *avenae*
evm.model.NODE_13755_length_8677_cov_0.62.1	secreted	Hypothetical protein *P. striiformis*
evm.model.NODE_13939_length_8621_cov_1.12668.3	secreted	---NA---
evm.model.NODE_139_length_51599_cov_0.560033.2	secreted	Hypothetical protein *P. coronata* var. *avenae* f. sp. *avenae*
evm.model.NODE_1401_length_25092_cov_0.323334.1	secreted	---NA---
evm.model.NODE_14121_length_8545_cov_0.464531.1	secreted	Secreted protein *M. larici-populina*
evm.model.NODE_14478_length_8456_cov_1.05451.2	secreted	---NA---
evm.model.NODE_14556_length_8430_cov_0.588582.2	secreted	---NA---
evm.model.NODE_14970_length_8304_cov_0.597261.1	secreted	---NA---
evm.model.NODE_15002_length_8298_cov_0.549137.1	secreted	---NA---

evm.model.NODE_15054_length_8284_cov_1.25043.1	secreted	Secreted protein *M. larici-populina*
evm.model.NODE_150611_length_1345_cov_0.1	cytoplasm	Secreted protein *M. larici-populina*
evm.model.NODE_15174_length_8249_cov_0.443487.1	nucleus	---NA---
evm.model.NODE_1521_length_24252_cov_1.0121.1	cytoplasm	---NA---
evm.model.NODE_15340_length_8203_cov_0.106625.1	secreted	---NA---
evm.model.NODE_15375_length_8185_cov_0.378348.2	secreted	---NA---
evm.model.NODE_1543_length_24159_cov_0.485562.1	secreted	---NA---
evm.model.NODE_154410_length_1299_cov_0.384812.1	secreted	---NA---
evm.model.NODE_15472_length_8166_cov_1.05996.1	secreted	Hypothetical protein *P. triticina*
evm.model.NODE_15519_length_8153_cov_0.999377.2	secreted	---NA---
evm.model.NODE_15626_length_8122_cov_1.19235.1	secreted	---NA---
evm.model.NODE_15688_length_8108_cov_1.01428.1	cytoplasm	Chitin deacetylase *P. graminis* f. sp. *tritici*
evm.model.NODE_15804_length_8083_cov_0.214429.1	secreted	Hypothetical protein *P. coronata* var. *avenae* f. sp. *avenae*
evm.model.NODE_15944_length_8047_cov_1.14973.1	secreted	---NA---
evm.model.NODE_1600_length_23783_cov_1.50397.5	secreted	---NA---
evm.model.NODE_161229_length_1221_cov_4.3766.1	nucleus	Hypothetical protein *P. sorghi*
evm.model.NODE_16422_length_7909_cov_0.220044.1	secreted	---NA---
evm.model.NODE_16423_length_7930_cov_0.859926.2	secreted	---NA---
evm.model.NODE_16665_length_7877_cov_0.280351.1	secreted	---NA---
evm.model.NODE_16670_length_7878_cov_1.91511.2	secreted	---NA---

evm.model.NODE_167661_length_1151_cov_0.768555.1	secreted	---NA---
evm.model.NODE_16776_length_7854_cov_0.763427.3	secreted	---NA---
evm.model.NODE_17047_length_7793_cov_0.273379.1	vacuole	SCP domain-containing protein *P. striiformis*
evm.model.NODE_17070_length_7788_cov_0.437671.1	secreted	Hypothetical protein *P. striiformis* f. sp. *tritici*
evm.model.NODE_1717_length_23147_cov_0.744494.2	secreted	---NA---
evm.model.NODE_17345_length_7727_cov_0.360395.1	secreted	---NA---
evm.model.NODE_17377_length_7721_cov_0.241375.1	secreted	---NA---
evm.model.NODE_17418_length_7712_cov_0.404087.1	secreted	---NA---
evm.model.NODE_17469_length_7699_cov_0.658743.1	secreted	---NA---
evm.model.NODE_1747_length_22938_cov_1.23273.1	secreted	---NA---
evm.model.NODE_17596_length_7670_cov_0.351982.1	secreted	Carboxylic ester hydrolase *Helicocarpus griseus*
evm.model.NODE_1768_length_22731_cov_0.761502.2	secreted	---NA---
evm.model.NODE_17742_length_7635_cov_0.85895.1	cytoplasm	Chitin deacetylase *M. larici-populina*
evm.model.NODE_17766_length_7629_cov_0.216742.1	secreted	---NA---
evm.model.NODE_17812_length_7621_cov_1.97278.4	secreted	Hypothetical protein *P. striiformis*
evm.model.NODE_17921_length_7595_cov_0.373058.1	secreted	---NA---
evm.model.NODE_18659_length_7423_cov_1.75308.2	vacuole	---NA---
evm.model.NODE_18795_length_7393_cov_0.537022.1	secreted	---NA---
evm.model.NODE_18838_length_7381_cov_0.855114.1	secreted	Hypothetical protein *P. graminis* f. sp. *tritici*
evm.model.NODE_19449_length_7248_cov_1.41983.2	secreted	---NA---

evm.model.NODE_20012_length_7131_cov_0.803969.1	secreted	---NA---
evm.model.NODE_20016_length_7129_cov_0.858183.1	secreted	---NA---
evm.model.NODE_20061_length_7120_cov_1.91105.4	secreted	---NA---
evm.model.NODE_20239_length_7088_cov_0.730068.1	secreted	Hypothetical protein *P. coronata* var. *avenae* f. sp. *avenae*
evm.model.NODE_20426_length_7056_cov_0.480445.1	secreted	---NA---
evm.model.NODE_20451_length_7051_cov_0.568602.1	secreted	---NA---
evm.model.NODE_20477_length_7046_cov_0.544154.1	secreted	---NA---
evm.model.NODE_20576_length_7027_cov_1.6387.2	secreted	---NA---
evm.model.NODE_2061_length_21333_cov_0.314864.1	secreted	---NA---
evm.model.NODE_20670_length_7007_cov_0.489971.1	secreted	Hypothetical protein *P. graminis* f. sp. *tritici*
evm.model.NODE_20733_length_6994_cov_1.04733.1	secreted	---NA---
evm.model.NODE_2075_length_21285_cov_0.389734.2	secreted	Hypothetical protein *P. graminis* f. sp. *tritici*
evm.model.NODE_2099_length_21180_cov_0.647858.3	secreted	---NA---
evm.model.NODE_21040_length_6916_cov_0.875441.2	secreted	Hypothetical protein *P. graminis* f. sp. *tritici*
evm.model.NODE_2137_length_21017_cov_0.479943.1	secreted	Hypothetical protein *P. coronata* var. *avenae* f. sp. *avenae*
evm.model.NODE_21468_length_6852_cov_0.295613.1	secreted	---NA---
evm.model.NODE_214_length_45606_cov_0.34733.1	nucleus	---NA---
evm.model.NODE_215_length_45608_cov_0.342099.2	secreted	Hypothetical protein *M. larici-populina*
evm.model.NODE_2160_length_20942_cov_0.93375.2	secreted	NA
evm.model.NODE_21744_length_6797_cov_0.678561.2	secreted	Hypothetical protein *P. sorghi*

evm.model.NODE_21756_length_6789_cov_0.714179.1	secreted	---NA---
evm.model.NODE_21773_length_6791_cov_0.847539.1	secreted	---NA---
evm.model.NODE_22544_length_6661_cov_0.699265.1	secreted	---NA---
evm.model.NODE_2266_length_20454_cov_0.872091.3	secreted	---NA---
evm.model.NODE_22848_length_6612_cov_1.14079.1	secreted	---NA---
evm.model.NODE_2287_length_20383_cov_0.512243.1	secreted	---NA---
evm.model.NODE_23109_length_6569_cov_0.855324.2	secreted	---NA---
evm.model.NODE_23344_length_6532_cov_0.712769.1	secreted	---NA---
evm.model.NODE_23552_length_6500_cov_0.90805.1	secreted	---NA---
evm.model.NODE_24357_length_6382_cov_0.354117.1	secreted	---NA---
evm.model.NODE_2496_length_19561_cov_0.842996.3	secreted	Hypothetical protein *P. coronata* var. *avenae* f. sp. *avenae*
evm.model.NODE_25339_length_6259_cov_1.47048.2	nucleus	---NA---
evm.model.NODE_2556_length_19410_cov_0.342789.1	secreted	Hypothetical protein *P. coronata* var. *avenae* f. sp. *avenae*
evm.model.NODE_25723_length_6213_cov_1.77834.1	secreted	---NA---
evm.model.NODE_25911_length_6188_cov_0.873618.2	secreted	---NA---
evm.model.NODE_262_length_42745_cov_0.94878.1	secreted	---NA---
evm.model.NODE_2638_length_19144_cov_0.79755.1	secreted	Sod_Cu domain-containing protein *P. graminis* f. sp. *tritici*
evm.model.NODE_2644_length_19126_cov_0.597874.1	secreted	Hypothetical protein *P. triticina*
evm.model.NODE_26533_length_6113_cov_2.23154.2	secreted	---NA---
evm.model.NODE_26623_length_6099_cov_0.992802.1	cytoplasm	Chitin deacetylase *P. graminis* f. sp. *tritici*

evm.model.NODE_26741_length_6086_cov_0.331096.1	secreted	---NA---
evm.model.NODE_27074_length_6045_cov_1.07722.1	secreted	---NA---
evm.model.NODE_2715_length_18873_cov_0.615565.1	secreted	---NA---
evm.model.NODE_2770_length_18665_cov_1.63449.1	secreted	Hypothetical protein *P. graminis* f. sp. *tritici*
evm.model.NODE_27877_length_5954_cov_0.473314.1	secreted	---NA---
evm.model.NODE_28014_length_5936_cov_0.422104.1	secreted	---NA---
evm.model.NODE_28303_length_5903_cov_0.666551.1	nucleus	Inhibitor I9 domain-containing protein
evm.model.NODE_2856_length_18375_cov_1.15493.1	secreted	---NA---
evm.model.NODE_28608_length_5870_cov_0.279122.1	secreted	Secreted protein *M. larici-populina*
evm.model.NODE_28763_length_5852_cov_0.907265.1	secreted	---NA---
evm.model.NODE_2876_length_18335_cov_0.47221.3	secreted	---NA---
evm.model.NODE_29272_length_5795_cov_1.39132.1	secreted	Lipase_3 domain-containing protein *P. striiformis* f. sp. *tritici*
evm.model.NODE_2985_length_18064_cov_0.808674.5	cytoplasm	---NA---
evm.model.NODE_30167_length_5704_cov_0.64246.1	secreted	---NA---
evm.model.NODE_30292_length_5692_cov_0.54583.1	secreted	---NA---
evm.model.NODE_30385_length_5682_cov_0.453105.1	nucleus	Hypothetical protein *P. graminis* f. sp. *tritici*
evm.model.NODE_30437_length_5676_cov_0.30474.1	secreted	---NA---
evm.model.NODE_30470_length_5673_cov_1.08186.1	secreted	---NA---
evm.model.NODE_30484_length_5672_cov_0.655005.1	cytoplasm	Sod_Cu domain-containing protein *P. graminis* f. sp. *tritici*
evm.model.NODE_306_length_40808_cov_0.610555.1	secreted	---NA---

evm.model.NODE_31145_length_5605_cov_0.239321.1	endoplasmic reticulum membrane	Hypothetical protein *P. graminis* f. sp. *tritici*
evm.model.NODE_31334_length_5585_cov_0.0443386.1	secreted	---NA---
evm.model.NODE_31345_length_5584_cov_0.223016.1	secreted	Dimer_Tnp_hAT domain-containing protein
evm.model.NODE_31408_length_5577_cov_0.620367.1	secreted	---NA---
evm.model.NODE_31568_length_5559_cov_0.333211.1	secreted	---NA---
evm.model.NODE_31591_length_5557_cov_0.401105.1	secreted	Hypothetical protein *P. coronata* var. *avenae* f. sp. *avenae*
evm.model.NODE_31592_length_5557_cov_0.88232.1	nucleus	Hypothetical protein *P. coronata* var. *avenae* f. sp. *avenae*
evm.model.NODE_31678_length_5549_cov_0.815382.1	secreted	---NA---
evm.model.NODE_3255_length_17366_cov_0.286377.1	secreted	---NA---
evm.model.NODE_32908_length_5423_cov_1.11782.2	secreted	Hypothetical protein *P. graminis* f. sp. *tritici*
evm.model.NODE_33375_length_5373_cov_1.81395.1	nucleus	---NA---
evm.model.NODE_33392_length_5371_cov_0.889207.2	secreted	---NA---
evm.model.NODE_33603_length_5352_cov_1.82086.2	secreted	Alpha-galactosidase *P. graminis* f. sp. *tritici*
evm.model.NODE_33895_length_5326_cov_0.483362.1	secreted	---NA---
evm.model.NODE_33933_length_5321_cov_0.561995.1	secreted	---NA---
evm.model.NODE_3408_length_16981_cov_1.40977.3	secreted	Hypothetical protein *P. graminis* f. sp. *tritici*
evm.model.NODE_34254_length_5289_cov_0.923867.1	secreted	---NA---
evm.model.NODE_3425_length_16954_cov_1.12177.2	secreted	---NA---
evm.model.NODE_34381_length_5277_cov_0.283883.1	secreted	---NA---
evm.model.NODE_34818_length_5238_cov_0.799452.1	secreted	Hypothetical protein *P. triticina*

evm.model.NODE_34859_length_5234_cov_0.768357.1	secreted	---NA---
evm.model.NODE_3491_length_16812_cov_1.27576.3	secreted	---NA---
evm.model.NODE_35022_length_5219_cov_0.809505.2	secreted	---NA---
evm.model.NODE_35140_length_5210_cov_0.691324.1	secreted	---NA---
evm.model.NODE_35185_length_5204_cov_1.13098.1	secreted	---NA---
evm.model.NODE_35347_length_5190_cov_0.343935.1	secreted	---NA---
evm.model.NODE_35350_length_5186_cov_0.240221.1	secreted	---NA---
evm.model.NODE_354_length_39246_cov_0.895862.1	secreted	---NA---
evm.model.NODE_3559_length_16610_cov_0.298914.1	secreted	---NA---
evm.model.NODE_35654_length_5164_cov_0.948978.1	cytoplasm	Hypothetical protein *P. coronata* var. *avenae* f. sp. *avenae*
evm.model.NODE_36327_length_5104_cov_0.212578.1	secreted	Hypothetical protein *P. striiformis* f. sp. *tritici*
evm.model.NODE_36746_length_5068_cov_0.660393.1	mitochondrion	Alpha/Beta hydrolase protein *Pseudomassariella vexata*
evm.model.NODE_37124_length_5036_cov_1.03585.1	secreted	---NA---
evm.model.NODE_3753_length_16153_cov_0.416838.1	secreted	---NA---
evm.model.NODE_3763_length_16150_cov_0.576671.1	secreted	---NA---
evm.model.NODE_37766_length_4983_cov_0.484349.1	chloroplast	---NA---
evm.model.NODE_38089_length_4957_cov_0.561698.1	endoplasmic reticulum	Thioredoxin domain-containing protein *P. triticina*
evm.model.NODE_38840_length_4894_cov_1.57562.1	secreted	---NA---
evm.model.NODE_38995_length_4882_cov_1.60126.4	secreted	---NA---
evm.model.NODE_39546_length_4840_cov_0.859962.1	cytoplasm	---NA---

evm.model.NODE_4004_length_15711_cov_0.468848.2	plasma membrane	---NA---
evm.model.NODE_40050_length_4800_cov_0.812326.1	secreted	Hypothetical protein *P. graminis* f. sp. *tritici*
evm.model.NODE_40251_length_4784_cov_0.630878.1	secreted	Hypothetical protein *Aspergillus wentii*
evm.model.NODE_41125_length_4715_cov_0.45728.1	secreted	---NA---
evm.model.NODE_41221_length_4707_cov_0.434061.2	secreted	---NA---
evm.model.NODE_41239_length_4704_cov_0.740991.1	secreted	---NA---
evm.model.NODE_41885_length_4657_cov_0.907506.1	secreted	Hypothetical protein *P. sorghi*
evm.model.NODE_41959_length_4652_cov_0.226519.2	secreted	---NA---
evm.model.NODE_42552_length_4612_cov_0.33913.1	secreted	Hypothetical protein *M. larici-populina*
evm.model.NODE_42655_length_4604_cov_0.279875.1	secreted	Secreted protein *M. larici-populina*
evm.model.NODE_4272_length_15245_cov_1.3394.7	secreted	Hypothetical protein *P. coronata* var. *avenae* f. sp. *avenae*
evm.model.NODE_4275_length_15239_cov_1.17988.2	cytoplasm	---NA---
evm.model.NODE_42799_length_4595_cov_0.305282.1	secreted	---NA---
evm.model.NODE_4300_length_15213_cov_1.43309.2	secreted	---NA---
evm.model.NODE_43077_length_4576_cov_0.219825.1	secreted	Hypothetical protein *P. coronata* var. *avenae* f. sp. *avenae*
evm.model.NODE_4319_length_15189_cov_1.76232.5	secreted	---NA---
evm.model.NODE_4319_length_15189_cov_1.76232.8	secreted	---NA---
evm.model.NODE_4351_length_15142_cov_1.48465.1	secreted	---NA---
evm.model.NODE_43844_length_4524_cov_1.04298.2	secreted	---NA---
evm.model.NODE_44175_length_4501_cov_0.595107.1	mitochondrion	Hypothetical protein *P. striiformis* f. sp. *tritici*

evm.model.NODE_4428_length_15041_cov_0.398283.1	secreted	---NA---
evm.model.NODE_4445_length_15006_cov_0.703475.2	secreted	---NA---
evm.model.NODE_44719_length_4465_cov_1.06524.2	secreted	---NA---
evm.model.NODE_47016_length_4308_cov_0.743902.1	secreted	DPBB_1 domain-containing protein *P. striiformis* f. sp. *tritici*
evm.model.NODE_471_length_36147_cov_0.628061.4	secreted	Hypothetical protein *P. graminis* f. sp. *tritici*
evm.model.NODE_47265_length_4293_cov_0.247.1	secreted	Hypothetical protein *P. striiformis* f. sp. *tritici*
evm.model.NODE_47421_length_4284_cov_0.770026.1	secreted	---NA---
evm.model.NODE_47468_length_4281_cov_0.437891.1	secreted	---NA---
evm.model.NODE_47864_length_4256_cov_0.806733.1	secreted	---NA---
evm.model.NODE_48455_length_4220_cov_0.780601.1	secreted	---NA---
evm.model.NODE_487_length_35803_cov_0.914396.3	secreted	---NA---
evm.model.NODE_49333_length_4167_cov_0.681188.1	secreted	Hypothetical protein *P. coronata* var. *avenae* f. sp. *avenae*
evm.model.NODE_4936_length_14262_cov_0.336753.1	secreted	DPBB_1 domain-containing protein
evm.model.NODE_49674_length_4146_cov_0.940035.1	secreted	---NA---
evm.model.NODE_4_length_99494_cov_0.351008.4	secreted	---NA---
evm.model.NODE_5026_length_14122_cov_0.672621.3	secreted	---NA---
evm.model.NODE_50324_length_4107_cov_0.0743719.1	secreted	Secreted protein *M. larici-populina*
evm.model.NODE_50423_length_4101_cov_1.02718.1	secreted	Hypothetical protein *Talaromyces marneffei*
evm.model.NODE_51001_length_4068_cov_1.38848.1	secreted	---NA---
evm.model.NODE_51346_length_4048_cov_2.22494.1	secreted	---NA---

evm.model.NODE_5144_length_13967_cov_0.811199.2	secreted	---NA---
evm.model.NODE_5174_length_13932_cov_0.457081.3	cytoplasm	Hypothetical protein *P. striiformis* f. sp. *tritici*
evm.model.NODE_5238_length_13853_cov_0.473956.1	secreted	---NA---
evm.model.NODE_52873_length_3961_cov_0.143453.1	secreted	Hypothetical protein *P. graminis* f. sp. *tritici*
evm.model.NODE_53034_length_3952_cov_1.53203.1	secreted	Hypothetical protein *P. striiformis* f. sp. *tritici*
evm.model.NODE_5371_length_13696_cov_0.641241.1	secreted	---NA---
evm.model.NODE_53733_length_3913_cov_1.12097.1	cytoplasm	Hypothetical protein *P. sorghi*
evm.model.NODE_54407_length_3875_cov_0.682836.1	secreted	---NA---
evm.model.NODE_54623_length_3866_cov_0.69671.1	cytoplasm	Hypothetical protein *P. coronata* var. *avenae* f. sp. *avenae*
evm.model.NODE_55075_length_3839_cov_0.0344828.1	secreted	SurE domain-containing protein *P. graminis* f. sp. *tritici*
evm.model.NODE_55497_length_3818_cov_1.60634.1	cytoplasm	Hypothetical protein *P. graminis* f. sp. *tritici*
evm.model.NODE_5556_length_13483_cov_0.842554.2	secreted	---NA---
evm.model.NODE_55_length_65597_cov_0.286605.1	secreted	Phosphatidylglycerol/phosphatidylinositol transfer protein *P. graminis* f. sp. *tritici*
evm.model.NODE_5615_length_13416_cov_0.518602.2	secreted	---NA---
evm.model.NODE_5695_length_13335_cov_0.919443.1	secreted	---NA---
evm.model.NODE_5720_length_13298_cov_0.474148.1	secreted	---NA---
evm.model.NODE_573_length_34048_cov_0.387171.1	secreted	---NA---
evm.model.NODE_57798_length_3696_cov_0.819277.1	secreted	---NA---

APPENDIX D. Sequences of 7 effector candidates validated in this work

>evm.model.NODE_11108_length_9646_cov_0.920475.1
MLMILLPIYLFALSALGASCSDPSAKLSSVPSSTSLSLPLDQQHDSRCFTTPQTDYGPTVDLNGQPVRYGPKENT
SYAPKTRTNSSDPVWGQPTIRFANGSSCCQHLSQVREYIDYLDETIVKYLSIRQQFVVEAGRFKASKQEVRAPPR
AVGVVKNAQAIAQKVGLAPWVAQVSYTALLNSFVELELCLFDEDVAKKNFAPHP
>evm.model.NODE_12491_length_9093_cov_0.505688.1
MFSFSLLTLFSAFFLAPTLVVLRKSTAGVELPDDPKAKVKVYSTAKMDLWNRKHSNWTWTLDGNNDFRIVTGYDR
VGWFGAYVNNSMQHRTLNVKIRSGLMHCGRSQTYFVNVTDASQNVIEQFNFKINTRGPLIDNWRLLNGTRLKSSY
VWGRGWRTLSGDIRREKKGPEVAHIHCGNDALNCSIYTNDEIPIDYLIALHTSGNVREAFCNF
>evm.model.NODE_15054_length_8284_cov_1.25043.1
MMGSLNQLVHLAFFLAAMATSIGAASSPQTLKCTTFDKRTTATAACNDVRGSRCSHGCTSQIVAKQCKHNNIGPD
SEENCTFAFGKSTAYSYTCINEKGSYTCTGKTSGVATCKGCTFPN
>evm.model.NODE_2160_length_20942_cov_0.93375.2
MLSISLLTLLGAFLAPTLVLLKKSTDDIDLPDNPNAQVKVYHTKKHCVYGDKSGNWTWTLEGAPELKIPGGYTTK
GGFQAYVNNEMSDKITTITARVC
>evm.model.NODE_23389_length_6527_cov_0.825156.1
MHSSALLTFSMTVVCSTVLATPAPQFGPAGFGGGQYSNGQFGNGGYANGGFGNGGFNQGFNGGAERNGGQGSSSS
FSQSSGQSSQSSGGNAGGFLSGLSNGYGNGGFNNYGNRNGGGYFRNNQLGGFGNGFGGYGNGFGGYGNGFGGVGG
GYGLGPGGGFGGPFNRFGGGFGGPGLGGGFGGPGFGGPGLGGGFGGRLYRRQVSTDEPDSPDSILSTTFTKTPKT
IASTQTKVQSSAVPHPTHHAVIIPDKDSHHSLDAVQTAM
>evm.model.NODE_30385_length_5682_cov_0.453105.1
MLAIILLLIIIHSIDPTILIETSSTNQVNSINHISNQSNPINQSNRSLSTTNYLCRPIGPCLPCTSQELTSPVCE
VYHNKRLVNCLDQSSSTILQRSEDIIKASDQNKLDNGLSKVEFQTWEACERVISQERKDYFEFI
>evm.model.NODE_28303_length_5903_cov_0.666551.1
MLATPLYLLLWLCLSLGQFQSSPSTQLASDLAQTNQLLQASVELGDSSNHKRKPSRRPNHKESKMSYIITFKEDT
TQQQLDDYEHQLVSQGGHITHRYTSVLKGFAVKIEPSALNSLQQNPQITGIEPDGEVHTS

3 CHAPTER 2 – COMPARISON OF EFFECTOR CANDIDATE PROTEINS FROM THREE BIOTYPES OF *Austropuccinia psidii*

ABSTRACT

Austropuccinia psidii is a biotrophic rust fungus that infects plants of the Myrtaceae family. First reported on guava in Brazil in 1884, it has since been reported to infect many other myrtaceous species and has spread globally. Several biotypes of *A. psidii* have been identified that differ in host range. In 2010, myrtle rust was detected in Australia, the centre of origin for the majority of Myrtaceae species. A Brazilian biotype (MF-1) is known to successfully infect *Eucalyptus* species, while the Australian pandemic (Au) and the South African (SA) biotypes infect distinct Myrtaceae species. Little is known about the complex pathogen-host interactions underlying myrtle rust. Proteins secreted into hosts by rust pathogens, termed effectors, are acknowledged to be fundamental for their pathogenicity, thus investigate these proteins may help understand mechanism involved in pathogen-host interaction. We predicted the effector candidates for each biotype and identified polymorphisms to be validated by PCR. We computationally predicted the effector candidates of three *A. psidii* biotypes: Au (di-haploid), SA (diploid), and MF-1 (diploid), estimated at 671, 365, and 282 candidates for each, respectively. We found 269 effector candidates with the strongest evidence of homology among the three biotypes, Au and MF-1 biotypes shared 351 of effector candidates, Au and SA biotypes shared 397, and MF-1 and SA shared 161. We also performed an orthology analysis and identified the SA and MF-1 biotypes closest, concerning effector candidates. The Au biotype showed a greater number of unique protein clusters compared to other biotypes. Our findings showed differences related to the number of effector candidates, however, no differences concerning effector localizations, and the most effector candidates have no predicted functional annotation. The localization prediction *in silico* showed a percentage similar to effector candidates from the biotypes targeting apoplast, nucleus, mitochondria, and chloroplasts. The effector candidates showed polymorphisms by PCR validation, however, supplementary studies are necessary to comprehend the implication of that to host variability.

Keywords: Secreted proteins; Myrtle rust; Effectoromic; Comparative genomic analyses; Pandemic biotype; *Eucalyptus* rust; Obligate pathogens

3.1 Introduction

Austropuccinia psidii (G. Winter) Beenken comb. nov. (Beenken, 2017) is a biotrophic fungus, the causal agent of myrtle rust, considered native of South America (Coutinho et al., 1998; Glen et al., 2007). The first report of this pathogen was in Brazil infecting guava (*Psidium guajava* L.) and named *Puccinia psidii* in 1884 (Winter, 1884). Just in 1912 *A. psidii* was detected in *Eucalyptus* (Joffily, 1944). Since first reported in Brazil, *A. psidii* spread quickly to neighbouring countries Paraguay and Uruguay (Carnegie & Pegg, 2018; Spegazzini, 1884), and is now worldwide spread (Carnegie & Pegg, 2018). Despite efforts to minimise the incursion of myrtle rust into Australia, in 2010 the pandemic biotype was detected in New South Wales (Carnegie et al., 2010). It was reported a single genotype in Australia

(Sandhu et al., 2016), the pandemic biotype, and appears to be the same found in Hawaii and New Caledonia (Machado et al., 2015; Sandhu et al., 2016; Stewart et al., 2018). In 2013, *A. psidii* was first reported in South Africa (Roux et al., 2013) and by 2016 was considered widespread, and pieces of evidence indicate only one genotype affecting native and non-native genera and species of Myrtaceae (Roux et al., 2016). The pathogen is a major threat to biodiversity in Australia since the country hosts 2,280 myrtaceous species (Berthon et al., 2018) among the 5,950 globally described (Christenhusz & Byng, 2016). In Australia, 232 species from natural infection and 115 from artificial inoculation were known to be affected by the pandemic biotype (Carnegie et al., 2016). In South Africa, the genotype infects non-native species (*Myrtus communis* and *Backhousia citriodora*) and native species (*Eugenia erythrophyllum, E. verdoornii*, *Heteropyxis canescens, H. natalanesis*, *Syzygium cordatum, S. legatii*) with different degrees of susceptibility (Roux et al., 2016). The South African biotype apparently is genetically unrelated to currently genotyped biotypes (Roux et al., 2016). In Brazil, there is the highest genetic variability among the *A. psidii* populations (Quecine et al., 2014; Stewart et al., 2018). The MF-1 biotype was collected from eucalypt plants in Brazil, and it appears to be more selective to *Eucalyptus* species (Leite, 2012; unpublished data).

Despite its global impact and wide host range, *A. psidii* genome was only recently available, to knowledge biotrophic fungi in general have a large genome, with high repeat regions, and limitations related to DNA extraction, therefore genome sequencing and assembly are a challenge (McTaggart et al., 2018). Initially, it was estimated size of 103-145 Mb to *A. psidii* genome using paired-end sequences of 250 bp from Illumina MiSeq (Tan et al., 2014). McTaggart et al. (2018) used Chromium 10X Library to sequence and assembly the South African biotype genome, to overcome the biotrophic fungi limitations. This technology was efficient to sequence 1.2 Gb of this pathogen using a small quantity of DNA. Tobias et al. (2020) estimated the genome size 1.02 Gb of the pandemic biotype from Australia, sequenced by PacBio and scaffolds assembly by Hi-C technology. The authors observed more repetitive regions (>90%) when compared to other Pucciniales species genomes, and the large genome may be associated with expansion due to transposable elements from Gypsy family (Tobias et al., 2020). It was sequenced and assembled a 630 Mb genome of MF-1 biotype from Brazil, using a combination of sequence data from 454 Plataform, MiSeq (Illumina), SMRT (PacBio), and HiSeq 2.5 (Illumina) (unpublished data – deposited at NCBI, Accession Number: AVOT00000000). The size differences among the biotypes are probably associated with sequencing techniques used for each, and their limitations.

Beyond the information about the genomes and their variability, some biotypes have apparent host biological specificity, for example, the MF-1 strain appears to successful infect *Eucalyptus* species but not *Syzygium jambos* (unpublished data), also in Brazil, guava isolates did not infect successfully eucalyptus and *vice-versa* (Ferreira, 1983; Quecine et al., 2016). Quecine et al. (2014) based on physiological variability among *A. psidii* populations investigated the genetic diversity in populations isolated from guava, syzygium, jaboticaba and eucalypt. The results showed a higher level of diversity

in guava, jaboticaba and syzygium than eucalypt. These physiologic and genetic variabilities suggest an evolution of host-specific genotypes (Quecine et al., 2014).

To study the variability among pathogenic strains, information from the genome is useful to identify sequence variations, since there is selective pressure to avoid host recognition (Tsushima et al., 2019). To successfully infect the plant, phytopathogens must overcome the plant's defenses, one alternative is the use of effectors to avoid recognition (Jaswal et al., 2020), which is particularly essential to biotrophic pathogens because of their lifestyle. Effectors are described as molecules secreted by an organism, which modulate the functions and physiology of another organism (Dalio et al., 2017). Thus, the study of effector candidate genes has been useful to understand the interaction of rust-host (Lorrain, Petre, et al., 2018). Schwessinger et al. (2020) compared the whole genomic of two isolates from *Puccinia striiformis* f.sp. *tritici*, the causal agent of stripe rust of wheat. The authors observed that 30% of the predicted candidate effector genes were variable between the two isolates, which may explain host adaptation and different phenotypes. It was hypothesised the variations of effector candidates may be due to de novo evolution, horizontal gene transfer or gene loss after divergence (Tsushima et al., 2019) or mutations caused by small insertions and deletions, structural variations, and the move of transposable elements (Schwessinger et al., 2020). Moreover, for rust pathogens, the set of effectors used by *Puccinia* group may not be the same as *Melampsora* group, suggesting that the difference is associated with their ability to infect a distinct set of host species (Bruce et al., 2014).

Here, we hypothesized that the comparative analysis of those three biotypes may show a variation among candidate genes to effectors. The biotypes might request a wide and variable repertoire of effector candidates to overcome defense responses from different hosts. Therefore, in this study, we identified the effector candidates from the three biotypes, the South African (SA), the Brazilian (MF-1), and the Australian pandemic (Au). Then, we predicted their subcellular localization and functions. Some effectors were searched for polymorphisms (indels and SNPs), using bioinformatic tools to elucidate if the differences among the effectors would be connected to the several hosts affected by *A. psidii*. This is the first study comparing effector candidates from biotypes of *A. psidii*, and also the first detailed report of effector candidates from South African and Australian biotypes.

3.2 Materials and Methods

3.2.1 *Austropuccinia psidii* biotypes and biological material

Information about the genome from three biotypes of *A. psidii* was used in this work. The haploid genome of the Australian biotype is available under the BioSample: SAMEA6153110 and the di-haploid genome is available at doi.org/10.5281/zenodo.3567172 (Tobias et al., 2020). The diploid genome of the *A. psidii* biotype from South Africa is available under the BioSample: SAMN09635590 (McTaggart et al., 2018). The MF-1 biotype diploid genome is available under the BioSample:

SAMN17798859. The other biotypes used in this work are listed in Table 1. To simplify we referred to the biotypes as Au: the Australian pandemic biotype, SA: the South African biotype, MF-1: the Brazilian biotype from *E. grandis* (University of São Paulo), Bz: the Brazilian biotype from *E. grandis* (Federal University of Viçosa), Ja: the Brazilian biotype from *S. jambos* and Pi:the Brazilian biotype from *E. uniflora* (Table 1).

The Plant Breeding Institute at the University of Sydney provided the DNA from Au and Bz. The Au pandemic biotype was first isolated from *Agonis flexuosa*, then the susceptible host *S. jambos* (rose-apple) was used to increase the urediniospores for DNA extraction (Tobias et al., 2020). SA biotype was isolated from the *M. communis* tree in South Africa, and the DNA was extracted from urediniospores increased in *S. jambos* (McTaggart et al., 2018). The South African DNA was provided by Forestry and Agricultural Biotechnology Institute at the University of Pretoria. The Laboratory of Genetics of Microorganisms "Prof. João Lucio de Azevedo" at the University of São Paulo provided DNA from three biotypes of *A. psidii*. MF-1 biotype was isolated from a single pustule in *E. grandis* leaves (Leite, 2012), and the urediniospores were increased in the susceptible species of *E. grandis* M09D1 for DNA extraction. Urediniospores isolated from *S. jambos* and *E. uniflora* were collected in São Paulo state, Brazil, then DNA from these urediniospores was extracted using Fungi/Yeast Genomic DNA Isolation Kit (Norgen Biotek Corp.) following the manufacturer's instructions. Only the biotypes Ja (*S. jambos)* and Pi (*E. uniflora)* are not monopostular.

Table 1. List of information about genomes rusts used in this work

Fungi biotype	Host from	Country of Origin	Genome representation	Genome size	Sequencing Technology	BioSample
A. psidii (Au)	*Agonis flexuosa*	New South Wales - Australia	Full	1.02 Gb	Pacific BioScience SMRT® cells	SAMEA6153110 (Tobias et al., 2020)
A. psidii (MF-1)	*Eucalyptus spp.*	São Paulo - Brazil	Partial	630 Mb	454 Plataform Pacific BioScience SMRT® cells HiSeq; 10X	SAMN17798859*
A. psidii (SA)	*Myrtus communis*	South Africa	Full	1.2 Gb	Illumina HiSeq; 10X Chromium	SAMN09635590 (Alistair R. McTaggart, Duong, et al., 2018)
A. psidii (Bz)	*Eucalyptus grandis*	Minas Gerais - Brazil	-	-	-	-
A. psidii (Ja)	*Syzigium jambos*	São Paulo - Brazil	-	-	-	-
A. psidii (Pi)	*Eugenia uniflora*	São Paulo - Brazil	-	-	-	-
P. gramminis f. sp. *tritici*	wheat	Pennsylvania	Full	88.6 Mb	Sanger whole-genome shotgun strategy	SAMN00013043 (Duplessis et al., 2011)
P. striiformis f. sp. *tritici*	-	-	Full	83 Mb	PacBio	SAMN07430048*

- No information available
* Projects with no publication informed

3.2.2 Effector candidate's prediction, subcellular localization and functional analyses

The predicted proteins from the MF-1, Au and SA biotypes were used to predict the effector candidates. The amino acid sequences were submitted to SignalP 4.1 (Nielsen, 2017) to check the presence of peptide signal. The proteins with the presence of peptide signal were carried out in EffectorP 2.0 (Sperschneider., 2018) to check whether they are effector candidates or not.

The software LOCALIZER was used to predict the subcellular localization of the effector candidates from each biotype, using default parameters (Sperschneider et al., 2017). This machine learning method predicted the subcellular localization of effector proteins to nuclei, chloroplasts and mitochondria. The ApoplastP software was carried out to predict apoplastic effectors (Sperschneider et al., 2018).

The functional categorization was obtained by the Gene Ontology Consortium (GO) (Ashburner et al., 2000), the terms were derived from the Blast2GO software (Conesa et al., 2005), using the default parameters. The obtained annotations were previously simplified by GO Slim.

3.2.3 Comparative genomic analyses

The OrthoFinder version 2.2.7 (Emms & Kelly, 2018) was used to perform a phylogenetic tree using the coding sequence fasta file from *A. psidii* MF-1, Au, SA, *P. gramminis f. sp. tritici* and *P. striiformis f. sp. tritici* (Table 1). We also constructed a phylogenetic tree using the effector candidates fasta file to verify the similarity among the biotypes. The output newick file for the species rooted tree (based on orthogroups) for both the OrthoFinder trees (total proteins and effector candidates) were input into Dendroscope/3.0 to visualize. It was performed a Blast local with Au, MF-1 and SA biotypes effector candidates using e-value: 10^{-5}, the effector candidates were considered as homologs with identity $\geq$ 40% and e-value: 10^{-5}.

Effector candidates from the three biotypes were submitted to OrthoVenn2 (Xu et al., 2019) to estimate the orthologous clusters at the protein level. The results from Orthovenn2 are available at https://orthovenn2.bioinfotoolkits.net/task/result/92ac8cb420fb39438bedaaaa49277af2#blast-multiple-alignments.

3.2.4 Primer's design and PCR validation

We selected 9 effector candidates from the Au biotype, which presented or not homology to other biotypes, to validated polymorphisms by PCR. OligoPerfect (https://apps.thermofisher.com/apps/oligoperfect/#!/design) was used to design the primers to 9 effector

candidates selected from Au biotype (Table 2). The parameters used were primer size: 18-24; primer Tm (°C): 52-58; primer GC (%): 40-60, and to generated amplicons at least with 200 pb. Then, the primers were verified in the Au genome sequence to check for introns and exons, and the size of the amplicon generated.

Table 2. List of primers from the effector candidates used in this work

Effector candidate	Primer Forward (5'-3')	Primer Reverse (5'-3')	Reference
APSI_P006.9475.t1	GGAGTACTCATTCTACGGAAAT	GTAGAGAGGATGAGAGACAAAA	This study
APSI_P005.10513.t1	ATAGCAAGTGTCAAACCTCGAA	TCAACAGTCACTTGCTTCTCAT	This study
APSI_P014.1260.t1	TTCCTTTTAGGCTTGATGCTTG	GTTTTCGGAGGTCTCATTCATA	This study
APSI_P009.18175.t1	CTCTGGAGAGTCTCAAATTTGT	TTCGGTTAATCGGATATACCTC	This study
APSI_P001.6777.t1	AATGCCAATATCGCTCTCAGAA	TGAAAATGAGCGACTGTCTTCT	This study
APSI_P004.3573.t1	CATTTGTAATCATATCGAGCCC	GGGACAAGTAAATGGGGTATTA	This study
APSI_P007.14323.t1	TTGCTCTCATCTTGCAACTAAG	CTAGAGCAATCGAACTTGGATA	This study
APSI_H011.7881.t1	ATAGACTTCGTATTGCTCCTTC	CTCCCTCTATTACCTTCGAATT	This study
APSI_P017.12300.t1	AATTCCTTCTCAAATCCAACGG	GGCGGTCATGACAGAATAAT	This study

The PCR reactions were performed using a final volume of 40 µl containing 2x SensiFAST™ SYBR® No-ROX mix (1X) (Bioline Reagents Ltd., London, UK), Forward and Reverse primer (400 nM), MiliQ water to complete the volume and 20 ng/µl of DNA. The cycling conditions were initial denaturation 95 °C - 5 minutes; Denaturation 95 °C - 30 seconds, Annealing 58 °C - 1 minute, Extension 72 °C - 1 minute, by 40 cycles; Extension final 72 °C - 4 minutes. The PCR products were observed in agarose gel (1%) and then purified using Isolate II PCR and Gel Kit, following the manufacturer's instructions, and the amplicons were sequenced by Sanger Method. It was performed a multiple alignment with the coding sequence from Au biotype and the sequenced amplicons using Geneious Prime 2021.1.1.

3.3 Results

3.3.1 Effector candidate's prediction, subcellular localization and functional analyses

Among the predicted proteins from the biotypes Au showed the highest number of proteins with signal peptide, as well the number of effector candidates predicted (Table 3).

Table 3. Predicted gene of Au, SA and MF-1 biotypes in each step of the prediction

A. psidii biotype*	Predicted proteins	Presence of peptide signal**	Effector candidates***
Au	35,196	2,082	671
MF-1	47,121	1,165	282
SA	19,482	1,150	365

*Au: Australian biotype; MF-1: Brazilian biotype; SA: South-African biotype
** Peptide signal presence identified by SignalP 4.1 (Nielsen, 2017)
*** Effector candidates predicted by EffectorP 2.0 (Sperschneider et al., 2018)

It was predicted among 671 effector candidates of Au biotype, 9.38% targeting the nucleus, 5.96% the mitochondria, 10.13% the chloroplasts, 43.81% was predicted as apoplastic and 30.72% as non-apoplastic with unknown localization (Table 4). Among the 282 effector candidates of MF-1 biotype, it was found 11.7% localized in the nucleus, 4.96% in the mitochondria, 9.92 in the chloroplast, 46.92% were predicted as apoplastic and 26.50% as non-apoplastic with unknown localization (Table 4). It was predicted among the 364 effector candidates of the SA biotype 10.95% effector candidates targeting the nucleus, 5.75% mitochondria, 10.13% chloroplasts, 44.92% were predicted as apoplastic and 28.25% as non-apoplastic with unknown localization (Table 4).

Table 4. Percentage of effector candidates from the biotypes in their predicted localization

A. psidii biotype	Apoplastic* (%)	Nucleus**(%)	Mitochondria**(%)	Chloroplast**(%)	Unknown subcellular localization (%)
Au	43.81	9.38	5.96	10.13	30.72
MF-1	46.92	11.7	4.96	9.92	26.50
SA	44.92	10.95	5.75	10.13	28.25

*Percentage from the number of effector candidates predicted as apoplastic by the ApoplastP;
**Percentage of effector candidates predicted in nucleus, mitochondria and chloroplast by LOCALIZER;
Au: Australian biotype; MF-1: Brazilian biotype; SA: South African biotype;

Regarding the annotation and functional characterization, it was observed that the Au biotype showed 56.78% of non-annotated proteins, 29.66% hypothetical with unknown function and 13.56% annotated with known function. For effector candidates from the SA biotype 54.40% were described as non-annotated, 32.70% hypothetical and 12.90% annotated. For the MF-1 biotype 59.57% were described as non-annotated, 30.85% hypothetical and 9.57% annotated. The complete lists of GO terms are shown in Appendix A, B, C. The effector candidates were categorized according to biological process terms using Blast2GO. The most abundant categories for all biotypes were carbohydrate metabolic process, transport and lipid metabolic process (Figure 1).

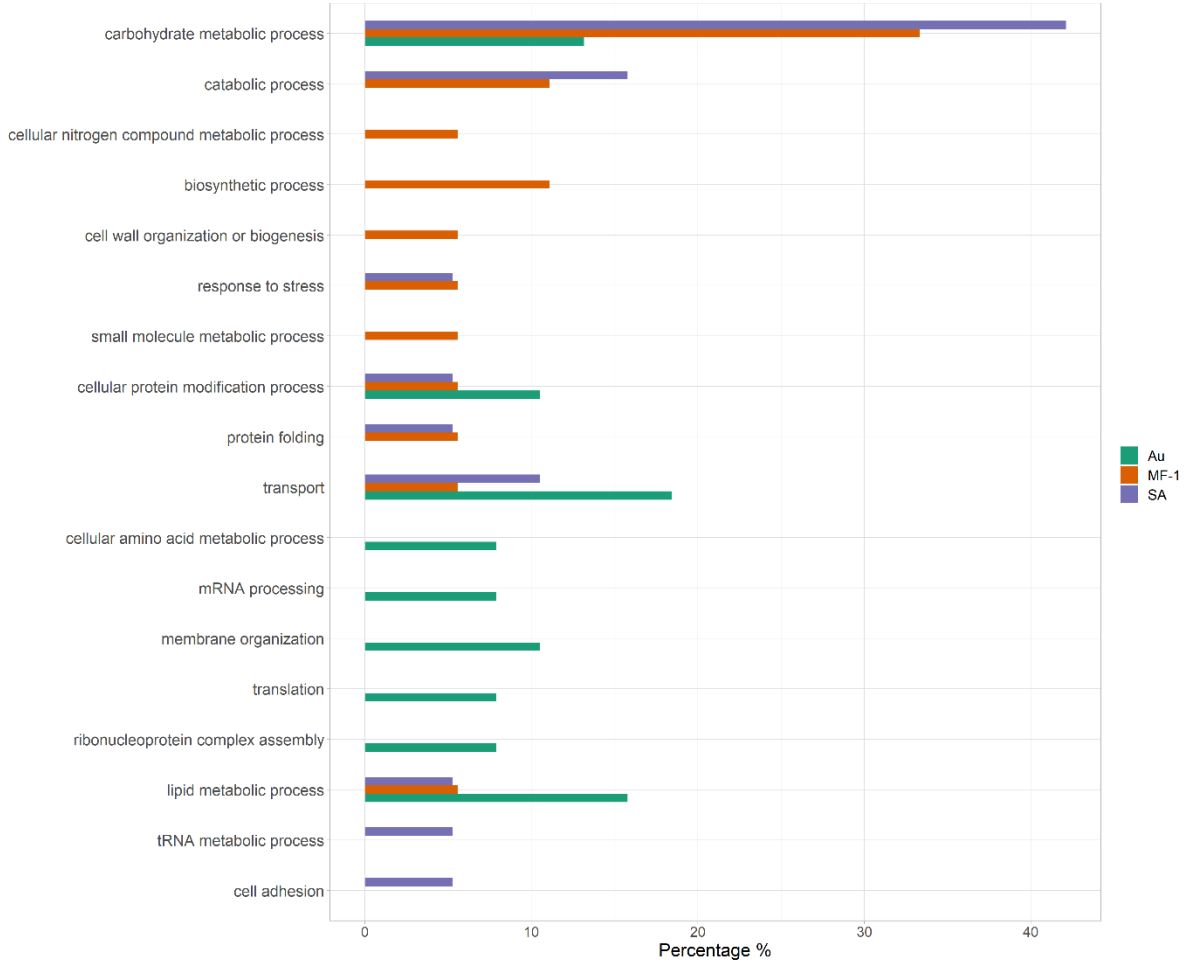

Figure 1. Gene ontology of biological process terms of effector candidates from Au (green), MF-1 (orange) and SA (purple) biotypes. Bar graph represents the term percentage (%) in the analysis.

3.3.2 Comparative genomic analyses

The phylogenetic trees showed the first branch, separating *Puccinia* and *Austropuccinia* species. In the total proteins tree the branch with *A. psidii* was divided into two branches, the MF-1 biotype was separated from Au and SA biotypes (Figure 2a). However, at the effector candidate's phylogenetic tree in the branch of *A. psidii* biotypes, the Au biotype was separated of MF-1 and SA (Figure 2b).

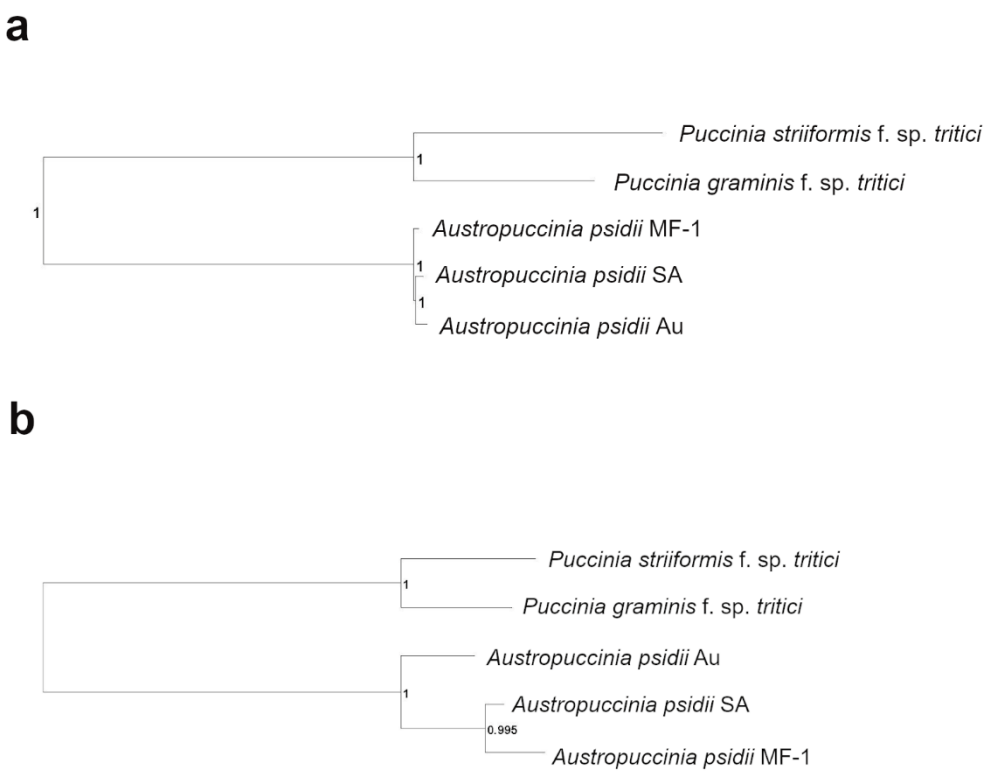

Figure 2. (a) Phylogenetic trees of total proteins sequences from *A. psidii* MF-1, SA and Au biotypes (b) Phylogenetic tree of effector candidates sequences from *A. psidii* MF-1, SA and Au biotypes. *P. graminis* f. sp. *tritici* and *P. striiformis* f. sp. *tritici* were used as out-groups. The internal node values are species tree inference from all genes (STAG) supports (Emms & Kelly, 2018)

We found 269 effector candidates with the strongest evidence of homology among the three biotypes, using Blast local with previous parameters. Au and MF-1 biotypes shared 351 effector candidates with evidence of homology, Au and SA biotypes shared 397, and MF-1 and SA shared 161. It was found 192 effector candidates exclusively of Au biotype, 75 of MF-1 biotype and 128 of SA biotype (Appendix D, E).

The biotype effector candidates orthologs were grouped in clusters by OrthoVenn2 (Figure 3). The 50 unique clusters of Au biotype have 143 effector candidates, 25 clusters showed non-annotated function, 1 (one) cluster was identified with molecular function, and 24 identified as involved in biological process. 24 effector candidates comprehend the 11 unique clusters of SA biotype with no annotated function. The 4 unique clusters of MF-1 biotype with 8 proteins, did not have any annotation. Among the 107 shared clusters of effector candidates, 10 are involved in biological processes and one with cellular component function. The other clusters were not functionally identified (Figure 3). It was found 194 clusters for the biotype MF-1, 305 for the Au biotype and 235 for the SA biotype. The three biotypes also shared 107 clusters of 387 effector candidates (Figure 4). Figure 4 shows the number of clusters and proteins inside of each cluster and the percentage of each biotype protein.

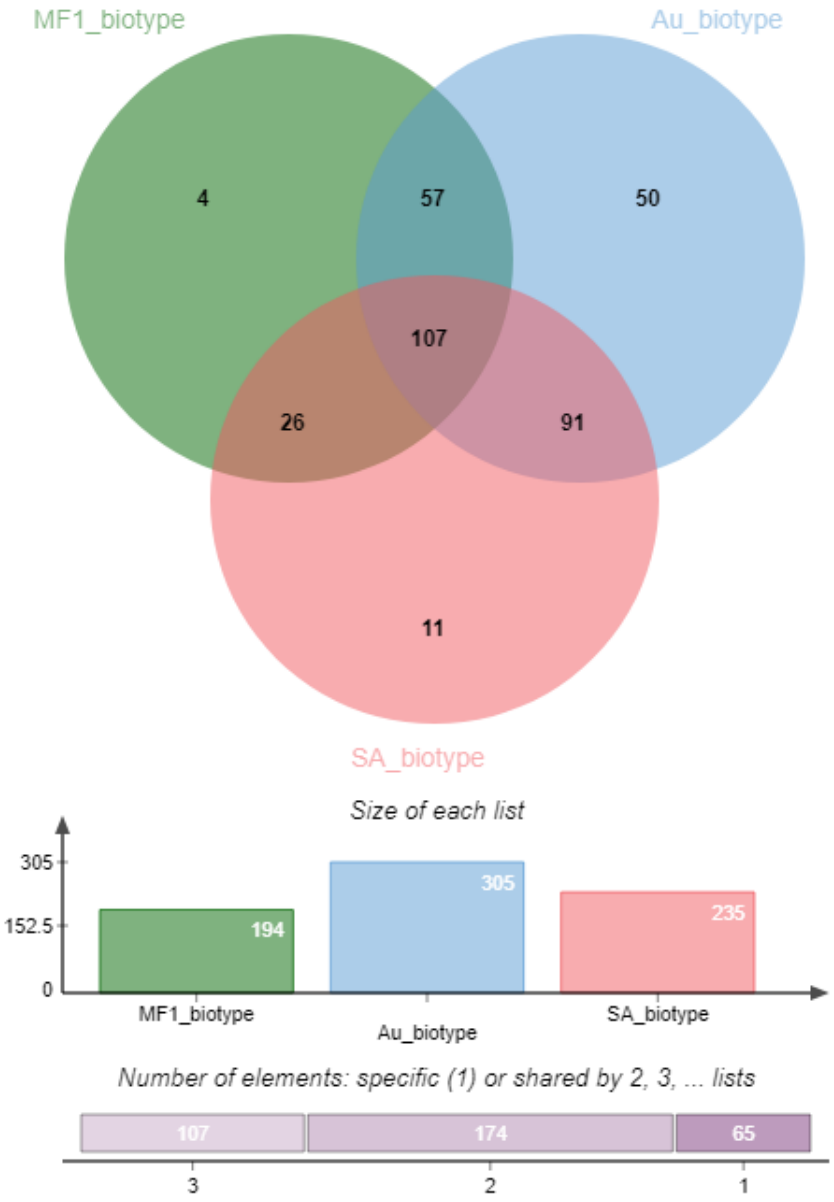

Figure 3. Venn Diagram of effector candidate's clusters from the three biotypes MF-1 (green), SA (pink) and Au (blue). The Venn diagram show the number of unique and shared orthologous effector candidates of each biotype. The bar charts show the number of clusters of each biotype. The purple bars show the number of cluster unique (1), shared by two biotypes (2) and shared by three biotypes (3)

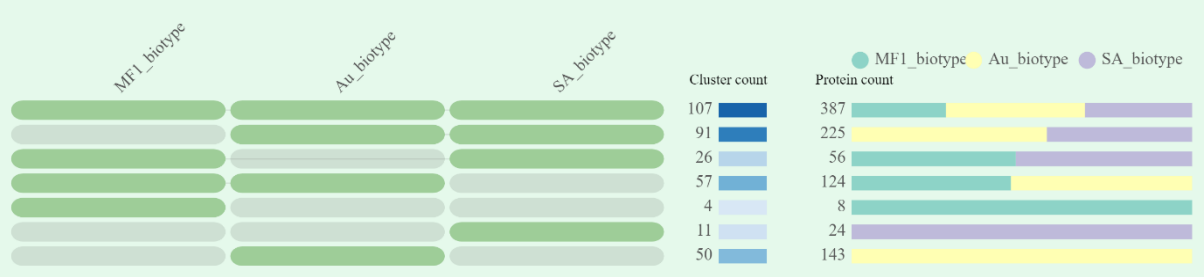

Figure 4. Representation of the numbers of cluster in each biotype's association (left), and the number of proteins for each cluster shared (right). MF-1 biotype represented by green, Au biotype represented by yellow, and SA represented by purple

3.3.3 Effector candidate's polymorphisms validated by PCR

It is described in Table 5 the information about the nine effector candidates selected previously, which were validated by PCR.

Table 5. Identification, description of function, localization and homologs of effector candidates selected from Au biotype

Au effector candidates	Function description[1]	Localization[2]	Homologs from MF-1[3]	Homologs from SA[3]
APSI_P006.9475.t1	Non-annotated	Non-apoplastic	evm.model.NODE_4428_length_15041_cov_0.398283.1	g11725.t1
APSI_P005.10513.t1	E3KLB4_PUCGT - Chitin deacetylase (*P. graminis* f. sp. *tritici)*	Non-apoplastic	evm.model.NODE_15688_length_8108_cov_1.014283.1	g14051.t1
APSI_P014.1260.t1	Non-annotated	Nucleus	-	g14667.t1
APSI_P009.18175.t1	Non-annotated	Apoplastic	evm.model.NODE_47468_length_4281_cov_0.437891.1	-
APSI_P001.6777.t1	Non-annotated	Non-apoplastic	evm.model.NODE_21040_length_6916_cov_0.875441.2	g14717.t1
APSI_P004.3573.t1	Non-annotated	Apoplastic	evm.model.NODE_25723_length_6213_cov_1.778344.1	-
APSI_P007.14323.t1	Non-annotated	Apoplastic	-	g6765.t1
APSI_H011.7881.t1	Non-annotated	Apoplastic	evm.model.NODE_47265_length_4293_cov_0.247.1	-
APSI_P017.12300.t1	A0A2N5VSF3_9BASI - hypothetical protein	Apoplastic	evm.model.NODE_43077_length_4576_cov_0.219825.1	g14456.t1

[1] Function description obtained by Blast2GO
[2] Localization predicted by ApoplastP and LOCALIZER
[3] Effector candidates homologs obtained by Blast local (e-value: 10-5; identity: ≥ 40%)
- No homologs found

We used biotypes with genome information (MF-1, SA, and Au) and the biotypes without genome information (Bz, Ja, and Pi) to perform the PCRs. All the amplicons were aligned to Au coding sequences since this biotype was used as a reference to primer design (Table 6).

Primers of three effector candidates, APSI_P006.9475.t1, APSI_P014.1260.t1, and APSI_P001.6777.t1 were amplified just for two DNA biotypes, Au and Bz. The alignments showed regions conserved, and a few polymorphisms were found (Figure 5a, b, c). It was found homologs in

MF-1 and SA biotypes for APSI_P006.9475.t1 and APSI_P001.6777.t1 effector candidates, however, by PCR they did not amplify.

For other sequences, the alignments were mostly conserved, as APSI_P009.18175.t1, APSI_H011.7881.t1, and APSI_P017.12300.t1 (Figure 5d, e, f). The primer from the APSI_P005.10513.t1 amplified for Au, Bz, MF-1, and Ja, and the alignment showed conserved among the biotypes with a few SNPs (Figure 5g). It was found homologs of MF-1 biotype for APSI_H011.7881.t1, APSI_P009.18175.t1, and APSI_P004.3573.t1 effector candidates, and just a homolog of SA biotype for APSI_P007.14323.t1, however, we found all these effector candidates by PCR for both biotypes.

In the case of APSI_P004.3573.t1 and APSI_P007.14323.t1 effector candidates, we found polymorphisms for Au, Bz, and SA alignments, whereas MF-1, Ja and Pi showed conserved amplicons among the biotypes for APSI_P004.3573.t1 effector candidate (Figure 5h, i). The SA biotype showed the worst alignments for effector candidates, which might be associated with the low quantity of DNA.

Table 6. Primers of effector candidates amplified by PCR in *A. psidii* biotypes samples

Au effector candidates	**Au**	**MF-1**	**SA**	**Bz**	**Ja**	**Pi**
APSI_P006.9475.t1	+	-	-	+	-	-
APSI_P005.10513.t1	+	+	-	+	+	-
APSI_P014.1260.t1	+	-	-	+	-	-
APSI_P009.18175.t1	+	+	+	+	+	+
APSI_P001.6777.t1	+	-	-	+	-	-
APSI_P004.3573.t1	+	+	+	+	+	+
APSI_P007.14323.t1	+	+	+	+	+	+
APSI_H011.7881.t1	+	+	+	+	+	+
APSI_P017.12300.t1	+	+	+	+	+	-

+ the primer was amplified for the biotype
- the primer was not amplified for the biotype
Au: Australian pandemic biotype; MF-1: Brazilian biotype of *E. grandis* from São Paulo; SA: South African biotype; Bz: Brazilian biotype of *E. grandis* from Minas Gerais; Ja: Brazilian biotype of *S. jambos* from São Paulo; Pi: Brazilian biotype of *E. uniflora* from São Paulo

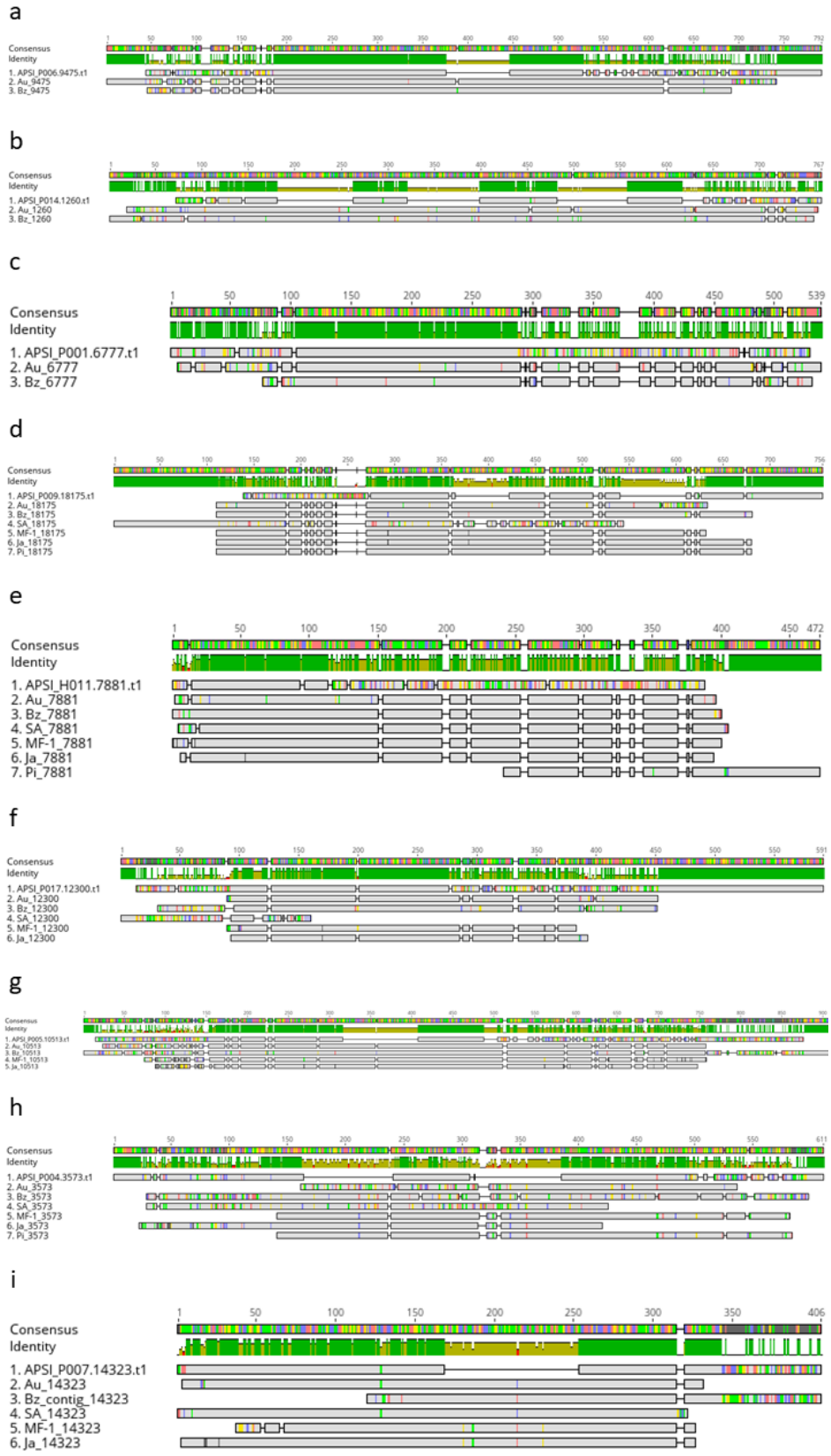

Figure 5. Representation of amplicons alignment by Geneious Prime (2021.1.1) (a) Au and Bz amplicons of APSI_P006.9475.t1 (b) Au and Bz amplicons of APSI_P014.1260.t1 (c) Au and Bz amplicons of APSI_P001.6777 (d) Au, Bz, SA, MF-1, Ja and Pi amplicons of APSI_P00918175 (e) Au, Bz, SA, MF-1, Ja and Pi amplicons of APSI_H011.7881.t1 (f) Au, Bz, SA, MF-1 and Ja amplicons of APSI_P017.12300.t1 (g) Au, Bz, MF-1 and Ja amplicons of APSI_P005.101513.t1 (h) Au, Bz, SA, MF-1, Ja and Pi amplicons of APSI_P004.3573.t1 (i) Au, Bz, SA, MF-1, Ja and Pi amplicons of APSI_P007.14323.t1

3.4 Discussion

A. psidii was first described as infecting guava (Winter, 1884), later *Eucalyptus* spp. (Joffily, 1944), and to date 480 myrtaceous species are infected (Soewarto et al., 2019). It was hypothesized that *A. psidii* jumped from guava to eucalypt, however, Graça et al. (2013) showed that they are distinct biotypes. However, it is unknown exactly the *A. psidii* biotypes evolution, also the high number of hosts impair the comprehension of its sexual cycle, infection mechanisms and genome evolution. We aimed at this study to identify and compare the effector candidates from three *A. psidii* biotypes with draft genome available, that also infect different hosts. The study of effector candidates might elucidate the differences among proteins involved during the infection of several hosts by *A. psidii*. This is the first effector candidate's comparative analysis of *A. psidii* biotypes.

From the prediction of effector candidates by machine learning method EffectorP 2.0, we observed a great variation related to the number of effector candidates among the biotypes. The Au biotype showed a higher number of effector candidates (671), followed by the SA biotype (375) and MF-1 (282). In general, the number of effector candidates found for other rusts is similar to this work. It was described 382 predicted secreted proteins of *Hemileia vastatrix* (coffee rust) (Fernandez et al., 2012), 520 secreted proteins for *P. graminis* f. sp. *tritici* (steam wheat rust) (Upadhyaya et al., 2015), and 1,184 small proteins for *M. larici-populina* (leaf rust in poplars) (Duplessis et al., 2011). However, few works comparing the number of effector candidates among strains, isolates or biotypes of rust fungi have been found. Link et al. (2014) compared the haustorial gene expression of *Uromyces appendiculatus* and *Phakopsora pachyrizi*, the bean and soybean rust, respectively. The authors found 149 secreted proteins for *P. pachyrizi* and 395 for *U. appendiculatus*, they performed a clustering analyses and found 134 families that shared at least two secreted proteins and identified genes that probably are associated with haustorium and pathogenicity biology. To effector candidates from another rust species, *P. striiformis* f. sp. *tritici*, was observed a difference between the number of effectors from two strains. It was found 969 effector candidates in the haplotype assembly Pst-104E strain (Schwessinger et al., 2018), and 557 effector candidates in the haplotype assembly Pst-DK0911 strain (Schwessinger et al., 2020), however, the methods used for prediction were not the same. Certainly, the different methods influence the prediction, mainly using different versions from one software, EffectorP 1.0 for Pst-104E strain and EffectorP 2.0 for Pst-DK0911 strain (Schwessinger et al., 2018, 2020). Thus, the difference in the number of effector candidates from these two strains of *P. striiformis* f. sp. *tritici*, found by the authors, may be associated with the prediction method instead of host, since both strains infect wheat.

In our study, the same method was used to predict the effector candidates from the three biotypes, and we found a different number of effector candidates for each biotype, which might be related to biotypes evolution and/or the number of hosts infected by each biotype. Moreover, the variation found may be related to genome annotation, since the Au biotype genome was a di-haploid

annotation and assembled in scaffolds, generating the primary (66 scaffolds) and the secondary (67 scaffolds) assemblies (Tobias et al., 2020), which was used for all analyses. Whereas the SA biotype was assembled in 147,937 scaffolds using short reads (McTaggart al., 2018), and the MF-1 biotype was assembled in 168,000 contigs using short reads. Thus, it could be associated with the number of coding sequences predicted for each biotype genome used to perform the predictions. However, it does not dispose of the hypothesis that could be required for the pandemic Au biotype a considerable bigger repertoire of effector to infect several hosts, overcoming distinct defense responses, meanwhile, for the other biotypes that infect a smaller range of hosts, a smaller effector repertoire may be requested.

The prediction of effector localization is crucial to determine its function (Jiang, 2011). The effector can act in the apoplast named apoplastic, and/or cytoplasmatic, those delivered to the host cell, targeting multiple compartments (Win et al., 2012). The apoplastic effectors play their function in the host intercellular space, are rich in cysteine, and in general, they are host-specific or isolate-specific (De Jonge et al., 2011). The cytoplasmic effectors are delivered by the haustorium inside the host cell (Win et al., 2012), and among the functions associated with these effectors are inhibiting signalling cascades mediated by MAP kinases, modification of defense responses transcriptome and transcriptional reprogramming (Göhre & Robatzek, 2008). Using a heterologous system, it was observed rust effectors triggering different cell compartments, as the nucleus, mitochondria, chloroplast and other compartments (Lorrain et al., 2018). It is known that apoplastic effectors from obligate pathogens present functions associated with the first contact with the host, as enzyme inhibitors and inhibition of PRRs activation (Göhre & Robatzek, 2008). Although the differences concerning the number of effector candidates from *A. psidii* biotypes, we found a similar percentage of apoplastic effectors for all biotypes, around 45%. Almost half of the effector candidates targeted the apoplast, and the other half targeted the other cell compartments. Moreover, the percentage of apoplastic effectors predicted were not different to other rusts, *P. striiformis f. sp. tritici* PST-130 (61.2%), *P. graminis f. sp. tritici* (61.6%), *M. larici-populina* (58.7%) and *P. triticina* (53.51%) (Sperschneider et al., 2018). The percentage of effector targeting nucleus, mitochondria and chloroplast are similar among the biotypes as well, around 10% targeting nucleus and chloroplasts, and around 5% targeting mitochondria. For other rusts, it was found a lower percentage, 4.5% nucleus, 3.35% targeting chloroplast, and 0.93% mitochondria (Sperschneider et al., 2017). Therefore, it was not found an association with the effector candidate's localization and host-specificity. We observed a redundancy in the effector candidate's localization using ApoplastP and LOCALIZER, in a few cases the apoplastic effector candidates were also predicted targeting a cellular component. This redundancy represented approximately 10% of effector candidates predicted, and may be associated with software false positive (Sperschneider et al., 2018) or the possibility of an effector plays a function in apoplast and plant cell (Rocafort et al., 2020).

Quecine et al. (2016) evaluated the proteome from two populations of *A. psidii*, guava and eucalypt, and observed a change in the abundance of proteins between the samples also unique proteins for each sample. The authors found among the most abundant biological process terms, the carbohydrate

metabolic process term, which was found in this work as most abundant for all biotypes. We also observed some unique terms for each biotype, as it was observed for *A. psidii* guava populations, the authors supposed that these unique terms may be associated with the higher diversity of this population (Quecine et al., 2016). Here, the fact that we found unique terms for the biotypes may be associated with the host variability. The three biotypes abundantly shared two GO terms, carbohydrate metabolic process and transport, those functions might be associate with the biotrophic lifestyle. The transport function was described to play a role in the exportation of compounds, which may be involved in pathogenesis and virulence, and uptake of nutrients (Liang et al., 2018; Verma et al., 2016). Whereas the carbohydrate-active enzymes might be involved in the cell wall degradation by the pathogens, acting as pathogenicity factors to facilitate the infection and obtain nutrients (Zhao et al., 2014).

Orthologous genes are found in different species and diverged at some point by speciation, deriving from a common ancestral gene from an ancestor species (Moreira, 2014). Identification of orthologous genes and their similarities is important in studies of comparative genomics to investigate the evolution of the genes, also the construction of a phylogenetic tree showing the relationships between gene sequences is fundamental to studies of comparative research (Emms & Kelly, 2018). The phylogenetic tree from the total proteins showed Au and SA biotypes in the same branch, whereas the MF-1 was separated. However, using the effector candidates sequences we observed the SA and MF-1 biotype in the same branch. These results imply that the pandemic Au biotype has evolved separately, may present distinct effector candidates to infect several hosts. The most effector candidates showed homology by Blast local using our criteria, and 192 effector candidates were exclusive of Au biotype, 75 of MF-1 biotype and 128 of SA biotype. The study of those exclusive effector candidates is interesting in order to understand their role in speciation and specialization (Long et al., 2003; Plissonneau et al., 2017).

We observed that the Au biotype shared the highest number of effector candidates to the other biotypes by Orthovenn2, but also it was the biotype with the highest number of unique effector candidate's clusters, composed of 143 effector candidates. Upadhyaya et al. (2015) compared 5 isolates of *P. graminis* f. sp. *tritici*, and constructed a pan-genome, and based on that they identify 520 secreted proteins, founding 25 effector candidates with variations between pt 21-0 isolate and other two derived isolates, which might explain the virulence of the derived isolates. Our findings showed that 387 orthologs of effector candidates are shared among the biotypes, opening new possibilities on studies focused on core effectors that might be important to understand the infection process and as a target for resistance breeding (Lorrain et al., 2018).

The effectors show a high degree of variation compared to housekeeping genes, and they are in co-evolution with the host (Dodds et al., 2006; Jones & Dangl, 2006; Yoshida et al., 2009). Effectors are under evolution pressure since the urge to avoid being recognized by the host and to ensure its survival, due to its lifestyle. The effector's mutations can be a consequence of SNPs, small insertions and deletions, structural variations, and the move of transposable elements (Schwessinger et al., 2020).

Regarding the validation of effector candidates, we observed that the Au pandemic biotype and Bz biotype showed conservation related to the effector candidates validated, however, they are probably not related (Stewart et al., 2018). The Bz and MF-1 biotypes were isolated from *Eucalyptus* in different regions in Brazil, however, we observed a difference between the biotypes, which impairs that even they originated from the same host, a few variations were found. The effector candidate's validation by PCR showed conserved regions among the biotypes with regions presenting polymorphisms, however, further studies are requested to investigate if the polymorphisms are associated with the host variability.

Based on *A. psidii* genotyping, Stewart et al. (2018) investigated the genetic and genotypic variability of biotypes from *A. psidii* considering the geographic location, the authors assigned 9 clusters (C1-C9) to the *A. psidii* isolates. The work showed the existence of multiple genetic clusters associated with the myrtle rust, and the isolates from Brazil were grouped at C2 and C3, whereas the SA and Au were not included. However, they showed strong evidence that the Au biotype will be a member of C1, together with Hawaii isolate, whereas the genotype relationships of SA biotype are still unclear. Moreover, the study of *A. psidii* variability even at the genomic level is growing, which may help understand its genetic variability, consequently the host association.

Our results might support our hypothesis that the Au biotype requires a greater variety of effector candidates to infect several hosts and developed its own effector candidate's repertoire to succeed in infection hosts, based on the homology analysis. However, our analysis limitation is associated with the genome annotation from the biotypes, using short reads of SA and MF-1 the probability of overlapping is higher than with long reads of Au. This limitation could explain the high number of Au effector candidates, as well the unique protein clusters compared to other biotypes. Further studies will be required to understand the role of homologs and/or unique effector candidates in the evolution of *A. psidii* and host range.

References

Beenken, L. (2017). Austropuccinia: A new genus name for the myrtle rust *Puccinia psidii* placed within the redefined family sphaerophragmiaceae (pucciniales). *Phytotaxa*, *297*(1), 53–61. https://doi.org/10.11646/phytotaxa.297.1.5

Berthon, K., Esperon-Rodriguez, M., Beaumont, L. J., Carnegie, A. J., & Leishman, M. R. (2018). Assessment and prioritisation of plant species at risk from myrtle rust (*Austropuccinia psidii*) under current and future climates in Australia. *Biological Conservation*, *218*(May 2017), 154–162. https://doi.org/10.1016/j.biocon.2017.11.035

Bruce, M., Neugebauer, K. A., Joly, D. L., Migeon, P., Cuomo, C. A., Wang, S., Akhunov, E., Bakkeren, G., Kolmer, J. A., & Fellers, J. P. (2014). Using transcription of six *Puccinia triticina* races to identify the effective secretome during infection of wheat. *Frontiers in Plant Science*, *4*(JAN), 1–7. https://doi.org/10.3389/fpls.2013.00520

Carnegie, A. J., Amrit, K., Pegg, G. S., Entwistle, P., Nagel, M., & Giblin, F. (2016). Impact of the invasive rust *Puccinia psidii* (myrtle rust) on native Myrtaceae in natural ecosystems in Australia. *Biological Invasions*, *18*(1), 127–144. https://doi.org/10.1007/s10530-015-0996-y

Carnegie, A. J., Lidbetter, J. R., Walker, J., Horwood, M. A., Tesoriero, L., Glen, M., & Priest, M. J. (2010). *Uredo rangelii*, a taxon in the guava rust complex, newly recorded on Myrtaceae in Australia. *Australasian Plant Pathology*, *39*(5), 463–466. https://doi.org/10.1071/AP10102

Carnegie, A. J., & Pegg, G. S. (2018). Lessons from the incursion of myrtle rust in Australia. *Annual Review of Phytopathology*, *56*, 457–478. https://doi.org/10.1146/annurev-phyto-080516-035256

Christenhusz, M. J. M., & Byng, J. W. (2016). The number of known plants species in the world and its annual increase. *Phytotaxa*, *261*(3), 201–217. https://doi.org/10.11646/phytotaxa.261.3.1

Coutinho, T. A., Wingfield, M. J., Alfenas, A. C., & Crous, P. W. (1998). *Eucalyptus* rust: A disease with the potential for serious international implications. *Plant Disease*, *82*(7), 819–825. https://doi.org/10.1094/PDIS.1998.82.7.819

Dalio, R. J. D., Magalhaes, D. M., Rodrigues, C. M., Arena, G. D., Oliveira, T. S., Souza-Neto, R. R., Picchi, S. C., Martins, P. M. M., Santos, P. J. C., Maximo, H. J., Pacheco, I. S., De Souza, A. A., & Machado, M. A. (2017). PAMPs, PRRs, effectors and R-genes associated with citrus-pathogen interactions. *Annals of Botany*, *119*(5), 749–774. https://doi.org/10.1093/aob/mcw238

De Jonge, R., Bolton, M. D., & Thomma, B. P. H. J. (2011). How filamentous pathogens co-opt plants: The ins and outs of fungal effectors. *Current Opinion in Plant Biology*, *14*(4), 400–406. https://doi.org/10.1016/j.pbi.2011.03.005

Dodds, P. N., Lawrence, G. J., Catanzariti, A. M., Teh, T., Wang, C. I. A., Ayliffe, M. A., Kobe, B., & Ellis, J. G. (2006). Direct protein interaction underlies gene-for-gene specificity and coevolution of the flax resistance genes and flax rust avirulence genes. *Proceedings of the National Academy of Sciences of the United States of America*, *103*(23), 8888–8893. https://doi.org/10.1073/pnas.0602577103

Duplessis, S., Cuomo, C. A., Lin, Y. C., Aerts, A., Tisserant, E., Veneault-Fourrey, C., Joly, D. L., Hacquard, S., Amselem, J., Cantarel, B. L., Chiu, R., Coutinho, P. M., Feaue, N., Field, M., Frey, P., Gelhaye, E., Goldberg, J., Grabherr, M. G., Kodira, C. D., … Martin, F. (2011). Obligate biotrophy features unraveled by the genomic analysis of rust fungi. *Proceedings of the National Academy of Sciences of the United States of America*, *108*(22), 9166–9171. https://doi.org/10.1073/pnas.1019315108

Emms, D. M., & Kelly, S. (2018). OrthoFinder: Phylogenetic orthology inference for comparative genomics. *BioRxiv*, 1–14. https://doi.org/10.1101/466201

Fernandez, D., Tisserant, E., Talhinhas, P., Azinheira, H., Vieira, A., Petitot, A. S., Loureiro, A., Poulain, J., da Silva, C., do Céu Silva, M., & Duplessis, S. (2012). 454-pyrosequencing of *Coffea arabica* leaves infected by the rust fungus *Hemileia vastatrix* reveals in planta-expressed pathogen-secreted proteins and plant functions in a late compatible plant-rust interaction. *Molecular Plant Pathology*, *13*(1), 17–37. https://doi.org/10.1111/j.1364-3703.2011.00723.x

Ferreira, F. (1983). Ferrugem do Eucalipto. *Revista Árvore*, *7*, 92–109.

Glen, M., Alfenas, A. C., Zauza, E. A. V., Wingfield, M. J., & Mohammed, C. (2007). *Puccinia psidii*: A threat to the Australian environment and economy - A review. *Australasian Plant Pathology*, *36*(1), 1–16. https://doi.org/10.1071/AP06088

Göhre, V., & Robatzek, S. (2008). Breaking the barriers: Microbial effector molecules subvert plant immunity. *Annual Review of Phytopathology*, *46*, 189–215. https://doi.org/10.1146/annurev.phyto.46.120407.110050

Graça, R. N., Ross-Davis, A. L., Klopfenstein, N. B., Kim, M. S., Peever, T. L., Cannon, P. G., Aun, C. P., Mizubuti, E. S. G., & Alfenas, A. C. (2013). Rust disease of eucalypts, caused by *Puccinia psidii*, did not originate via host jump from guava in Brazil. *Molecular Ecology*, *22*(24), 6033–6047. https://doi.org/10.1111/mec.12545

Jaswal, R., Kiran, K., Rajarammohan, S., Dubey, H., Singh, P. K., Sharma, Y., Deshmukh, R., Sonah, H., Gupta, N., & Sharma, T. R. (2020). Effector Biology of Biotrophic Plant Fungal Pathogens: Current Advances and Future Prospects. *Microbiological Research*, *241*(December 2019), 126567. https://doi.org/10.1016/j.micres.2020.126567

Jiang, R. H. Y. (2011). Dynamics of effectors in host–pathogen interactions. *Mycology*, *2*(3), 210–217. https://doi.org/10.1080/21501203.2011.605181

Joffily, J. (1944). Ferrugem do eucalipto. *Bragantia*, *4*(8), 475–487. https://doi.org/10.1590/s0006-87051944000300001

Jones, J. D. G., & Dangl, J. L. (2006). The plant immune system. *Nature*, *444*(7117), 323–329.

Leite, T. F. (2012). Estabelecimento de um patossistema modelo e análise da interação molecular planta-patógeno entre Eucalyptus grandis e Puccinia psidii Winter por meio da técnica de RNA-Seq. In *Thesis*. University of São Paulo.

Liang, P., Liu, S., Xu, F., Jiang, S., Yan, J., He, Q., Liu, W., Lin, C., Zheng, F., Wang, X., & Miao, W. (2018). Powdery Mildews Are Characterized by Contracted Carbohydrate Metabolism and Diverse Effectors to Adapt to Obligate Biotrophic Lifestyle. *Frontiers in Microbiology*, *9*(December), 1–14. https://doi.org/10.3389/fmicb.2018.03160

Link, T. I., Lang, P., Scheffler, B. E., Duke, M. V., Graham, M. A., Cooper, B., Tucker, M. L., van de Mortel, M., Voegele, R. T., Mendgen, K., Baum, T. J., & Whitham, S. A. (2014). The haustorial transcriptomes of *Uromyces appendiculatus* and *Phakopsora pachyrhizi* and their candidate effector families. *Molecular Plant Pathology*, *15*(4), 379–393. https://doi.org/10.1111/mpp.12099

Long, M., Betrán, E., Thornton, K., & Wang, W. (2003). The origin of new genes: Glimpses from the young and old. *Nature Reviews Genetics*, *4*(11), 865–875. https://doi.org/10.1038/nrg1204

Lorrain, C., Marchal, C., Hacquard, S., Delaruelle, C., Pétrowski, J., Petre, B., Hecker, A., Frey, P., & Duplessis, S. (2018). The rust fungus *Melampsora larici-populina* expresses a conserved genetic program and distinct sets of secreted protein genes during infection of its two host plants, larch and poplar. *Molecular Plant-Microbe Interactions*, *31*(7), 695–706. https://doi.org/10.1094/MPMI-12-17-0319-R

Lorrain, C., Petre, B., & Duplessis, S. (2018). Show me the way: rust effector targets in heterologous plant systems. *Current Opinion in Microbiology*, *46*, 19–25. https://doi.org/10.1016/j.mib.2018.01.016

Machado, P. S., Glen, M., Pereira, O. L., Silva, A. A., & Alfenas, A. C. (2015). Epitypification of *Puccinia psidii*, Causal Agent of Guava Rust. *Tropical Plant Pathology*, *40*(1), 5–12. https://doi.org/10.1007/s40858-014-0002-8

McTaggart, A. R., Duong, T., Le, V. Q., Shuey, L. S., Smidt, W., Naidoo, S., Wingfield, M. J., & Wingfield, B. D. (2018). Chromium sequencing: The doors open for genomics of obligate plant pathogens. *BioTechniques*, *65*(5), 253–257. https://doi.org/10.2144/BTN-2018-0019

McTaggart, Alistair R., Duong, T. A., Le, V. Q., Shuey, L. S., Smidt, W., Naidoo, S., Wingfield, M. J., & Wingfield, B. D. (2018). Chromium sequencing: The doors open for genomics of obligate plant pathogens. *BioTechniques*, *65*(5), 253–257. https://doi.org/10.2144/BTN-2018-0019

Moreira, D. (2014). Orthologous Gene. In R. Amils, M. Gargaud, J. Cernicharo Quintanilla, H. J. Cleaves, W. M. Irvine, D. Pinti, & M. Viso (Eds.), *Encyclopedia of Astrobiology* (p. 1). Springer Berlin Heidelberg. https://doi.org/10.1007/978-3-642-27833-4_1731-3

Nielsen, H. (2017). Predicting secretory proteins with signalP. In D. Kihara (Ed.), *Protein Function Prediction (Methods in Molecular Biology)* (Vol. 1611, pp. 59–73). Springer. https://doi.org/10.1007/978-1-4939-7015-5_6

Panstruga, R. (2009). Terrific Protein Traffic : The Mystery. *Science*, *748*(May), 748–751. https://doi.org/10.1126/science.1171652

Plissonneau, C., Benevenuto, J., Mohd-Assaad, N., Fouché, S., Hartmann, F. E., & Croll, D. (2017). Using population and comparative genomics to understand the genetic basis of effector-driven fungal pathogen evolution. *Frontiers in Plant Science*, *8*(FEBRUARY), 1–15. https://doi.org/10.3389/fpls.2017.00119

Quecine, M. C., Bini, A. P., Romagnoli, E. R., Andreote, F. D., Moon, D. H., & Labate, C. A. (2014). Genetic variability in *Puccinia psidii* populations as revealed by PCR-DGGE and T-RFLP markers. *Plant Disease*, *98*(1), 16–23. https://doi.org/10.1094/PDIS-03-13-0332-RE

Quecine, M. C., Leite, T. F., Bini, A. P., Regiani, T., Franceschini, L. M., Budzinski, I. G. F., Marques, F. G., Labate, M. T. V., Guidetti-Gonzalez, S., Moon, D. H., & Labate, C. A. (2016). Label-free quantitative proteomic analysis of *Puccinia psidii* uredospores reveals differences of fungal populations infecting eucalyptus and guava. *PLoS ONE*, *11*(1), 1–19. https://doi.org/10.1371/journal.pone.0145343

Rocafort, M., Fudal, I., & Mesarich, C. H. (2020). Apoplastic effector proteins of plant-associated fungi and oomycetes. *Current Opinion in Plant Biology*, *56*, 9–19. https://doi.org/10.1016/j.pbi.2020.02.004

Roux, J., Granados, G. M., Shuey, L., Barnes, I., Wingfield, M. J., & McTaggart, A. R. (2016). A unique genotype of the rust pathogen, *Puccinia psidii*, on Myrtaceae in South Africa. *Australasian Plant Pathology*, *45*(6), 645–652. https://doi.org/10.1007/s13313-016-0447-y

Roux, J., Greyling, I., Coutinho, T. A., Verleur, M., & Wingfeld, M. J. (2013). The Myrtle rust pathogen, *Puccinia psidii*, discovered in Africa. *IMA Fungus*, *4*(1), 155–159. https://doi.org/10.5598/imafungus.2013.04.01.14

Sandhu, K. S., Karaoglu, H., Zhang, P., & Park, R. F. (2016). Simple sequence repeat markers support the presence of a single genotype of *Puccinia psidii* in Australia. *Plant Pathology*, *65*(7), 1084–1094. https://doi.org/10.1111/ppa.12501

Schwessinger, B., Chen, Y. J., Tien, R., Vogt, J. K., Sperschneider, J., Nagar, R., McMullan, M., Sicheritz-Ponten, T., Sørensen, C. K., Hovmøller, M. S., Rathjen, J. P., & Justesen, A. F. (2020). Distinct Life Histories Impact Dikaryotic Genome Evolution in the Rust Fungus *Puccinia striiformis* Causing Stripe Rust in Wheat. *Genome Biology and Evolution*, *12*(5), 597–617. https://doi.org/10.1093/gbe/evaa071

Schwessinger, B., Sperschneider, J., Cuddy, W. S., Garnica, D. P., Miller, M. E., Taylor, J. M., Dodds, P. N., Figueroa, M., Park, R. F., & Rathjen, P. (2018). A near-complete haplotype-phased genome of the dikaryotic. *MBio*, *9*, e02275-17.

Soewarto, J., Giblin, F., & Carnegie, A. J. (2019). Austropuccinia psidii (myrtle rust) global host list. *Version 2. Australian Network for Plant Conservation*. http://www.anpc.asn.au/myrtle-rust

Spegazzini, C. . (1884). Fungi Guaranitici. Pugillus1. *An. Soc. Cient. Argent*, *17*, 119–134.

Sperschneider, J., Catanzariti, A. M., Deboer, K., Petre, B., Gardiner, D. M., Singh, K. B., Dodds, P. N., & Taylor, J. M. (2017). LOCALIZER: Subcellular localization prediction of both plant and effector proteins in the plant cell. *Scientific Reports*, *7*(March), 1–14. https://doi.org/10.1038/srep44598

Sperschneider, J., Dodds, P. N., Gardiner, D. M., Singh, K. B., & Taylor, J. M. (2018). Improved prediction of fungal effector proteins from secretomes with EffectorP 2.0. *Molecular Plant Pathology*, *19*(9), 2094–2110. https://doi.org/10.1111/mpp.12682

Sperschneider, J., Dodds, P. N., Singh, K. B., & Taylor, J. M. (2018). ApoplastP: prediction of effectors and plant proteins in the apoplast using machine learning. *New Phytologist*, *217*(4), 1764–1778. https://doi.org/10.1111/nph.14946

Stewart, J. E., Ross-Davis, A. L., Graça, R. N., Alfenas, A. C., Peever, T. L., Hanna, J. W., Uchida, J. Y., Hauff, R. D., Kadooka, C. Y., Kim, M. S., Cannon, P. G., Namba, S., Simeto, S., Pérez, C. A., Rayamajhi, M. B., Lodge, D. J., Arguedas, M., Medel-Ortiz, R., López-Ramirez, M. A., … Klopfenstein, N. B. (2018). Genetic diversity of the myrtle rust pathogen (*Austropuccinia psidii*) in the Americas and Hawaii: Global implications for invasive threat assessments. *Forest Pathology*, *48*(1), 1–13. https://doi.org/10.1111/efp.12378

Tan, M. K., Collins, D., Chen, Z., Englezou, A., & Wilkins, M. R. (2014). A brief overview of the size and composition of the myrtle rust genome and its taxonomic status. *Mycology*, *5*(2), 52–63. https://doi.org/10.1080/21501203.2014.919967

Tobias, P. A., Schwessinger, B., Deng, C. H., Wu, C., Dong, C., Sperschneider, J., Jones, A., Smith, G. R., Tibbits, J., Chagné, D., & Park, R. F. (2020). Long read assembly of the pandemic strain of *Austropuccinia psidii* (myrtle rust) reveals an unusually large (gigabase sized) and repetitive fungal genome. *BioRxiv*, 1–44. http://biorxiv.org/content/early/2020/03/20/2020.03.18.996108.abstract

Tsushima, A., Gan, P., Kumakura, N., Narusaka, M., Takano, Y., Narusaka, Y., & Shirasu, K. (2019). Genomic plasticity mediated by transposable elements in the plant pathogenic fungus *Colletotrichum higginsianum*. *Genome Biology and Evolution*, *11*(5), 1487–1500. https://doi.org/10.1093/gbe/evz087

Upadhyaya, N. M., Garnica, D. P., Karaoglu, H., Sperschneider, J., Nemri, A., Xu, B., Mago, R., Cuomo, C. A., Rathjen, J. P., Park, R. F., Ellis, J. G., & Dodds, P. N. (2015). Comparative genomics of australian isolates of the wheat stem rust pathogen *Puccinia graminis* f. sp. *tritici* reveals extensive polymorphism in candidate effector genes. *Frontiers in Plant Science*, *5*(JAN), 1–13. https://doi.org/10.3389/fpls.2014.00759

Verma, S., Gazara, R. K., Nizam, S., Parween, S., Chattopadhyay, D., & Verma, P. K. (2016). Draft genome sequencing and secretome analysis of fungal phytopathogen *Ascochyta rabiei* provides insight into the necrotrophic effector repertoire. *Scientific Reports*, *6*(April), 1–14. https://doi.org/10.1038/srep24638

Win, J., Chaparro-Garcia, A., Belhaj, K., Saunders, D. G. O., Yoshida, K., Dong, S., Schornack, S., Zipfel, C., Robatzek, S., Hogenhout, S. A., & Kamoun, S. (2012). Effector biology of plant-associated organisms: Concepts and perspectives. *Cold Spring Harbor Symposia on Quantitative Biology*, *77*, 235–247. https://doi.org/10.1101/sqb.2012.77.015933

Winter, G. (1884). Repertorium. Rabenhorstii fungi europaei et extraeuraopaei Cent. XXXI et XXXII. *Hedwigia*, *23*, 164–172.

Xu, L., Dong, Z., Fang, L., Luo, Y., Wei, Z., Guo, H., Zhang, G., Gu, Y. Q., Coleman-Derr, D., Xia, Q., & Wang, Y. (2019). OrthoVenn2: A web server for whole-genome comparison and annotation of orthologous clusters across multiple species. *Nucleic Acids Research*, *47*(W1), W52–W58. https://doi.org/10.1093/nar/gkz333

Yoshida, K., Saitoh, H., Fujisawa, S., Kanzaki, H., Matsumura, H., Yoshida, K., Tosa, Y., Chuma, I., Takano, Y., Win, J., Kamoun, S., & Terauchi, R. (2009). Association genetics reveals three novel avirulence genes from the rice blast fungal pathogen *Magnaporthe oryzae*. *Plant Cell*, *21*(5), 1573–1591. https://doi.org/10.1105/tpc.109.066324

Zhao, Z., Liu, H., Wang, C., & Xu, J. R. (2014). Correction to Comparative analysis of fungal genomes reveals different plant cell wall degrading capacity in fungi [BMC Genomics 14(2013) 274]. *BMC Genomics*, *15*(1). https://doi.org/10.1186/1471-2164-15-6

Appendices

APPENDIX A. List of GO terms obtained by Blast2GO from effector candidates of Au biotype

ID Sequence	Description
APSI_P002.15036.t1	hypothetical protein PGT21_002604
APSI_P006.9603.t1	---NA---
APSI_P012.8977.t1	hypothetical protein PTTG_00895
APSI_P011.205.t1	family 4 carbohydrate esterase
APSI_P001.6419.t1	hypothetical protein PTTG_08542
APSI_P005.10553.t1	---NA---
APSI_P014.966.t1	---NA---
APSI_P018.7675.t1	---NA---
APSI_P006.9922.t1	---NA---
APSI_P010.11572.t1	---NA---
APSI_P024.16551.t1	---NA---
APSI_P003.2383.t1	polar growth protein
APSI_P015.12851.t1	---NA---
APSI_P002.15354.t1	hypothetical protein PCANC_17395
APSI_P010.12024.t1	---NA---
APSI_P006.9367.t1	family 23 glycoside hydrolase
APSI_P019.7991.t1	---NA---
APSI_P019.8249.t1	hypothetical protein PGT21_035967
APSI_P001.6256.t1	---NA---
APSI_P004.3527.t1	hypothetical protein VP01_649g4
APSI_P022.4793.t1	---NA---
APSI_P011.762.t1	---NA---
APSI_P004.3511.t1	ACrystal Structure of Ustilago sphaerogena Ribonuclease U2 Complexed with adenosine 3'-monophosphate
APSI_P009.18222.t1	hypothetical protein PSTG_04609
APSI_P005.10609.t1	---NA---
APSI_P010.12051.t1	---NA---
APSI_P016.16215.t1	ACrystal Structure of Ustilago sphaerogena Ribonuclease U2 Complexed with adenosine 3'-monophosphate
APSI_P025.26.t1	---NA---
APSI_P007.13556.t1	---NA---
APSI_P002.15484.t1	hypothetical protein PGTG_02169
APSI_P001.6777.t1	hypothetical protein PTTG_28580
APSI_P009.18196.t1	---NA---
APSI_P011.649.t1	cystathionine beta-lyase
APSI_P006.10044.t1	hypothetical protein PGTG_09756
APSI_P010.11524.t1	secreted protein
APSI_P001.6831.t1	---NA---
APSI_P025.78.t1	---NA---
APSI_P001.6355.t1	---NA---
APSI_P001.6451.t1	hypothetical protein M408DRAFT_234221
APSI_P014.1260.t1	hypothetical protein PTTG_10178

APSI_P008.16939.t1	---NA---
APSI_P007.14386.t1	GPI anchored CFEM domain protein C
APSI_P017.12604.t1	---NA---
APSI_P003.2486.t1	uncharacterized protein VP01_444g8
APSI_P018.7580.t1	hypothetical protein PGTG_00965
APSI_P001.7305.t2	hypothetical protein PCASD_07877
APSI_P011.466.t1	secreted protein
APSI_P009.18151.t1	hypothetical protein PCASD_07877
APSI_P004.2813.t1	hypothetical protein PTTG_04707
APSI_P003.2523.t1	hypothetical protein PCASD_22376
APSI_P001.6620.t1	---NA---
APSI_P011.602.t1	---NA---
APSI_P014.1138.t1	---NA---
APSI_P014.965.t1	---NA---
APSI_P012.8789.t1	---NA---
APSI_P009.18155.t1	hypothetical protein PGTG_17519
APSI_P006.10210.t1	hypothetical protein PGTG_09326
APSI_P019.8320.t1	---NA---
APSI_P015.13117.t1	---NA---
APSI_P006.9804.t1	secreted protein
APSI_P016.16247.t1	---NA---
APSI_P001.6257.t1	---NA---
APSI_P011.371.t1	hypothetical protein PGT21_035712
APSI_P014.1291.t1	---NA---
APSI_P021.13431.t1	---NA---
APSI_P009.17648.t1	hypothetical protein PCASD_07877
APSI_P001.6823.t1	60S ribosomal protein L29
APSI_P005.11126.t1	CSEP-35, partial
APSI_P002.15786.t1	---NA---
APSI_P003.1899.t1	---NA---
APSI_P007.14266.t1	hypothetical protein PCANC_20635
APSI_P002.15364.t1	hypothetical protein PTTG_12365
APSI_P001.7258.t1	hypothetical protein PGT21_010376
APSI_P025.103.t1	---NA---
APSI_P019.7994.t1	nuclease
APSI_P004.3462.t1	family 5 carbohydrate esterase
APSI_P002.15562.t1	---NA---
APSI_P008.16775.t1	---NA---
APSI_P018.7751.t1	---NA---
APSI_P009.17671.t1	---NA---
APSI_P012.8996.t1	hypothetical protein PSTG_09941
APSI_P001.6658.t1	hypothetical protein PTTG_04707
APSI_P004.3640.t1	---NA---
APSI_P006.9920.t1	---NA---
APSI_P018.7749.t2	hypothetical protein PGT21_010826
APSI_P001.6772.t1	---NA---

APSI_P002.15163.t1	hypothetical protein PTTG_28579
APSI_P003.2484.t1	hypothetical protein PGT21_006688
APSI_P006.9441.t1	hypothetical protein PSHT_00658
APSI_P010.12049.t1	---NA---
APSI_P029.3864.t1	secreted protein
APSI_P010.12130.t1	---NA---
APSI_P002.15781.t1	---NA---
APSI_P001.6770.t1	hypothetical protein PTTG_00841
APSI_P001.5595.t2	---NA---
APSI_P003.2073.t1	---NA---
APSI_P017.12463.t1	---NA---
APSI_P002.15287.t1	hypothetical protein VP01_2502g1
APSI_P001.5860.t1	hypothetical protein CROQUDRAFT_359464
APSI_P009.17593.t1	hypothetical protein PSTG_01739
APSI_P005.10513.t1	hypothetical protein PTTG_02142
APSI_P021.13316.t1	---NA---
APSI_P009.18190.t1	hypothetical protein PCASD_07877
APSI_P012.9215.t1	Peptidyl-prolyl cis-trans isomerase B
APSI_P018.7748.t2	hypothetical protein PTTG_04753
APSI_P008.16995.t1	---NA---
APSI_P017.12631.t1	---NA---
APSI_P008.17008.t1	hypothetical protein PCANC_17395
APSI_P005.10482.t1	hypothetical protein PGTUg99_005444
APSI_P008.16894.t1	---NA---
APSI_P002.14778.t1	hypothetical protein PGTUg99_012885
APSI_P015.12819.t1	---NA---
APSI_P010.12124.t1	---NA---
APSI_P014.1225.t1	hypothetical protein PCASD_22545
APSI_P019.8113.t1	---NA---
APSI_P026.906.t1	---NA---
APSI_P006.9765.t1	---NA---
APSI_P015.13113.t1	---NA---
APSI_P003.2387.t1	---NA---
APSI_P005.11039.t1	hypothetical protein PGTG_06052
APSI_P013.4314.t1	---NA---
APSI_P005.11314.t1	hypothetical protein VP01_673g2
APSI_P018.7571.t1	---NA---
APSI_P025.77.t1	---NA---
APSI_P016.16105.t1	---NA---
APSI_P013.4035.t1	---NA---
APSI_P001.7354.t1	---NA---
APSI_P003.1814.t1	---NA---
APSI_P014.1378.t1	hypothetical protein PCASD_09322
APSI_P003.1584.t1	---NA---
APSI_P011.659.t1	hypothetical protein PSTG_15024
APSI_P016.16116.t2	---NA---

APSI_P005.10630.t1	hypothetical protein PSTG_15912
APSI_P005.10487.t1	hypothetical protein PCASD_12679
APSI_P001.6338.t1	succinate dehydrogenase (ubiquinone) membrane anchor subunit
APSI_P006.9745.t1	---NA---
APSI_P003.2719.t1	---NA---
APSI_P001.6864.t1	small nuclear ribonucleoprotein G
APSI_P003.1555.t1	---NA---
APSI_P005.11042.t1	hypothetical protein PGTG_06052
APSI_P010.12123.t1	---NA---
APSI_P004.3623.t1	hypothetical protein PTTG_11722
APSI_P022.4675.t1	---NA---
APSI_P013.4384.t1	---NA---
APSI_P006.9571.t1	hypothetical protein VP01_1014g3
APSI_P018.7863.t1	---NA---
APSI_P012.9173.t1	hypothetical protein PGT21_020166
APSI_P014.1460.t1	---NA---
APSI_P017.12533.t1	---NA---
APSI_P016.16246.t1	---NA---
APSI_P005.11068.t1	hypothetical protein PCANC_03411
APSI_P011.212.t1	hypothetical protein, variant
APSI_P001.6259.t1	---NA---
APSI_P005.10457.t1	---NA---
APSI_P019.8306.t1	---NA---
APSI_P010.11706.t1	---NA---
APSI_P003.1934.t1	hypothetical protein PGTUg99_011480
APSI_P016.16102.t1	---NA---
APSI_P011.198.t1	---NA---
APSI_P001.5424.t1	---NA---
APSI_P013.3893.t1	---NA---
APSI_P005.10940.t1	---NA---
APSI_P009.17723.t1	---NA---
APSI_P006.10022.t1	---NA---
APSI_P008.16771.t1	---NA---
APSI_P006.9317.t1	---NA---
APSI_P015.12854.t1	---NA---
APSI_P009.17651.t1	hypothetical protein PCASD_07877
APSI_P012.8825.t1	---NA---
APSI_P011.451.t1	secreted protein
APSI_P007.14191.t1	---NA---
APSI_P015.13112.t1	---NA---
APSI_P009.17955.t1	---NA---
APSI_P001.6786.t1	---NA---
APSI_P015.12821.t1	---NA---
APSI_P005.11052.t1	hypothetical protein HWV62_24866
APSI_P018.7552.t1	hypothetical protein PGT21_025600
APSI_P012.9228.t1	---NA---

APSI_P004.3557.t1	hydrolase 76 protein
APSI_P018.7577.t1	hypothetical protein PGTG_00965
APSI_P006.9913.t1	---NA---
APSI_P010.11859.t1	hypothetical protein PGTG_12331
APSI_P007.13871.t1	---NA---
APSI_P004.3443.t1	---NA---
APSI_P006.9908.t1	---NA---
APSI_P005.10801.t1	---NA---
APSI_P004.2955.t1	hypothetical protein PGTUg99_033111
APSI_P017.12414.t1	---NA---
APSI_P014.1073.t1	---NA---
APSI_P001.7080.t1	---NA---
APSI_P005.10948.t1	---NA---
APSI_P015.12682.t1	---NA---
APSI_P001.7305.t1	hypothetical protein PCASD_07877
APSI_P008.17405.t1	---NA---
APSI_P023.8485.t1	---NA---
APSI_P005.10475.t1	secreted protein
APSI_P003.2401.t1	hypothetical protein PTTG_12380, partial
APSI_P010.12091.t1	---NA---
APSI_P004.3683.t1	---NA---
APSI_P001.7224.t1	---NA---
APSI_P016.16287.t1	---NA---
APSI_P009.17508.t1	---NA---
APSI_P001.5855.t1	hypothetical protein CROQUDRAFT_699647
APSI_P002.15332.t1	hypothetical protein PSTT_04396
APSI_P002.15483.t1	hypothetical protein PGTG_02169
APSI_P008.16742.t1	hypothetical protein PTTG_08460
APSI_P014.977.t1	---NA---
APSI_P023.8467.t1	---NA---
APSI_P009.18175.t1	---NA---
APSI_P017.12167.t1	hypothetical protein PTTG_12661
APSI_P011.414.t1	secreted protein
APSI_P008.17264.t1	hypothetical protein VP01_1014g3
APSI_P001.5334.t1	hypothetical protein PCASD_09108
APSI_P006.9550.t1	nuclease
APSI_P010.12119.t1	---NA---
APSI_P001.7100.t1	---NA---
APSI_P002.14561.t1	hypothetical protein CROQUDRAFT_659295
APSI_P004.2826.t1	---NA---
APSI_P013.4315.t1	---NA---
APSI_P006.9501.t1	secreted protein
APSI_P003.2095.t1	---NA---
APSI_P016.16039.t1	---NA---
APSI_P009.17696.t1	---NA---
APSI_P001.7435.t1	---NA---

APSI_P029.3884.t1	secreted protein
APSI_P014.1360.t1	---NA---
APSI_P005.10459.t1	secreted protein
APSI_P006.9475.t1	---NA---
APSI_P003.2310.t1	---NA---
APSI_P003.1841.t1	---NA---
APSI_P004.3492.t1	---NA---
APSI_P022.4818.t1	---NA---
APSI_P003.2394.t1	hypothetical protein VP01_4052g4
APSI_P005.10949.t1	---NA---
APSI_P012.9205.t1	hypothetical protein PGT21_026392
APSI_P001.6649.t1	---NA---
APSI_P013.3906.t1	hypothetical protein PSTT_10230
APSI_P020.4846.t1	---NA---
APSI_P013.4116.t1	uncharacterized protein MELLADRAFT_109863
APSI_P001.7180.t1	hypothetical protein PCASD_22252
APSI_P011.707.t1	---NA---
APSI_P015.13124.t1	---NA---
APSI_P005.11140.t1	CSEP-35, partial
APSI_P020.4880.t1	---NA---
APSI_P002.15052.t1	hypothetical protein PCANC_21128
APSI_P016.16126.t1	Alpha/Beta hydrolase protein
APSI_P006.9494.t1	---NA---
APSI_P003.1911.t1	---NA---
APSI_P003.1780.t1	---NA---
APSI_P008.17145.t1	hypothetical protein PTTG_01817
APSI_P002.15177.t1	hypothetical protein VP01_1014g3
APSI_P009.17587.t1	---NA---
APSI_P018.7870.t1	hypothetical protein PGTG_17002
APSI_P006.9892.t1	---NA---
APSI_P007.14323.t1	---NA---
APSI_P008.17121.t1	secreted protein
APSI_P004.3158.t1	hypothetical protein TWF706_004243
APSI_P004.3404.t1	---NA---
APSI_P016.16235.t1	---NA---
APSI_P002.15789.t1	---NA---
APSI_P007.13902.t1	putative uncharacterized protein 86B
APSI_P005.10357.t1	hypothetical protein PGT21_012530
APSI_P025.73.t1	---NA---
APSI_P006.9715.t1	---NA---
APSI_P021.13365.t1	hypothetical protein PCANC_18328
APSI_P013.4092.t3	glycosylphosphatidylinositol anchor biosynthesis
APSI_P010.12148.t1	hypothetical protein PCANC_26603
APSI_P010.11494.t1	---NA---
APSI_P005.10833.t1	hypothetical protein VP01_4042g2
APSI_P009.17592.t1	hypothetical protein PSTT_12330

APSI_P002.15557.t1	---NA---
APSI_P027.7471.t1	---NA---
APSI_P003.1676.t1	hypothetical protein CROQUDRAFT_61041
APSI_P001.7237.t1	---NA---
APSI_P003.2206.t1	---NA---
APSI_P010.12112.t1	hypothetical protein PGTG_12331
APSI_P022.4814.t1	---NA---
APSI_P012.8857.t1	---NA---
APSI_P012.9231.t1	hypothetical protein PSTG_03083
APSI_P004.2893.t1	---NA---
APSI_P006.10218.t1	zinc metalloprotease
APSI_P002.15459.t1	---NA---
APSI_P014.1514.t1	hypothetical protein PSTG_10920
APSI_P016.16116.t1	---NA---
APSI_P023.8461.t1	---NA---
APSI_P024.16473.t1	---NA---
APSI_P009.18250.t1	---NA---
APSI_P007.14199.t1	---NA---
APSI_P017.12300.t1	Mitochondrial carrier protein ymc2
APSI_P019.8008.t1	---NA---
APSI_P018.7749.t1	hypothetical protein PGT21_010826
APSI_P013.3907.t1	---NA---
APSI_P023.8520.t1	---NA---
APSI_P013.4080.t1	Long chronological lifespan protein 2
APSI_P008.16758.t1	---NA---
APSI_P005.11212.t1	small subunit ribosomal protein S10e
APSI_P006.9443.t1	---NA---
APSI_P019.8195.t1	hypothetical protein, variant
APSI_P008.17140.t1	hypothetical protein PTTG_01817
APSI_P009.18252.t1	---NA---
APSI_P005.10417.t1	---NA---
APSI_P005.10938.t1	---NA---
APSI_P015.12681.t1	---NA---
APSI_P023.8350.t1	---NA---
APSI_P023.8518.t1	---NA---
APSI_P006.9522.t1	secreted protein
APSI_P004.3483.t1	---NA---
APSI_P005.10507.t1	---NA---
APSI_P007.13867.t1	---NA---
APSI_P009.18208.t1	---NA---
APSI_P004.3446.t1	---NA---
APSI_P008.16895.t1	---NA---
APSI_P022.4680.t1	---NA---
APSI_P009.17668.t1	---NA---
APSI_P012.8774.t1	---NA---
APSI_P005.11073.t1	hypothetical protein PGTUg99_025605

APSI_P003.1924.t1	hypothetical protein PTTG_01451, partial
APSI_P012.9139.t1	---NA---
APSI_P013.3895.t1	---NA---
APSI_P007.14189.t1	uncharacterized protein MELLADRAFT_106648
APSI_P001.6438.t1	---NA---
APSI_P017.12449.t1	---NA---
APSI_P007.13786.t1	carbohydrate esterase family 1 protein
APSI_P005.10407.t1	---NA---
APSI_P001.6666.t1	---NA---
APSI_P018.7748.t1	hypothetical protein PTTG_04753
APSI_P002.15545.t1	---NA---
APSI_P023.8517.t1	---NA---
APSI_P018.7519.t1	hypothetical protein PCANC_22108
APSI_P001.6422.t1	hypothetical protein PTTG_08542
APSI_P008.16939.t2	---NA---
APSI_P005.10528.t1	hypothetical protein CROQUDRAFT_670094
APSI_P005.10668.t1	---NA---
APSI_P006.9601.t1	---NA---
APSI_P024.16506.t1	---NA---
APSI_P017.12375.t1	---NA---
APSI_P007.14181.t1	---NA---
APSI_P002.14561.t2	hypothetical protein CROQUDRAFT_659295
APSI_P001.5292.t1	uncharacterized protein MELLADRAFT_85819
APSI_P004.3816.t1	---NA---
APSI_P001.7184.t1	hypothetical protein VP01_1014g3
APSI_P008.16998.t1	---NA---
APSI_P009.18162.t1	hypothetical protein PCASD_07877
APSI_P014.1455.t1	---NA---
APSI_P008.17031.t1	hypothetical protein, variant
APSI_P013.4169.t1	---NA---
APSI_P007.13627.t1	---NA---
APSI_P003.1876.t1	---NA---
APSI_P007.13696.t1	hypothetical protein PGTG_00119
APSI_P009.17929.t1	---NA---
APSI_P003.2485.t1	uncharacterized protein VP01_444g8
APSI_P017.12429.t1	---NA---
APSI_P004.2961.t1	uncharacterized protein MELLADRAFT_102180
APSI_P004.3021.t1	secreted protein
APSI_P004.3573.t1	---NA---
APSI_P002.15153.t1	hypothetical protein PGT21_018723
APSI_P019.8218.t1	phenylalanyl-tRNA synthetase
APSI_P017.12375.t2	---NA---
APSI_P005.10730.t1	hypothetical protein PSTG_09842
APSI_P006.9653.t1	phosphatidylserine decarboxylase
APSI_P004.2937.t1	aldehyde dehydrogenase (NAD+)
APSI_P007.14430.t1	---NA---

APSI_P008.17394.t1	---NA---
APSI_P012.9030.t1	---NA---
APSI_P010.12120.t1	---NA---
APSI_P006.9736.t1	---NA---
APSI_P012.8606.t1	hypothetical protein VP01_1014g3
APSI_H005.1788.t1	---NA---
APSI_H004.2917.t1	---NA---
APSI_H011.7922.t1	hypothetical protein PCASD_07877
APSI_H003.4396.t1	secreted protein
APSI_H002.13098.t1	hypothetical protein VP01_853g10
APSI_H002.12351.t1	hypothetical protein PGTG_04832
APSI_H020.87.t1	---NA---
APSI_H001.7110.t2	hypothetical protein, variant
APSI_H001.6138.t1	hypothetical protein VP01_1014g3
APSI_H006.14420.t1	hypothetical protein M408DRAFT_234221
APSI_H001.6253.t1	---NA---
APSI_H004.3191.t1	hypothetical protein PSTG_02653
APSI_H011.7909.t1	---NA---
APSI_H004.3438.t1	---NA---
APSI_H004.3166.t1	hypothetical protein PGT21_030525
APSI_H004.3327.t1	---NA---
APSI_H003.4728.t3	---NA---
APSI_H004.3321.t1	---NA---
APSI_H016.15417.t2	6,7-dimethyl-8-ribityllumazine synthase
APSI_H005.1280.t1	hypothetical protein PCANC_20687
APSI_H011.7947.t1	hypothetical protein PCASD_07877
APSI_H020.373.t1	hypothetical protein VP01_1014g3
APSI_H017.8136.t1	hypothetical protein PGTG_06052
APSI_H003.4610.t1	---NA---
APSI_H002.13405.t1	---NA---
APSI_H006.14609.t1	hypothetical protein PTTG_01451, partial
APSI_H003.5320.t1	hypothetical protein PSTG_03083
APSI_H004.3315.t1	---NA---
APSI_H012.10730.t1	---NA---
APSI_H008.9266.t1	---NA---
APSI_H011.7921.t1	hypothetical protein PCASD_07877
APSI_H005.1404.t1	---NA---
APSI_H008.9963.t1	small nuclear ribonucleoprotein G
APSI_H014.2269.t1	hypothetical protein PGT21_002604
APSI_H003.5152.t1	---NA---
APSI_H004.3230.t1	---NA---
APSI_H005.1520.t1	---NA---
APSI_H006.15147.t2	---NA---
APSI_H001.6654.t1	---NA---
APSI_H002.12863.t1	uncharacterized protein MELLADRAFT_85819
APSI_H019.11126.t1	---NA---

APSI_H007.8636.t1	---NA---
APSI_H006.14419.t1	---NA---
APSI_H003.5322.t1	hypothetical protein PSTG_03083
APSI_H002.13389.t2	---NA---
APSI_H003.4232.t1	---NA---
APSI_H013.5636.t1	---NA---
APSI_H006.14788.t2	RNA polymerase III C11 subunit
APSI_H004.3139.t1	---NA---
APSI_H017.8167.t1	hypothetical protein PGTG_06052
APSI_H017.8128.t1	hypothetical protein PGTG_06052
APSI_H002.13405.t3	---NA---
APSI_H008.9416.t1	---NA---
APSI_H004.3130.t1	---NA---
APSI_H009.11505.t1	hypothetical protein CROQUDRAFT_670077
APSI_H016.15335.t1	---NA---
APSI_H015.402.t1	---NA---
APSI_H004.3254.t1	hypothetical protein ASPWEDRAFT_44265
APSI_H011.7549.t1	---NA---
APSI_H008.9936.t1	---NA---
APSI_H004.3137.t1	---NA---
APSI_H007.8902.t1	---NA---
APSI_H017.8139.t1	hypothetical protein HWV62_24866
APSI_H017.8334.t1	hypothetical protein VP01_673g2
APSI_H002.12434.t1	hypothetical protein PSTG_12889
APSI_H015.414.t1	hypothetical protein CROQUDRAFT_49918
APSI_H011.7941.t1	hypothetical protein PSTG_01881
APSI_H004.3602.t1	carbohydrate esterase family 1 protein
APSI_H005.1601.t1	---NA---
APSI_H006.14364.t1	---NA---
APSI_H005.1650.t1	GPI anchored CFEM domain protein C
APSI_H005.1156.t1	hypothetical protein PGT21_035294
APSI_H011.7445.t1	hypothetical protein PCASD_07877
APSI_H008.9302.t1	---NA---
APSI_H005.958.t1	---NA---
APSI_H010.14291.t1	hypothetical protein PTTG_27146
APSI_H009.11834.t1	hypothetical protein PGTG_16623
APSI_H003.5224.t1	hypothetical protein PSTG_01739
APSI_H003.4333.t1	---NA---
APSI_H010.13775.t1	Dcp1p-Dcp2p decapping enzyme complex alpha subunit
APSI_H003.4419.t1	hypothetical protein PGTUg99_007592
APSI_H005.941.t1	---NA---
APSI_H006.15057.t1	uncharacterized protein VP01_444g8
APSI_H001.5919.t1	DNA-directed RNA polymerase III subunit
APSI_H001.6936.t1	hypothetical protein PSTG_10920
APSI_H007.8999.t1	secreted protein
APSI_H010.14175.t1	hypothetical protein PCANC_17395

APSI_H003.4229.t1	---NA---
APSI_H001.5956.t1	---NA---
APSI_H009.11923.t1	secreted protein
APSI_H003.4925.t1	asparagine-linked glycosylation protein
APSI_H005.1524.t1	uncharacterized protein MELLADRAFT_106648
APSI_H016.15662.t1	phenylalanine ammonia-lyase
APSI_H002.12594.t1	---NA---
APSI_H004.3630.t1	adenosinetriphosphatase
APSI_H013.5580.t1	---NA---
APSI_H005.1704.t1	---NA---
APSI_H016.15382.t1	hypothetical protein PGTUg99_014499
APSI_H002.13062.t1	---NA---
APSI_H001.7055.t1	hypothetical protein PGT21_035967
APSI_H004.3192.t1	hypothetical protein PSTG_02653
APSI_H012.10628.t1	---NA---
APSI_H002.13295.t1	secreted protein
APSI_H014.2201.t1	hypothetical protein PGT21_003963
APSI_H002.13034.t1	2,3-bisphosphoglycerate-independent phosphoglycerate mutase
APSI_H003.5003.t1	hypothetical protein PGT21_025960
APSI_H008.9977.t1	---NA---
APSI_H010.14290.t1	hypothetical protein PGTG_02169
APSI_H014.2315.t1	---NA---
APSI_H005.1636.t1	hypothetical protein PSTG_13167
APSI_H006.15054.t1	hypothetical protein PSHT_06615
APSI_H012.10741.t1	---NA---
APSI_H010.13681.t1	---NA---
APSI_H016.15367.t1	---NA---
APSI_H006.15147.t3	---NA---
APSI_H007.8945.t1	---NA---
APSI_H016.15354.t1	---NA---
APSI_H007.8559.t1	---NA---
APSI_H002.12404.t1	---NA---
APSI_H011.7944.t1	hypothetical protein PCASD_07877
APSI_H002.12334.t1	secreted protein
APSI_H008.10082.t1	---NA---
APSI_H001.7323.t1	nuclease
APSI_H003.5243.t1	---NA---
APSI_H014.2402.t1	---NA---
APSI_H027.3774.t1	hypothetical protein VP01_1014g3
APSI_H007.8961.t1	hypothetical protein PGTG_09756
APSI_H013.5633.t1	---NA---
APSI_H007.8761.t1	---NA---
APSI_H007.8744.t1	---NA---
APSI_H005.1565.t1	hypothetical protein PCANC_20635
APSI_H002.13097.t1	hypothetical protein PTTG_04779
APSI_H005.1816.t1	---NA---

APSI_H004.3650.t1	hypothetical protein PSTG_07801
APSI_H017.8250.t1	small subunit ribosomal protein S10e
APSI_H003.4226.t1	---NA---
APSI_H001.6793.t1	---NA---
APSI_H003.4473.t1	---NA---
APSI_H003.4621.t1	---NA---
APSI_H002.12217.t1	hypothetical protein PCANC_17395
APSI_H019.10994.t1	---NA---
APSI_H003.4728.t1	---NA---
APSI_H012.10636.t1	---NA---
APSI_H010.14030.t1	---NA---
APSI_H008.9532.t1	protein RCC2 homolog
APSI_H020.197.t1	---NA---
APSI_H001.6977.t1	FK506-binding protein 2
APSI_H010.14266.t1	---NA---
APSI_H014.2421.t1	---NA---
APSI_H003.4491.t1	---NA---
APSI_H020.150.t1	---NA---
APSI_H009.11351.t1	methylthioribulose-1-phosphate dehydratase
APSI_H003.4911.t1	---NA---
APSI_H018.10277.t1	hypothetical protein PSTT_11306, partial
APSI_H002.13237.t1	hypothetical protein CROQUDRAFT_661367
APSI_H008.9981.t1	hypothetical protein PTTG_00841
APSI_H006.14618.t1	---NA---
APSI_H004.2990.t1	hypothetical protein PGTUg99_017339
APSI_H020.265.t1	hypothetical protein PCASD_07877
APSI_H002.12188.t1	---NA---
APSI_H003.4911.t2	---NA---
APSI_H001.6016.t1	---NA---
APSI_H001.6500.t1	---NA---
APSI_H020.214.t1	hypothetical protein PGTUg99_035882
APSI_H009.11370.t1	---NA---
APSI_H014.2401.t1	---NA---
APSI_H001.6605.t1	---NA---
APSI_H002.13405.t5	---NA---
APSI_H003.4613.t1	---NA---
APSI_H020.352.t1	hypothetical protein VP01_1014g3
APSI_H003.4166.t1	60S ribosomal protein L38
APSI_H006.14750.t1	secreted protein
APSI_H006.14979.t1	---NA---
APSI_H003.4583.t1	---NA---
APSI_H011.7469.t1	---NA---
APSI_H003.3953.t1	---NA---
APSI_H004.3151.t1	Alpha/Beta hydrolase protein
APSI_H001.5883.t1	hypothetical protein P167DRAFT_464349, partial
APSI_H011.7875.t1	hypothetical protein PSTG_04609

APSI_H023.7995.t1	hypothetical protein, partial
APSI_H016.15346.t1	---NA---
APSI_H011.7901.t1	hypothetical protein PSTG_01871
APSI_H001.7002.t1	Retrovirus-related Pol polyprotein from type-1 retrotransposable element R2
APSI_H003.5302.t1	Peptidyl-prolyl cis-trans isomerase B
APSI_H009.11786.t1	Long chronological lifespan protein 2
APSI_H016.15417.t1	6,7-dimethyl-8-ribityllumazine synthase
APSI_H017.8154.t1	hypothetical protein PCANC_22040
APSI_H012.10563.t1	---NA---
APSI_H011.7479.t1	---NA---
APSI_H001.7111.t2	hypothetical protein PTTG_02666
APSI_H001.6143.t1	---NA---
APSI_H018.10369.t1	---NA---
APSI_H003.5272.t1	hypothetical protein PGT21_020166
APSI_H003.4519.t1	---NA---
APSI_H006.15147.t1	---NA---
APSI_H004.3417.t1	---NA---
APSI_H015.658.t1	protein RCC2 homolog
APSI_H002.12405.t1	---NA---
APSI_H013.5638.t1	---NA---
APSI_H002.12181.t1	hypothetical protein PGT21_025508
APSI_H006.15291.t1	---NA---
APSI_H004.2950.t1	---NA---
APSI_H006.15277.t1	---NA---
APSI_H004.3625.t1	---NA---
APSI_H011.7447.t1	hypothetical protein PCASD_07877
APSI_H009.11522.t1	---NA---
APSI_H008.9642.t1	hypothetical protein PCASD_25670
APSI_H004.3432.t1	---NA---
APSI_H005.1083.t1	---NA---
APSI_H008.9972.t1	---NA---
APSI_H004.3737.t1	hypothetical protein PGTUg99_014316
APSI_H013.5578.t1	---NA---
APSI_H002.12403.t1	---NA---
APSI_H015.607.t1	---NA---
APSI_H014.2116.t1	hypothetical protein PGT21_012530
APSI_H002.13405.t2	---NA---
APSI_H010.13761.t1	---NA---
APSI_H008.9895.t1	---NA---
APSI_H001.7110.t1	hypothetical protein PTTG_02666
APSI_H002.13439.t1	alpha,alpha-trehalose-phosphate synthase (UDP-forming)
APSI_H003.4924.t1	---NA---
APSI_H018.10384.t1	---NA---
APSI_H009.11254.t1	---NA---
APSI_H001.6259.t1	---NA---
APSI_H001.7111.t1	hypothetical protein, variant

APSI_H019.11152.t1	---NA---
APSI_H002.12498.t1	hypothetical protein PTTG_12661
APSI_H012.10577.t1	secreted protein
APSI_H018.10205.t1	---NA---
APSI_H001.6143.t2	---NA---
APSI_H004.2779.t1	---NA---
APSI_H004.2904.t1	---NA---
APSI_H001.5864.t1	---NA---
APSI_H007.8619.t1	---NA---
APSI_H004.2977.t1	hypothetical protein PGT21_035239
APSI_H002.12864.t1	---NA---
APSI_H003.4422.t1	hypothetical protein PGTUg99_007592
APSI_H010.13570.t2	hypothetical protein CROQUDRAFT_659295
APSI_H007.9034.t1	hypothetical protein PGTG_09326
APSI_H007.9071.t1	---NA---
APSI_H013.5415.t1	---NA---
APSI_H005.990.t1	---NA---
APSI_H014.2232.t1	---NA---
APSI_H001.6153.t1	hypothetical protein VP01_1014g3
APSI_H001.6954.t1	---NA---
APSI_H009.11931.t1	---NA---
APSI_H024.9216.t1	hypothetical protein PCANC_22108
APSI_H003.4866.t1	---NA---
APSI_H014.2291.t1	---NA---
APSI_H008.9486.t2	---NA---
APSI_H003.4898.t1	---NA---
APSI_H016.15485.t1	---NA---
APSI_H013.5645.t1	hypothetical protein PCANC_18328
APSI_H002.12785.t1	Mitochondrial carrier protein ymc2
APSI_H004.2899.t1	hypothetical protein PGTG_17002
APSI_H002.12353.t1	hypothetical protein PGTG_04832
APSI_H014.2344.t1	---NA---
APSI_H002.12843.t1	hypothetical protein PCASD_09108
APSI_H007.8820.t1	secreted protein
APSI_H011.7462.t1	---NA---
APSI_H017.8151.t1	hypothetical protein PGTUg99_022256
APSI_H009.11760.t1	uncharacterized protein MELLADRAFT_109863
APSI_H010.14187.t1	hypothetical protein PTTG_12365
APSI_H008.9395.t1	---NA---
APSI_H002.12958.t1	2,3-bisphosphoglycerate-independent phosphoglycerate mutase
APSI_H015.770.t1	hypothetical protein PTTG_11911
APSI_H011.7407.t1	---NA---
APSI_H002.12354.t1	hypothetical protein PTTG_01817
APSI_H003.4928.t1	---NA---
APSI_H012.10664.t1	hypothetical protein PSTG_15024
APSI_H010.13570.t1	hypothetical protein CROQUDRAFT_659295

APSI_H011.7930.t1	hypothetical protein PGTG_17519
APSI_H007.9111.t1	---NA---
APSI_H005.1264.t1	putative uncharacterized protein 86B
APSI_H001.6018.t1	---NA---
APSI_H011.7881.t1	---NA---
APSI_H020.290.t1	Dcp1p-Dcp2p decapping enzyme complex alpha subunit
APSI_H002.13389.t1	---NA---
APSI_H009.12003.t1	secreted protein
APSI_H010.13613.t1	single-strand binding protein family
APSI_H005.1513.t1	---NA---
APSI_H012.10558.t1	---NA---
APSI_H008.9467.t1	Hypothetical predicted protein
APSI_H018.10350.t1	---NA---
APSI_H003.5318.t1	hypothetical protein PCANC_04412
APSI_H006.14775.t5	---NA---
APSI_H004.2981.t1	---NA---
APSI_H004.3033.t1	---NA---
APSI_H016.15598.t1	family 4 carbohydrate esterase
APSI_H005.1070.t1	---NA---
APSI_H001.6817.t1	hypothetical protein PTTG_12151
APSI_H006.14597.t1	hypothetical protein CROQUDRAFT_671584
APSI_H002.12402.t1	---NA---
APSI_H002.13405.t4	---NA---
APSI_H010.14016.t1	---NA---
APSI_H012.10637.t1	---NA---
APSI_H003.4206.t1	uncharacterized protein MELLADRAFT_101620
APSI_H004.3492.t1	---NA---
APSI_H020.197.t2	---NA---
APSI_H007.9186.t1	---NA---
APSI_H020.231.t1	hypothetical protein PGT21_010376
APSI_H001.6945.t1	---NA---
APSI_H004.3379.t1	---NA---
APSI_H017.8157.t1	hypothetical protein PGTUg99_025605

APPENDIX B. List of GO terms obtained by Blast2GO from effector candidates of SA biotype

ID Sequence	Description
g2338.t1	---NA---
g4544.t1	competence protein ComEA
g11007.t1	hypothetical protein RR48_03454
g9203.t1	hypothetical protein VP01_1245g1
g16789.t1	hypothetical protein PGTUg99_007592
g14288.t1	---NA---
g13581.t1	hypothetical protein PCASD_22323
g16372.t1	---NA---
g3453.t1	small subunit ribosomal protein S10e
g11431.t1	---NA---
g3090.t1	Alpha/Beta hydrolase protein
g544.t1	---NA---
g17956.t1	---NA---
g16800.t1	---NA---
g15269.t1	---NA---
g2557.t1	secreted protein
g9355.t1	hypothetical protein PGTUg99_050157
g16493.t1	---NA---
g5667.t1	---NA---
g17727.t1	---NA---
g15194.t1	secreted protein
g3727.t1	---NA---
g645.t1	---NA---
g11235.t1	hypothetical protein PGTUg99_000817
g17107.t2	hypothetical protein PSTT_04396
g11445.t1	hypothetical protein PCASD_07724
g18175.t1	---NA---
g16285.t1	---NA---
g17785.t1	hypothetical protein PCASD_10515
g3709.t1	---NA---
g845.t1	hypothetical protein CROQUDRAFT_658791
g16748.t1	hypothetical protein M408DRAFT_234221
g14760.t1	hypothetical protein PTTG_01451, partial
g14075.t1	---NA---
g4969.t1	---NA---
g16980.t1	---NA---
g13732.t1	---NA---
g9058.t1	---NA---
g13741.t1	---NA---
g13921.t1	---NA---
g11674.t1	---NA---
g13948.t1	---NA---
g6049.t1	---NA---
g17424.t1	hypothetical protein PTTG_03168

g8042.t1	---NA---
g6743.t1	uncharacterized protein PAC_18923
g18168.t1	---NA---
g11152.t1	---NA---
g14855.t1	---NA---
g16373.t1	---NA---
g9148.t1	secreted protein
g2391.t1	secreted protein
g847.t1	---NA---
g13621.t1	DUF305 domain-containing protein
g3575.t1	hypothetical protein PSTG_04609
g2183.t1	hypothetical protein PGTG_12331
g10144.t1	---NA---
g9764.t1	---NA---
g14051.t1	hypothetical protein PGTG_11258
g13058.t1	---NA---
g13658.t1	hypothetical protein PCANC_17395
g2331.t1	---NA---
g5662.t1	---NA---
g5896.t1	hypothetical protein PSTT_11306, partial
g15492.t1	---NA---
g16121.t1	---NA---
g5960.t1	hypothetical protein PSTG_05541
g11599.t1	---NA---
g3834.t1	---NA---
g4160.t1	---NA---
g1911.t1	hypothetical protein PSTG_15024
g5938.t1	hypothetical protein PSTG_01861
g989.t1	hypothetical protein PSTT_09788
g17469.t1	hypothetical protein PGTUg99_019843
g5081.t1	family 10 glycoside hydrolase
g15193.t1	secreted protein
g16561.t1	---NA---
g3021.t1	---NA---
g7380.t1	neuromedin-U receptor 2-like isoform X3
g5074.t1	hypothetical protein PSTG_03813
g1482.t1	hypothetical protein PGTUg99_012885
g17901.t1	hypothetical protein PGT21_030525
g1326.t1	hypothetical protein PCASD_25670
g1006.t1	hypothetical protein PCASD_07877
g19.t1	---NA---
g6104.t1	---NA---
g2774.t1	---NA---
g16839.t1	---NA---
g12670.t1	uncharacterized protein MELLADRAFT_106648
g5985.t1	hydrolase 76 protein

g768.t1	hypothetical protein PSTG_09842
g5078.t1	family 10 glycoside hydrolase
g10611.t1	hypothetical protein PCASD_07877
g2174.t1	hypothetical protein PGTUg99_011480
g3569.t1	uncharacterized protein MELLADRAFT_109863
g4548.t1	uncharacterized protein LOC115743464
g1487.t1	GPI anchored CFEM domain protein C
g17437.t1	hypothetical protein PGT21_020166
g16704.t1	---NA---
g6738.t1	hypothetical protein PSTG_03813
g9926.t1	uncharacterized protein MELLADRAFT_71192
g2472.t1	---NA---
g9005.t1	---NA---
g17758.t1	hypothetical protein PTTG_12365
g18208.t1	---NA---
g5406.t1	hypothetical protein PCASD_18809
g16500.t1	hypothetical protein VP01_3183g3
g3290.t1	hypothetical protein CROQUDRAFT_359464
g16998.t1	---NA---
g11506.t1	hypothetical protein
g16473.t2	hypothetical protein TWF706_004243
g6612.t1	uncharacterized protein VP01_920g2
g12289.t1	hypothetical protein PSTT_13365
g15687.t1	---NA---
g11678.t1	---NA---
g3300.t1	hypothetical protein PTTG_12151
g14717.t1	hypothetical protein PTTG_28580
g11725.t1	---NA---
g3296.t1	hypothetical protein PTTG_04707
g11131.t1	---NA---
g14475.t1	hypothetical protein PCASD_01135
g9148.t2	hypothetical protein PSTG_08958
g2073.t1	single-strand binding protein family
g4287.t1	---NA---
g5561.t1	hypothetical protein PSTG_05541
g8821.t1	---NA---
g387.t1	hypothetical protein PTTG_06681, partial
g10769.t1	---NA---
g11393.t1	---NA---
g14813.t1	---NA---
g15716.t1	---NA---
g3796.t1	uncharacterized protein MELLADRAFT_106648
g1490.t1	---NA---
g12473.t1	hypothetical protein PCASD_18539
g977.t1	---NA---
g1245.t1	hypothetical protein PGTG_09326

g15544.t1	Peptidyl-prolyl cis-trans isomerase B
g5733.t1	hypothetical protein PTTG_00841
g14456.t1	Mitochondrial carrier protein ymc2
g2154.t1	secreted protein
g9814.t1	---NA---
g13646.t1	---NA---
g5872.t1	---NA---
g14392.t1	---NA---
g16911.t1	---NA---
g11170.t1	---NA---
g1647.t1	family 4 carbohydrate esterase
g2622.t1	hypothetical protein PCANC_06901
g10029.t1	---NA---
g13868.t1	---NA---
g2699.t1	secreted protein
g5914.t1	---NA---
g17398.t1	hypothetical protein VP01_2502g1
g9957.t1	---NA---
g199.t1	hypothetical protein PSTG_15974
g5402.t1	hypothetical protein PSTG_10920
g10309.t1	---NA---
g11280.t1	hypothetical protein PGT21_035294
g13910.t1	hypothetical protein BT93_B1004
g17974.t1	putative uncharacterized protein 86B
g15225.t1	2,3-bisphosphoglycerate-independent phosphoglycerate mutase
g1935.t1	---NA---
g3031.t1	---NA---
g15491.t1	---NA---
g2422.t1	hypothetical protein PGTG_04985
g13363.t1	alginate export family protein
g13719.t1	---NA---
g15077.t1	---NA---
g4663.t1	hypothetical protein PCANC_14728
g3551.t1	---NA---
g5449.t1	phosphatidylserine decarboxylase
g15424.t1	hypothetical protein PTTG_25649
g17575.t1	---NA---
g14397.t1	---NA---
g6089.t1	hypothetical protein PCASD_12679
g15807.t1	---NA---
g1894.t1	hypothetical protein PCANC_17395
g3088.t1	---NA---
g5954.t1	---NA---
g16463.t1	---NA---
g9823.t1	hypothetical protein VP01_237g11
g15825.t1	---NA---

g12271.t1	---NA---
g13636.t1	---NA---
g12892.t1	hypothetical protein PTTG_00841
g13308.t1	---NA---
g11867.t1	hypothetical protein PTTG_07960
g16530.t1	hypothetical protein PCANC_04412
g12043.t1	---NA---
g16952.t1	---NA---
g15287.t1	hypothetical protein PGTG_06052
g17580.t1	---NA---
g16975.t1	---NA---
g9995.t1	---NA---
g1595.t1	hypothetical protein PGTUg99_032783
g17682.t1	---NA---
g13857.t2	---NA---
g5661.t1	---NA---
g5738.t1	secreted protein
g14108.t1	---NA---
g5808.t1	---NA---
g12300.t1	hypothetical protein PGTUg99_014316
g10400.t1	---NA---
g12687.t1	---NA---
g18071.t1	---NA---
g9852.t1	---NA---
g930.t1	hypothetical protein PGTUg99_025605
g7048.t1	hypothetical protein RR46_05488
g13150.t1	---NA---
g9283.t1	---NA---
g14078.t1	---NA---
g17490.t1	---NA---
g12724.t1	---NA---
g16531.t1	hypothetical protein PCANC_04412
g11350.t1	---NA---
g10952.t1	sodium-dependent noradrenaline transporter-like
g12890.t1	---NA---
g17136.t1	---NA---
g12530.t1	hypothetical protein PGTUg99_005444
g16970.t1	---NA---
g16926.t1	---NA---
g1452.t1	hypothetical protein PGTUg99_036703
g17973.t1	putative uncharacterized protein 86B
g5660.t1	---NA---
g10858.t1	hypothetical protein CA237_10925
g10795.t1	---NA---
g5035.t1	---NA---
g11407.t1	hypothetical protein CROQUDRAFT_659295

g15601.t1	hypothetical protein VP01_3678g2
g2502.t1	hypothetical protein PCANC_21056
g13892.t1	hypothetical protein PSTG_01739
g13284.t1	---NA---
g4147.t1	---NA---
g5740.t1	hypothetical protein CROQUDRAFT_61041
g133.t1	Long chronological lifespan protein 2
g15514.t1	uncharacterized protein MELLADRAFT_85819
g5899.t1	hypothetical protein PCASD_03447
g3424.t1	hypothetical protein PTTG_01817
g3926.t1	---NA---
g2914.t1	---NA---
g7888.t1	hypothetical protein PSHT_14600
g4553.t1	---NA---
g12843.t1	hypothetical protein PTTG_01817
g16342.t1	---NA---
g130.t1	---NA---
g15597.t1	---NA---
g495.t1	---NA---
g13406.t1	---NA---
g836.t1	---NA---
g12728.t1	hypothetical protein PCASD_05829
g14173.t1	hypothetical protein VP01_1014g3
g10530.t1	---NA---
g17217.t1	---NA---
g17661.t1	hypothetical protein VP01_1014g3
g15265.t1	---NA---
g14283.t1	---NA---
g17255.t1	---NA---
g6676.t1	---NA---
g11292.t1	---NA---
g15702.t1	---NA---
g14240.t1	---NA---
g13520.t1	hypothetical protein PGT21_030525
g15640.t1	---NA---
g4948.t1	---NA---
g2856.t1	hypothetical protein PGT21_012530
g2424.t1	hypothetical protein PCANC_22040
g12112.t1	2,3-bisphosphoglycerate-independent phosphoglycerate mutase
g3932.t1	hypothetical protein PCANC_20635
g11381.t1	Phosphatidylglycerol/phosphatidylinositol transfer protein
g1718.t1	hypothetical protein PGT21_036673
g15997.t1	hypothetical protein PTTG_02065
g6221.t1	hypothetical protein PSTG_16974
g18421.t1	hypothetical protein PSHT_06615
g3653.t1	---NA---

g17076.t1	hypothetical protein PTTG_01817
g18171.t1	---NA---
g6831.t1	---NA---
g17782.t1	---NA---
g6788.t1	---NA---
g11393.t2	---NA---
g13487.t1	---NA---
g16284.t1	; MatureChain: 23-228 | Effector probability: 0.741
g6788.t2	---NA---
g3485.t1	---NA---
g3897.t2	hypothetical protein PGT21_025960
g18289.t1	---NA---
g2930.t1	hypothetical protein VP01_1014g3
g4784.t1	---NA---
g14881.t2	hypothetical protein VP01_1014g3
g16560.t1	---NA---
g16790.t1	hypothetical protein PCANC_22341
g17078.t1	hypothetical protein PTTG_01817
g6547.t1	---NA---
g15460.t1	uncharacterized protein VP01_362g24
g13441.t1	trehalose-6-phosphate synthase
g17175.t1	---NA---
g1121.t1	---NA---
g14667.t1	hypothetical protein PGT21_030071
g1477.t1	---NA---
g1263.t1	---NA---
g10367.t1	hypothetical protein PSTG_01739
g16369.t1	---NA---
g9384.t1	---NA---
g10687.t1	---NA---
g13801.t1	---NA---
g13476.t1	---NA---
g6327.t1	hypothetical protein PSTT_11306, partial
g2726.t1	---NA---
g6826.t1	---NA---
g8495.t1	cadherin-86C isoform X2
g8972.t1	---NA---
g15043.t1	---NA---
g2616.t1	---NA---
g10302.t1	hypothetical protein PCANC_18328
g7204.t1	chymotrypsin-like protease CTRL-1 isoform X3
g6765.t1	---NA---
g4950.t1	Dcp1p-Dcp2p decapping enzyme complex alpha subunit
g13814.t1	hypothetical protein PTTG_00841
g5886.t1	hypothetical protein PSTT_07418
g6647.t1	---NA---

g3151.t1	---NA---
g12327.t1	---NA---
g4213.t1	---NA---
g8946.t1	---NA---
g16473.t1	hypothetical protein TWF706_004243
g10334.t1	hypothetical protein PCANC_00258
g5574.t1	---NA---
g3741.t1	hypothetical protein CROQUDRAFT_61041
g317.t1	hypothetical protein, variant
g265.t1	---NA---
g6737.t1	hypothetical protein VP01_168g4
g17471.t1	---NA---
g11403.t1	hypothetical protein PGTG_17519
g4850.t1	---NA---
g2059.t2	---NA---
g11855.t1	---NA---
g5341.t1	---NA---
g7785.t1	DUF3297 family protein
g10013.t1	hypothetical protein PSTG_10920
g524.t2	---NA---
g7009.t1	---NA---
g13542.t1	---NA---
g889.t1	---NA---
g149.t1	hypothetical protein PTTG_12661
g15809.t1	hypothetical protein CROQUDRAFT_699647
g1555.t1	---NA---
g14932.t1	---NA---
g8025.t1	---NA---
g418.t1	hypothetical protein PCANC_26603
g549.t1	carbohydrate esterase family 1 protein
g13990.t1	hypothetical protein CROQUDRAFT_49918
g3159.t1	---NA---
g16960.t1	---NA---
g11682.t1	---NA---
g6986.t1	---NA---
g10389.t1	---NA---
g5555.t1	---NA---
g10920.t1	hypothetical protein PGTG_11258
g10035.t1	beta glucosidase precursor
g8578.t1	DUF411 domain-containing protein
g10438.t1	---NA---
g1485.t1	---NA---
g10696.t1	---NA---
g18533.t1	hypothetical protein PGTG_02169

APPENDIX C. List of GO terms obtained by Blast2GO from effector candidates of MF-1 biotype

ID Sequence	Description
evm.model.NODE_10061_length_10145_cov_0.0507087.1	alpha,alpha-trehalose-phosphate synthase (UDP-forming)
evm.model.NODE_10152_length_10096_cov_0.832481.1	hypothetical protein PSTG_09842
evm.model.NODE_10225_length_10054_cov_0.703536.1	---NA---
evm.model.NODE_10347_length_9998_cov_1.27474.2	hypothetical protein PSTG_08958
evm.model.NODE_10399_length_9973_cov_17.2373.3	---NA---
evm.model.NODE_104004_length_2112_cov_1.66801.1	---NA---
evm.model.NODE_10462_length_9942_cov_1.10912.2	hypothetical protein VP01_1014g3
evm.model.NODE_10530_length_9908_cov_0.717514.4	---NA---
evm.model.NODE_10569_length_9889_cov_0.720242.1	hypothetical protein PGTG_12331
evm.model.NODE_105_length_55253_cov_0.45355.1	---NA---
evm.model.NODE_1060_length_27712_cov_0.666751.1	---NA---
evm.model.NODE_1074_length_27621_cov_1.26717.2	hypothetical protein CROQUDRAFT_658791
evm.model.NODE_11108_length_9646_cov_0.920475.1	hypothetical protein PCASD_22376
evm.model.NODE_11112_length_9643_cov_0.62768.1	hypothetical protein PTTG_12365
evm.model.NODE_11176_length_9608_cov_0.896003.1	---NA---
evm.model.NODE_11209_length_9589_cov_0.266751.1	hypothetical protein PGT21_027923
evm.model.NODE_11232_length_9577_cov_1.54677.3	hypothetical protein PGTG_17519
evm.model.NODE_11274_length_9557_cov_0.67561.2	hypothetical protein, variant
evm.model.NODE_11428_length_9490_cov_0.763695.1	uncharacterized protein MELLADRAFT_85819
evm.model.NODE_114746_length_1891_cov_0.502268.1	---NA---
evm.model.NODE_11687_length_9385_cov_1.54699.2	---NA---
evm.model.NODE_1172_length_26737_cov_0.188193.1	putative uncharacterized protein 86B
evm.model.NODE_11786_length_9347_cov_1.30542.1	hypothetical protein PCASD_05829
evm.model.NODE_11794_length_9343_cov_0.50255.1	uncharacterized protein MELLADRAFT_124586
evm.model.NODE_1187_length_26556_cov_0.308868.2	---NA---
evm.model.NODE_11912_length_9294_cov_0.491655.1	---NA---
evm.model.NODE_11_length_86909_cov_0.133459.3	---NA---
evm.model.NODE_12087_length_9232_cov_0.709061.1	---NA---
evm.model.NODE_12169_length_9205_cov_0.451481.1	---NA---
evm.model.NODE_12191_length_9196_cov_0.891534.1	---NA---
evm.model.NODE_12201_length_9196_cov_0.656302.1	---NA---
evm.model.NODE_123330_length_1735_cov_1.20522.1	---NA---
evm.model.NODE_12378_length_9131_cov_0.962914.1	---NA---
evm.model.NODE_12491_length_9093_cov_0.505688.1	hypothetical protein PCANC_18523
evm.model.NODE_12507_length_9082_cov_0.159058.2	Reversal of tor2 lethality
evm.model.NODE_12611_length_9049_cov_0.544945.3	hypothetical protein PSTT_08273, partial
evm.model.NODE_127356_length_1668_cov_0.0661908.1	---NA---
evm.model.NODE_12741_length_9006_cov_0.176484.1	---NA---
evm.model.NODE_12743_length_9006_cov_0.699628.1	hypothetical protein PSHT_14808
evm.model.NODE_12793_length_8993_cov_0.571622.3	---NA---
evm.model.NODE_128173_length_1656_cov_0.691302.1	---NA---

evm.model.NODE_131451_length_1605_cov_1.44655.1	---NA---
evm.model.NODE_133257_length_1578_cov_1.36527.1	---NA---
evm.model.NODE_13415_length_8785_cov_0.517672.2	---NA---
evm.model.NODE_13447_length_8775_cov_0.4493.2	---NA---
evm.model.NODE_135553_length_1546_cov_1.04299.1	---NA---
evm.model.NODE_135553_length_1546_cov_1.04299.2	---NA---
evm.model.NODE_13633_length_8716_cov_0.215275.1	---NA---
evm.model.NODE_13647_length_8711_cov_0.688956.4	hypothetical protein CROQUDRAFT_670094
evm.model.NODE_13752_length_8677_cov_0.852865.1	hypothetical protein PCASD_05829
evm.model.NODE_13755_length_8677_cov_0.62.1	hypothetical protein PSTT_12330
evm.model.NODE_137688_length_1516_cov_1.0036.1	---NA---
evm.model.NODE_13939_length_8621_cov_1.12668.3	---NA---
evm.model.NODE_139_length_51599_cov_0.560033.2	hypothetical protein PCANC_22108
evm.model.NODE_1401_length_25092_cov_0.323334.1	---NA---
evm.model.NODE_14121_length_8545_cov_0.464531.1	uncharacterized protein MELLADRAFT_102573
evm.model.NODE_14478_length_8456_cov_1.05451.2	uncharacterized protein MELLADRAFT_124586
evm.model.NODE_14556_length_8430_cov_0.588582.2	---NA---
evm.model.NODE_14970_length_8304_cov_0.597261.1	---NA---
evm.model.NODE_15002_length_8298_cov_0.549137.1	---NA---
evm.model.NODE_15054_length_8284_cov_1.25043.1	CSEP-35, partial
evm.model.NODE_150611_length_1345_cov_0.1	hypothetical protein PCASD_18539
evm.model.NODE_15174_length_8249_cov_0.443487.1	---NA---
evm.model.NODE_1521_length_24252_cov_1.0121.1	---NA---
evm.model.NODE_15340_length_8203_cov_0.106625.1	---NA---
evm.model.NODE_15375_length_8185_cov_0.378348.2	---NA---
evm.model.NODE_1543_length_24159_cov_0.485562.1	---NA---
evm.model.NODE_154410_length_1299_cov_0.384812.1	---NA---
evm.model.NODE_15472_length_8166_cov_1.05996.1	hypothetical protein PCANC_04412
evm.model.NODE_15519_length_8153_cov_0.999377.2	---NA---
evm.model.NODE_15626_length_8122_cov_1.19235.1	---NA---
evm.model.NODE_15688_length_8108_cov_1.01428.1	hypothetical protein PGTG_11258
evm.model.NODE_15804_length_8083_cov_0.214429.1	hypothetical protein PCASD_09322
evm.model.NODE_15836_length_8076_cov_0.739338.1	hypothetical protein PGTG_02939
evm.model.NODE_15944_length_8047_cov_1.14973.1	---NA---
evm.model.NODE_1600_length_23783_cov_1.50397.5	---NA---
evm.model.NODE_161229_length_1221_cov_4.3766.1	hypothetical protein PSTG_11145
evm.model.NODE_16422_length_7909_cov_0.220044.1	---NA---
evm.model.NODE_16423_length_7930_cov_0.859926.2	---NA---
evm.model.NODE_16665_length_7877_cov_0.280351.1	---NA---
evm.model.NODE_16670_length_7878_cov_1.91511.2	---NA---
evm.model.NODE_16740_length_7856_cov_0.165482.1	hypothetical protein VP01_3183g3
evm.model.NODE_167661_length_1151_cov_0.768555.1	---NA---
evm.model.NODE_16776_length_7854_cov_0.763427.3	---NA---
evm.model.NODE_16851_length_7839_cov_0.835581.1	hypothetical protein PTTG_11740

evm.model.NODE_17047_length_7793_cov_0.273379.1	hypothetical protein PSTG_01739
evm.model.NODE_17070_length_7788_cov_0.437671.1	hypothetical protein PCANC_18328
evm.model.NODE_1717_length_23147_cov_0.744494.2	---NA---
evm.model.NODE_17345_length_7727_cov_0.360395.1	---NA---
evm.model.NODE_17377_length_7721_cov_0.241375.1	---NA---
evm.model.NODE_17418_length_7712_cov_0.404087.1	---NA---
evm.model.NODE_17469_length_7699_cov_0.658743.1	---NA---
evm.model.NODE_1747_length_22938_cov_1.23273.1	---NA---
evm.model.NODE_1751_length_22899_cov_0.396259.2	---NA---
evm.model.NODE_17596_length_7670_cov_0.351982.1	alpha beta-hydrolase
evm.model.NODE_17650_length_7657_cov_0.811421.1	hypothetical protein PSHT_10412
evm.model.NODE_1768_length_22731_cov_0.761502.2	---NA---
evm.model.NODE_17742_length_7635_cov_0.85895.1	family 4 carbohydrate
evm.model.NODE_17766_length_7629_cov_0.216742.1	---NA---
evm.model.NODE_17812_length_7621_cov_1.97278.4	hypothetical protein PSTT_07418
evm.model.NODE_17921_length_7595_cov_0.373058.1	---NA---
evm.model.NODE_1793_length_22625_cov_0.6064.2	CSEP-35, partial
evm.model.NODE_18203_length_7530_cov_0.816831.2	polar growth
evm.model.NODE_18659_length_7423_cov_1.75308.2	carboxypeptidase D
evm.model.NODE_18723_length_7409_cov_1.43408.1	hypothetical protein PGTG_00965
evm.model.NODE_18795_length_7393_cov_0.537022.1	---NA---
evm.model.NODE_18838_length_7381_cov_0.855114.1	hypothetical protein PGTUg99_019843
evm.model.NODE_19449_length_7248_cov_1.41983.2	---NA---
evm.model.NODE_20012_length_7131_cov_0.803969.1	---NA---
evm.model.NODE_20016_length_7129_cov_0.858183.1	---NA---
evm.model.NODE_20061_length_7120_cov_1.91105.4	uncharacterized protein VP01_362g24
evm.model.NODE_20239_length_7088_cov_0.730068.1	hypothetical protein PCANC_22341
evm.model.NODE_20426_length_7056_cov_0.480445.1	---NA---
evm.model.NODE_20451_length_7051_cov_0.568602.1	---NA---
evm.model.NODE_20477_length_7046_cov_0.544154.1	---NA---
evm.model.NODE_20576_length_7027_cov_1.6387.2	---NA---
evm.model.NODE_2061_length_21333_cov_0.314864.1	---NA---
evm.model.NODE_20670_length_7007_cov_0.489971.1	hypothetical protein PGT21_025600
evm.model.NODE_20733_length_6994_cov_1.04733.1	---NA---
evm.model.NODE_2075_length_21285_cov_0.389734.2	hypothetical protein PTTG_04707
evm.model.NODE_2099_length_21180_cov_0.647858.3	---NA---
evm.model.NODE_21040_length_6916_cov_0.875441.2	hypothetical protein PCANC_08280
evm.model.NODE_2137_length_21017_cov_0.479943.1	hypothetical protein PCASD_07877
evm.model.NODE_21468_length_6852_cov_0.295613.1	---NA---
evm.model.NODE_214_length_45606_cov_0.34733.1	---NA---
evm.model.NODE_215_length_45608_cov_0.342099.2	uncharacterized protein MELLADRAFT_109863
evm.model.NODE_2160_length_20942_cov_0.93375.2	---NA---
evm.model.NODE_21744_length_6797_cov_0.678561.2	hypothetical protein VP01_1014g3
evm.model.NODE_21756_length_6789_cov_0.714179.1	---NA---
evm.model.NODE_21773_length_6791_cov_0.847539.1	---NA---
evm.model.NODE_22544_length_6661_cov_0.699265.1	---NA---

evm.model.NODE_2266_length_20454_cov_0.872091.3	---NA---
evm.model.NODE_22848_length_6612_cov_1.14079.1	---NA---
evm.model.NODE_2287_length_20383_cov_0.512243.1	---NA---
evm.model.NODE_23109_length_6569_cov_0.855324.2	---NA---
evm.model.NODE_23344_length_6532_cov_0.712769.1	---NA---
evm.model.NODE_23552_length_6500_cov_0.90805.1	---NA---
evm.model.NODE_2361_length_20081_cov_0.466553.1	hypothetical protein PCANC_20635
evm.model.NODE_24204_length_6402_cov_0.414343.1	---NA---
evm.model.NODE_24357_length_6382_cov_0.354117.1	---NA---
evm.model.NODE_2488_length_19599_cov_1.25.3	hypothetical protein CROQUDRAFT_664478
evm.model.NODE_2496_length_19561_cov_0.842996.3	hypothetical protein PTTG_25847
evm.model.NODE_25339_length_6259_cov_1.47048.2	---NA---
evm.model.NODE_2556_length_19410_cov_0.342789.1	hypothetical protein PCANC_17395
evm.model.NODE_25723_length_6213_cov_1.77834.1	---NA---
evm.model.NODE_25911_length_6188_cov_0.873618.2	alpha beta-hydrolase
evm.model.NODE_262_length_42745_cov_0.94878.1	---NA---
evm.model.NODE_2638_length_19144_cov_0.79755.1	hypothetical protein PGT21_030525
evm.model.NODE_2644_length_19126_cov_0.597874.1	hypothetical protein PTTG_00895
evm.model.NODE_26533_length_6113_cov_2.23154.2	---NA---
evm.model.NODE_26623_length_6099_cov_0.992802.1	hypothetical protein PGT21_003963
evm.model.NODE_26741_length_6086_cov_0.331096.1	---NA---
evm.model.NODE_27074_length_6045_cov_1.07722.1	---NA---
evm.model.NODE_2715_length_18873_cov_0.615565.1	---NA---
evm.model.NODE_2744_length_18764_cov_0.703064.1	---NA---
evm.model.NODE_2770_length_18665_cov_1.63449.1	hypothetical protein PGTG_16623
evm.model.NODE_27877_length_5954_cov_0.473314.1	---NA---
evm.model.NODE_28014_length_5936_cov_0.422104.1	---NA---
evm.model.NODE_28303_length_5903_cov_0.666551.1	hypothetical protein CROQUDRAFT_89685
evm.model.NODE_2856_length_18375_cov_1.15493.1	---NA---
evm.model.NODE_28608_length_5870_cov_0.279122.1	uncharacterized protein MELLADRAFT_124586
evm.model.NODE_28763_length_5852_cov_0.907265.1	---NA---
evm.model.NODE_2876_length_18335_cov_0.47221.3	---NA---
evm.model.NODE_28797_length_5848_cov_0.290509.1	---NA---
evm.model.NODE_28950_length_5829_cov_1.03016.1	---NA---
evm.model.NODE_29272_length_5795_cov_1.39132.1	hypothetical protein PSTG_11669
evm.model.NODE_29340_length_5789_cov_1.35694.2	hypothetical protein PTTG_00474
evm.model.NODE_2985_length_18064_cov_0.808674.5	alpha,alpha-trehalose-phosphate synthase (UDP-forming)
evm.model.NODE_30167_length_5704_cov_0.64246.1	---NA---
evm.model.NODE_30292_length_5692_cov_0.54583.1	hypothetical protein PGT21_005845
evm.model.NODE_30385_length_5682_cov_0.453105.1	hypothetical protein PGT21_012530
evm.model.NODE_30437_length_5676_cov_0.30474.1	---NA---
evm.model.NODE_30470_length_5673_cov_1.08186.1	---NA---
evm.model.NODE_30484_length_5672_cov_0.655005.1	hypothetical protein PGTG_17002
evm.model.NODE_306_length_40808_cov_0.610555.1	---NA---

evm.model.NODE_31145_length_5605_cov_0.239321.1	hypothetical protein PTTG_01451, partial
evm.model.NODE_31334_length_5585_cov_0.0443386.1	---NA---
evm.model.NODE_31345_length_5584_cov_0.223016.1	hypothetical protein PGT21_026307
evm.model.NODE_31408_length_5577_cov_0.620367.1	---NA---
evm.model.NODE_31568_length_5559_cov_0.333211.1	---NA---
evm.model.NODE_31591_length_5557_cov_0.401105.1	hypothetical protein PCANC_23330
evm.model.NODE_31592_length_5557_cov_0.88232.1	hypothetical protein PCANC_15928
evm.model.NODE_31678_length_5549_cov_0.815382.1	---NA---
evm.model.NODE_3255_length_17366_cov_0.286377.1	---NA---
evm.model.NODE_3285_length_17284_cov_0.699598.2	hypothetical protein PCASD_16951
evm.model.NODE_32908_length_5423_cov_1.11782.2	hypothetical protein PGTUg99_033957
evm.model.NODE_33375_length_5373_cov_1.81395.1	hypothetical protein PSTT_10230
evm.model.NODE_33392_length_5371_cov_0.889207.2	---NA---
evm.model.NODE_33603_length_5352_cov_1.82086.2	hypothetical protein PSTG_07801
evm.model.NODE_33895_length_5326_cov_0.483362.1	---NA---
evm.model.NODE_33933_length_5321_cov_0.561995.1	---NA---
evm.model.NODE_3408_length_16981_cov_1.40977.3	hypothetical protein PGTG_06052
evm.model.NODE_34254_length_5289_cov_0.923867.1	---NA---
evm.model.NODE_3425_length_16954_cov_1.12177.2	---NA---
evm.model.NODE_34381_length_5277_cov_0.283883.1	---NA---
evm.model.NODE_34818_length_5238_cov_0.799452.1	hypothetical protein PCANC_21290
evm.model.NODE_34859_length_5234_cov_0.768357.1	---NA---
evm.model.NODE_3491_length_16812_cov_1.27576.3	---NA---
evm.model.NODE_35022_length_5219_cov_0.809505.2	---NA---
evm.model.NODE_35140_length_5210_cov_0.691324.1	---NA---
evm.model.NODE_35185_length_5204_cov_1.13098.1	---NA---
evm.model.NODE_35347_length_5190_cov_0.343935.1	---NA---
evm.model.NODE_35350_length_5186_cov_0.240221.1	---NA---
evm.model.NODE_354_length_39246_cov_0.895862.1	---NA---
evm.model.NODE_3559_length_16610_cov_0.298914.1	---NA---
evm.model.NODE_35654_length_5164_cov_0.948978.1	hypothetical protein PGTUg99_026562
evm.model.NODE_360_length_39094_cov_0.299261.2	hypothetical protein PSTG_02734
evm.model.NODE_36327_length_5104_cov_0.212578.1	hypothetical protein PSTG_05541
evm.model.NODE_36746_length_5068_cov_0.660393.1	Alpha Beta hydrolase
evm.model.NODE_37124_length_5036_cov_1.03585.1	---NA---
evm.model.NODE_3753_length_16153_cov_0.416838.1	---NA---
evm.model.NODE_3763_length_16150_cov_0.576671.1	---NA---
evm.model.NODE_37766_length_4983_cov_0.484349.1	---NA---
evm.model.NODE_38089_length_4957_cov_0.561698.1	hypothetical protein PTTG_01431
evm.model.NODE_38840_length_4894_cov_1.57562.1	---NA---
evm.model.NODE_38995_length_4882_cov_1.60126.4	---NA---
evm.model.NODE_39355_length_4852_cov_0.340106.1	hypothetical protein CROQUDRAFT_61041
evm.model.NODE_39546_length_4840_cov_0.859962.1	---NA---
evm.model.NODE_3999_length_15719_cov_1.10076.1	hypothetical protein CROQUDRAFT_359464

evm.model.NODE_4004_length_15711_cov_0.468848.2	plasma membrane H+-ATPase
evm.model.NODE_40050_length_4800_cov_0.812326.1	hypothetical protein PTTG_25649
evm.model.NODE_40251_length_4784_cov_0.630878.1	Guanyl-specific ribonuclease F1
evm.model.NODE_41125_length_4715_cov_0.45728.1	---NA---
evm.model.NODE_41221_length_4707_cov_0.434061.2	---NA---
evm.model.NODE_41239_length_4704_cov_0.740991.1	---NA---
evm.model.NODE_41885_length_4657_cov_0.907506.1	hypothetical protein PSHT_14635
evm.model.NODE_41959_length_4652_cov_0.226519.2	---NA---
evm.model.NODE_42552_length_4612_cov_0.33913.1	hypothetical protein CROQUDRAFT_699647
evm.model.NODE_42655_length_4604_cov_0.279875.1	hypothetical protein CROQUDRAFT_670837
evm.model.NODE_4272_length_15245_cov_1.3394.7	Encoded by
evm.model.NODE_4275_length_15239_cov_1.17988.2	---NA---
evm.model.NODE_42799_length_4595_cov_0.305282.1	---NA---
evm.model.NODE_4300_length_15213_cov_1.43309.2	---NA---
evm.model.NODE_43077_length_4576_cov_0.219825.1	Mitochondrial carrier ymc2
evm.model.NODE_4319_length_15189_cov_1.76232.5	---NA---
evm.model.NODE_4319_length_15189_cov_1.76232.8	---NA---
evm.model.NODE_4351_length_15142_cov_1.48465.1	---NA---
evm.model.NODE_43844_length_4524_cov_1.04298.2	---NA---
evm.model.NODE_44175_length_4501_cov_0.595107.1	hypothetical protein PSHT_05208
evm.model.NODE_4428_length_15041_cov_0.398283.1	---NA---
evm.model.NODE_4445_length_15006_cov_0.703475.2	---NA---
evm.model.NODE_44719_length_4465_cov_1.06524.2	---NA---
evm.model.NODE_47016_length_4308_cov_0.743902.1	hypothetical protein PSTG_15024
evm.model.NODE_471_length_36147_cov_0.628061.4	hypothetical protein PTTG_12151
evm.model.NODE_47265_length_4293_cov_0.247.1	hypothetical protein PSTG_10576
evm.model.NODE_47421_length_4284_cov_0.770026.1	---NA---
evm.model.NODE_47468_length_4281_cov_0.437891.1	---NA---
evm.model.NODE_47535_length_4276_cov_0.0556627.2	DEAH-box RNA helicase prp16
evm.model.NODE_47864_length_4256_cov_0.806733.1	---NA---
evm.model.NODE_48455_length_4220_cov_0.780601.1	---NA---
evm.model.NODE_487_length_35803_cov_0.914396.3	---NA---
evm.model.NODE_49333_length_4167_cov_0.681188.1	hypothetical protein PTTG_25847
evm.model.NODE_4936_length_14262_cov_0.336753.1	hypothetical protein CROQUDRAFT_651536
evm.model.NODE_49674_length_4146_cov_0.940035.1	---NA---
evm.model.NODE_4_length_99494_cov_0.351008.4	---NA---
evm.model.NODE_5026_length_14122_cov_0.672621.3	---NA---
evm.model.NODE_50324_length_4107_cov_0.0743719.1	uncharacterized protein MELLADRAFT_116225
evm.model.NODE_50423_length_4101_cov_1.02718.1	2,3-bisphosphoglycerate-independent phosphoglycerate mutase
evm.model.NODE_51001_length_4068_cov_1.38848.1	---NA---
evm.model.NODE_51346_length_4048_cov_2.22494.1	glycoside hydrolase family 7
evm.model.NODE_5144_length_13967_cov_0.811199.2	---NA---
evm.model.NODE_5174_length_13932_cov_0.457081.3	hypothetical protein PSTG_12325

evm.model.NODE_5238_length_13853_cov_0.473956.1	---NA---
evm.model.NODE_52444_length_3985_cov_0.487818.2	---NA---
evm.model.NODE_52873_length_3961_cov_0.143453.1	hypothetical protein PGTG_04481
evm.model.NODE_53034_length_3952_cov_1.53203.1	hypothetical protein CROQUDRAFT_49918
evm.model.NODE_5371_length_13696_cov_0.641241.1	---NA---
evm.model.NODE_53733_length_3913_cov_1.12097.1	hypothetical protein VP01_1014g3
evm.model.NODE_54407_length_3875_cov_0.682836.1	---NA---
evm.model.NODE_54623_length_3866_cov_0.69671.1	hypothetical protein PSTG_11929
evm.model.NODE_54833_length_3853_cov_7.91814.1	unnamed protein product
evm.model.NODE_55075_length_3839_cov_0.0344828.1	hypothetical protein PTTG_08460
evm.model.NODE_55497_length_3818_cov_1.60634.1	hypothetical protein PGTG_06052
evm.model.NODE_5556_length_13483_cov_0.842554.2	---NA---
evm.model.NODE_5586_length_13452_cov_2.96878.4	---NA---
evm.model.NODE_55_length_65597_cov_0.286605.1	hypothetical protein PGT21_020166
evm.model.NODE_5615_length_13416_cov_0.518602.2	---NA---
evm.model.NODE_56533_length_3763_cov_0.503575.1	hypothetical protein PCASD_22545
evm.model.NODE_5695_length_13335_cov_0.919443.1	---NA---
evm.model.NODE_5720_length_13298_cov_0.474148.1	---NA---
evm.model.NODE_573_length_34048_cov_0.387171.1	---NA---
evm.model.NODE_57798_length_3696_cov_0.819277.1	---NA---

APPENDIX D. Blast local of effector candidates from MF-1 and SA biotypes; parameters used: e-value: 10-5 and identity ≥ 40%

Au biotype	MF-1	SA
APSI_P002.15036.t1	evm.model.NODE_16851_length_7839_cov_0.835581.1;	g9203.t1
APSI_P006.9603.t1		
APSI_P012.8977.t1	evm.model.NODE_2644_length_19126_cov_0.597874.1;	g11445.t1
APSI_P011.205.t1	evm.model.NODE_17742_length_7635_cov_0.85895.1;	g1647.t1
APSI_P001.6419.t1		
APSI_P005.10553.t1		g5402.t1
APSI_P014.966.t1	evm.model.NODE_20733_length_6994_cov_1.04733.1;	g13646.t1
APSI_P018.7675.t1	evm.model.NODE_35185_length_5204_cov_1.13098.1;	g14932.t1
APSI_P006.9922.t1	evm.model.NODE_47864_length_4256_cov_0.806733.1;	g16800.t1
APSI_P010.11572.t1		
APSI_P024.16551.t1	evm.model.NODE_1187_length_26556_cov_0.308868.2;	g11393.t2
APSI_P003.2383.t1	evm.model.NODE_18203_length_7530_cov_0.816831.2;	
APSI_P015.12851.t1	evm.model.NODE_16665_length_7877_cov_0.280351.1;	g13308.t1
APSI_P002.15354.t1	evm.model.NODE_2556_length_19410_cov_0.342789.1;	g13658.t1
APSI_P010.12024.t1	evm.model.NODE_3491_length_16812_cov_1.27576.3;	g3834.t1
APSI_P006.9367.t1		
APSI_P019.7991.t1	evm.model.NODE_17377_length_7721_cov_0.241375.1;	g10309.t1
APSI_P019.8249.t1	evm.model.NODE_11786_length_9347_cov_1.30542.1;	g12728.t1
APSI_P001.6256.t1		g16463.t1
APSI_P004.3527.t1		g1452.t1
APSI_P022.4793.t1	evm.model.NODE_10225_length_10054_cov_0.703536.1;	
APSI_P011.762.t1		g18289.t1
APSI_P004.3511.t1	evm.model.NODE_40251_length_4784_cov_0.630878.1;	
APSI_P009.18222.t1		g3575.t1
APSI_P005.10609.t1		g14240.t1
APSI_P010.12051.t1		g16121.t1
APSI_P016.16215.t1	evm.model.NODE_40251_length_4784_cov_0.630878.1;	
APSI_P025.26.t1		
APSI_P007.13556.t1	evm.model.NODE_30167_length_5704_cov_0.64246.1;	g6986.t1
APSI_P002.15484.t1		g18533.t1
APSI_P001.6777.t1	evm.model.NODE_21040_length_6916_cov_0.875441.2;	g14717.t1
APSI_P009.18196.t1	evm.model.NODE_47421_length_4284_cov_0.770026.1;	g6831.t1
APSI_P011.649.t1		
APSI_P006.10044.t1		
APSI_P010.11524.t1	evm.model.NODE_1793_length_22625_cov_0.6064.2;	
APSI_P001.6831.t1	evm.model.NODE_1401_length_25092_cov_0.323334.1;	g9384.t1
APSI_P025.78.t1	evm.model.NODE_12201_length_9196_cov_0.656302.1;	g16960.t1
APSI_P001.6355.t1	evm.model.NODE_10530_length_9908_cov_0.717514.4;	g6647.t1
APSI_P001.6451.t1		g16748.t1
APSI_P014.1260.t1		g14667.t1
APSI_P008.16939.t1	evm.model.NODE_31568_length_5559_cov_0.333211.1;	g13476.t1
APSI_P007.14386.t1		g1487.t1
APSI_P017.12604.t1		

APSI_P003.2486.t1		g18421.t1
APSI_P018.7580.t1	evm.model.NODE_18723_length_7409_cov_1.43408.1;	
APSI_P001.7305.t2	evm.model.NODE_2137_length_21017_cov_0.479943.1;	g1006.t1
APSI_P011.466.t1	evm.model.NODE_42655_length_4604_cov_0.279875.1;	
APSI_P009.18151.t1	evm.model.NODE_2137_length_21017_cov_0.479943.1;	g5886.t1
APSI_P004.2813.t1	evm.model.NODE_2075_length_21285_cov_0.389734.2;	g3296.t1
APSI_P003.2523.t1	evm.model.NODE_11108_length_9646_cov_0.920475.1;	
APSI_P001.6620.t1	evm.model.NODE_34381_length_5277_cov_0.283883.1;	
APSI_P011.602.t1		
APSI_P014.1138.t1		
APSI_P014.965.t1	evm.model.NODE_20733_length_6994_cov_1.04733.1;	g13646.t1
APSI_P012.8789.t1	evm.model.NODE_41959_length_4652_cov_0.226519.2;	g16748.t1
APSI_P009.18155.t1	evm.model.NODE_11232_length_9577_cov_1.54677.3;	g11403.t1
APSI_P006.10210.t1		g1245.t1
APSI_P019.8320.t1		
APSI_P015.13117.t1	evm.model.NODE_12201_length_9196_cov_0.656302.1;	g10530.t1
APSI_P006.9804.t1	evm.model.NODE_42655_length_4604_cov_0.279875.1;	
APSI_P016.16247.t1		
APSI_P001.6257.t1		g16463.t1
APSI_P011.371.t1		g6221.t1
APSI_P014.1291.t1	evm.model.NODE_214_length_45606_cov_0.34733.1;	g12843.t1
APSI_P021.13431.t1		g11599.t1
APSI_P009.17648.t1		g10611.t1
APSI_P001.6823.t1		
APSI_P005.11126.t1	evm.model.NODE_1793_length_22625_cov_0.6064.2;	
APSI_P002.15786.t1		
APSI_P003.1899.t1	evm.model.NODE_11176_length_9608_cov_0.896003.1;	g16369.t1
APSI_P007.14266.t1	evm.model.NODE_2361_length_20081_cov_0.466553.1;	g3932.t1
APSI_P002.15364.t1	evm.model.NODE_11112_length_9643_cov_0.62768.1;	g17758.t1
APSI_P001.7258.t1		
APSI_P025.103.t1		
APSI_P019.7994.t1		
APSI_P004.3462.t1		
APSI_P002.15562.t1	evm.model.NODE_3255_length_17366_cov_0.286377.1;	
APSI_P008.16775.t1	evm.model.NODE_24357_length_6382_cov_0.354117.1;	
APSI_P018.7751.t1		
APSI_P009.17671.t1		g9852.t1
APSI_P012.8996.t1	evm.model.NODE_52873_length_3961_cov_0.143453.1;	g15601.t1
APSI_P001.6658.t1	evm.model.NODE_2075_length_21285_cov_0.389734.2;	g3296.t1
APSI_P004.3640.t1		g10769.t1
APSI_P006.9920.t1	evm.model.NODE_47864_length_4256_cov_0.806733.1;	g13741.t1
APSI_P018.7749.t2		
APSI_P001.6772.t1	evm.model.NODE_4300_length_15213_cov_1.43309.2;	g889.t1
APSI_P002.15163.t1	evm.model.NODE_21040_length_6916_cov_0.875441.2;	g14717.t1
APSI_P003.2484.t1		g18421.t1
APSI_P006.9441.t1	evm.model.NODE_1074_length_27621_cov_1.26717.2;	g845.t1

APSI_P010.12049.t1		g16121.t1
APSI_P029.3864.t1	evm.model.NODE_10347_length_9998_cov_1.27474.2;	g5740.t1
APSI_P010.12130.t1	evm.model.NODE_20426_length_7056_cov_0.480445.1;	g14078.t1
APSI_P002.15781.t1		
APSI_P001.6770.t1		g13814.t1
APSI_P001.5595.t2		g3485.t1
APSI_P003.2073.t1	evm.model.NODE_11912_length_9294_cov_0.491655.1;	g16800.t1
APSI_P017.12463.t1	evm.model.NODE_11_length_86909_cov_0.133459.3;	g13487.t1
APSI_P002.15287.t1	evm.model.NODE_3285_length_17284_cov_0.699598.2;	g17398.t1
APSI_P001.5860.t1	evm.model.NODE_3999_length_15719_cov_1.10076.1;	g3290.t1
APSI_P009.17593.t1	evm.model.NODE_17047_length_7793_cov_0.273379.1;	g10367.t1
APSI_P005.10513.t1	evm.model.NODE_15688_length_8108_cov_1.01428.1;	g14051.t1
APSI_P021.13316.t1	evm.model.NODE_12611_length_9049_cov_0.544945.3;	g5914.t1
APSI_P009.18190.t1	evm.model.NODE_47265_length_4293_cov_0.247.1;	g10611.t1
APSI_P012.9215.t1		g15544.t1
APSI_P018.7748.t2		
APSI_P008.16995.t1		
APSI_P017.12631.t1	evm.model.NODE_4445_length_15006_cov_0.703475.2;	g17471.t1
APSI_P008.17008.t1	evm.model.NODE_2556_length_19410_cov_0.342789.1;	g13658.t1
APSI_P005.10482.t1	evm.model.NODE_52873_length_3961_cov_0.143453.1;	
APSI_P008.16894.t1	evm.model.NODE_11912_length_9294_cov_0.491655.1;	g12530.t1
APSI_P002.14778.t1		g1482.t1
APSI_P015.12819.t1		
APSI_P010.12124.t1	evm.model.NODE_1751_length_22899_cov_0.396259.2;	g11431.t1
APSI_P014.1225.t1		
APSI_P019.8113.t1	evm.model.NODE_15375_length_8185_cov_0.378348.2;	g265.t1
APSI_P026.906.t1	evm.model.NODE_5556_length_13483_cov_0.842554.2;	g14855.t1
APSI_P006.9765.t1	evm.model.NODE_15340_length_8203_cov_0.106625.1;	
APSI_P015.13113.t1		
APSI_P003.2387.t1	evm.model.NODE_4_length_99494_cov_0.351008.4;	g977.t1
APSI_P005.11039.t1	evm.model.NODE_3408_length_16981_cov_1.40977.3;	
APSI_P013.4314.t1	evm.model.NODE_21468_length_6852_cov_0.295613.1;	g10696.t1
APSI_P005.11314.t1		g17424.t1
APSI_P018.7571.t1	evm.model.NODE_20477_length_7046_cov_0.544154.1;	g10438.t1
APSI_P025.77.t1	evm.model.NODE_12201_length_9196_cov_0.656302.1;	g16960.t1
APSI_P016.16105.t1	evm.model.NODE_2099_length_21180_cov_0.647858.3;	g18071.t1
APSI_P013.4035.t1	evm.model.NODE_15519_length_8153_cov_0.999377.2;	
APSI_P001.7354.t1		
APSI_P003.1814.t1		
APSI_P014.1378.t1	evm.model.NODE_15804_length_8083_cov_0.214429.1;	g13581.t1
APSI_P003.1584.t1	evm.model.NODE_24357_length_6382_cov_0.354117.1;	
APSI_P011.659.t1	evm.model.NODE_47016_length_4308_cov_0.743902.1;	g1911.t1
APSI_P016.16116.t2		
APSI_P005.10630.t1	evm.model.NODE_15836_length_8076_cov_0.739338.1;	g845.t1
APSI_P005.10487.t1		
APSI_P001.6338.t1		

APSI_P006.9745.t1		
APSI_P003.2719.t1	evm.model.NODE_16740_length_7856_cov_0.165482.1;	g16500.t1
APSI_P001.6864.t1		
APSI_P003.1555.t1	evm.model.NODE_24357_length_6382_cov_0.354117.1;	
APSI_P005.11042.t1	evm.model.NODE_3408_length_16981_cov_1.40977.3;	
APSI_P010.12123.t1	evm.model.NODE_20426_length_7056_cov_0.480445.1;	g14078.t1
APSI_P004.3623.t1	evm.model.NODE_49333_length_4167_cov_0.681188.1;	g3926.t1
APSI_P022.4675.t1		
APSI_P013.4384.t1	evm.model.NODE_2876_length_18335_cov_0.47221.3;	g3021.t1
APSI_P006.9571.t1	evm.model.NODE_10462_length_9942_cov_1.10912.2;	g14173.t1
APSI_P018.7863.t1		g9957.t1
APSI_P012.9173.t1	evm.model.NODE_55_length_65597_cov_0.286605.1;	g17437.t1
APSI_P014.1460.t1	evm.model.NODE_5026_length_14122_cov_0.672621.3;	
APSI_P017.12533.t1	evm.model.NODE_28950_length_5829_cov_1.03016.1;	g5872.t1
APSI_P016.16246.t1		
APSI_P005.11068.t1		g2424.t1
APSI_P011.212.t1	evm.model.NODE_11274_length_9557_cov_0.67561.2;	g317.t1
APSI_P001.6259.t1		g16463.t1
APSI_P005.10457.t1	evm.model.NODE_354_length_39246_cov_0.895862.1;	g2616.t1
APSI_P019.8306.t1		
APSI_P010.11706.t1		g2774.t1
APSI_P003.1934.t1	evm.model.NODE_29272_length_5795_cov_1.39132.1;	g2174.t1
APSI_P016.16102.t1	evm.model.NODE_2099_length_21180_cov_0.647858.3;	g18071.t1
APSI_P011.198.t1		
APSI_P001.5424.t1	evm.model.NODE_24357_length_6382_cov_0.354117.1;	
APSI_P013.3893.t1	evm.model.NODE_34254_length_5289_cov_0.923867.1;	g9814.t1
APSI_P005.10940.t1		
APSI_P009.17723.t1		g13058.t1
APSI_P006.10022.t1	evm.model.NODE_27074_length_6045_cov_1.07722.1;	g5808.t1
APSI_P008.16771.t1	evm.model.NODE_24357_length_6382_cov_0.354117.1;	
APSI_P006.9317.t1	evm.model.NODE_354_length_39246_cov_0.895862.1;	g2616.t1
APSI_P015.12854.t1	evm.model.NODE_16665_length_7877_cov_0.280351.1;	g13308.t1
APSI_P009.17651.t1		g10611.t1
APSI_P012.8825.t1	evm.model.NODE_53733_length_3913_cov_1.12097.1;	g16285.t1
APSI_P011.451.t1	evm.model.NODE_14121_length_8545_cov_0.464531.1;	
APSI_P007.14191.t1	evm.model.NODE_1060_length_27712_cov_0.666751.1;	g3796.t1
APSI_P015.13112.t1		
APSI_P009.17955.t1		g17490.t1
APSI_P001.6786.t1		g889.t1
APSI_P015.12821.t1		
APSI_P005.11052.t1		
APSI_P018.7552.t1	evm.model.NODE_20670_length_7007_cov_0.489971.1;	
APSI_P012.9228.t1	evm.model.NODE_15472_length_8166_cov_1.05996.1;	g16530.t1
APSI_P004.3557.t1		g5985.t1
APSI_P018.7577.t1	evm.model.NODE_18723_length_7409_cov_1.43408.1;	
APSI_P006.9913.t1	evm.model.NODE_104004_length_2112_cov_1.66801.1;	g13741.t1

APSI_P010.11859.t1	evm.model.NODE_10569_length_9889_cov_0.720242.1;	g2183.t1
APSI_P007.13871.t1		
APSI_P004.3443.t1		g4160.t1
APSI_P006.9908.t1	evm.model.NODE_47864_length_4256_cov_0.806733.1;	g16800.t1
APSI_P005.10801.t1		
APSI_P004.2955.t1		
APSI_P017.12414.t1	evm.model.NODE_3559_length_16610_cov_0.298914.1;	g17136.t1
APSI_P014.1073.t1		g5402.t1
APSI_P001.7080.t1		
APSI_P005.10948.t1		
APSI_P015.12682.t1		
APSI_P001.7305.t1	evm.model.NODE_2137_length_21017_cov_0.479943.1;	g1006.t1
APSI_P008.17405.t1		g17255.t1
APSI_P023.8485.t1	evm.model.NODE_2856_length_18375_cov_1.15493.1;	g15702.t1
APSI_P005.10475.t1	evm.model.NODE_52873_length_3961_cov_0.143453.1;	g12530.t1
APSI_P003.2401.t1		g387.t1
APSI_P010.12091.t1	evm.model.NODE_154410_length_1299_cov_0.384812.1;	g4948.t1
APSI_P004.3683.t1		g495.t1
APSI_P001.7224.t1	evm.model.NODE_14556_length_8430_cov_0.588582.2;	g3709.t1
APSI_P016.16287.t1	evm.model.NODE_20451_length_7051_cov_0.568602.1;	g15687.t1
APSI_P009.17508.t1		g18168.t1
APSI_P001.5855.t1	evm.model.NODE_42552_length_4612_cov_0.33913.1;	g15809.t1
APSI_P002.15332.t1		g17107.t2
APSI_P002.15483.t1		g18533.t1
APSI_P008.16742.t1	evm.model.NODE_55075_length_3839_cov_0.0344828.1;	
APSI_P014.977.t1		g3031.t1
APSI_P023.8467.t1		
APSI_P009.18175.t1	evm.model.NODE_47468_length_4281_cov_0.437891.1;	
APSI_P017.12167.t1		g149.t1
APSI_P011.414.t1	evm.model.NODE_14121_length_8545_cov_0.464531.1;	
APSI_P008.17264.t1	evm.model.NODE_21744_length_6797_cov_0.678561.2;	g17661.t1
APSI_P001.5334.t1	evm.model.NODE_11209_length_9589_cov_0.266751.1;	
APSI_P006.9550.t1		
APSI_P010.12119.t1	evm.model.NODE_1751_length_22899_cov_0.396259.2;	g11431.t1
APSI_P001.7100.t1	evm.model.NODE_16670_length_7878_cov_1.91511.2;	g17580.t1
APSI_P002.14561.t1	evm.model.NODE_29272_length_5795_cov_1.39132.1;	g11407.t1
APSI_P004.2826.t1		
APSI_P013.4315.t1	evm.model.NODE_23109_length_6569_cov_0.855324.2;	g10696.t1
APSI_P006.9501.t1	evm.model.NODE_11794_length_9343_cov_0.50255.1;	g15193.t1
APSI_P003.2095.t1	evm.model.NODE_11912_length_9294_cov_0.491655.1;	g16800.t1
APSI_P016.16039.t1	evm.model.NODE_4445_length_15006_cov_0.703475.2;	g17471.t1
APSI_P009.17696.t1	evm.model.NODE_13415_length_8785_cov_0.517672.2;	g16998.t1
APSI_P001.7435.t1	evm.model.NODE_12793_length_8993_cov_0.571622.3;	
APSI_P029.3884.t1	evm.model.NODE_10347_length_9998_cov_1.27474.2;	g5740.t1
APSI_P014.1360.t1	evm.model.NODE_38995_length_4882_cov_1.60126.4;	g5886.t1
APSI_P005.10459.t1		g11867.t1

APSI_P006.9475.t1	evm.model.NODE_4428_length_15041_cov_0.398283.1;	g11725.t1
APSI_P003.2310.t1	evm.model.NODE_28763_length_5852_cov_0.907265.1;	g836.t1
APSI_P003.1841.t1	evm.model.NODE_22544_length_6661_cov_0.699265.1;	g2616.t1
APSI_P004.3492.t1	evm.model.NODE_1717_length_23147_cov_0.744494.2;	
APSI_P022.4818.t1		
APSI_P003.2394.t1	evm.model.NODE_18203_length_7530_cov_0.816831.2;	
APSI_P005.10949.t1		
APSI_P012.9205.t1		
APSI_P001.6649.t1	evm.model.NODE_34381_length_5277_cov_0.283883.1;	
APSI_P013.3906.t1		
APSI_P020.4846.t1	evm.model.NODE_1768_length_22731_cov_0.761502.2;	g2914.t1
APSI_P013.4116.t1	evm.model.NODE_215_length_45608_cov_0.342099.2;	g3569.t1
APSI_P001.7180.t1	evm.model.NODE_12491_length_9093_cov_0.505688.1;	g14173.t1
APSI_P011.707.t1	evm.model.NODE_54833_length_3853_cov_7.91814.1;	
APSI_P015.13124.t1	evm.model.NODE_12201_length_9196_cov_0.656302.1;	g10530.t1
APSI_P005.11140.t1	evm.model.NODE_1793_length_22625_cov_0.6064.2;	
APSI_P020.4880.t1		
APSI_P002.15052.t1		
APSI_P016.16126.t1	evm.model.NODE_36746_length_5068_cov_0.660393.1;	g3090.t1
APSI_P006.9494.t1	evm.model.NODE_13415_length_8785_cov_0.517672.2;	g16926.t1
APSI_P003.1911.t1		
APSI_P003.1780.t1		
APSI_P008.17145.t1	evm.model.NODE_214_length_45606_cov_0.34733.1;	g17078.t1
APSI_P002.15177.t1	evm.model.NODE_21040_length_6916_cov_0.875441.2;	g14717.t1
APSI_P009.17587.t1	evm.model.NODE_31568_length_5559_cov_0.333211.1;	g13476.t1
APSI_P018.7870.t1	evm.model.NODE_30484_length_5672_cov_0.655005.1;	g13520.t1
APSI_P006.9892.t1	evm.model.NODE_17345_length_7727_cov_0.360395.1;	g1490.t1
APSI_P007.14323.t1		g6765.t1
APSI_P008.17121.t1	evm.model.NODE_50324_length_4107_cov_0.0743719.1;	
APSI_P004.3158.t1	evm.model.NODE_39546_length_4840_cov_0.859962.1;	g16473.t2
APSI_P004.3404.t1	evm.model.NODE_47864_length_4256_cov_0.806733.1;	g15702.t1
APSI_P016.16235.t1	evm.model.NODE_43844_length_4524_cov_1.04298.2;	g9005.t1
APSI_P002.15789.t1		
APSI_P007.13902.t1	evm.model.NODE_1172_length_26737_cov_0.188193.1;	g17973.t1
APSI_P005.10357.t1		g2856.t1
APSI_P025.73.t1	evm.model.NODE_12201_length_9196_cov_0.656302.1;	g16960.t1
APSI_P006.9715.t1		
APSI_P021.13365.t1	evm.model.NODE_17070_length_7788_cov_0.437671.1;	g10302.t1
APSI_P013.4092.t3		
APSI_P010.12148.t1	evm.model.NODE_53034_length_3952_cov_1.53203.1;	g418.t1
APSI_P010.11494.t1		g15491.t1
APSI_P005.10833.t1		g1245.t1
APSI_P009.17592.t1	evm.model.NODE_13755_length_8677_cov_0.62.1;	g768.t1
APSI_P002.15557.t1	evm.model.NODE_3255_length_17366_cov_0.286377.1;	
APSI_P027.7471.t1	evm.model.NODE_1747_length_22938_cov_1.23273.1;	g2331.t1
APSI_P003.1676.t1	evm.model.NODE_39355_length_4852_cov_0.340106.1;	g3741.t1

APSI_P001.7237.t1	evm.model.NODE_14556_length_8430_cov_0.588582.2;	g3709.t1
APSI_P003.2206.t1	evm.model.NODE_12201_length_9196_cov_0.656302.1;	g12890.t1
APSI_P010.12112.t1	evm.model.NODE_10569_length_9889_cov_0.720242.1;	g2183.t1
APSI_P022.4814.t1		
APSI_P012.8857.t1	evm.model.NODE_5371_length_13696_cov_0.641241.1;	
APSI_P012.9231.t1		
APSI_P004.2893.t1		
APSI_P006.10218.t1		
APSI_P002.15459.t1	evm.model.NODE_41959_length_4652_cov_0.226519.2;	g16980.t1
APSI_P014.1514.t1		g5402.t1
APSI_P016.16116.t1		
APSI_P023.8461.t1		
APSI_P024.16473.t1	evm.model.NODE_20012_length_7131_cov_0.803969.1;	
APSI_P009.18250.t1		g9283.t1
APSI_P007.14199.t1		g2331.t1
APSI_P017.12300.t1	evm.model.NODE_43077_length_4576_cov_0.219825.1;	g14456.t1
APSI_P019.8008.t1	evm.model.NODE_12087_length_9232_cov_0.709061.1;	g15687.t1
APSI_P018.7749.t1		
APSI_P013.3907.t1		g5574.t1
APSI_P023.8520.t1	evm.model.NODE_31568_length_5559_cov_0.333211.1;	g13476.t1
APSI_P013.4080.t1		g133.t1
APSI_P008.16758.t1	evm.model.NODE_28014_length_5936_cov_0.422104.1;	
APSI_P005.11212.t1		g3453.t1
APSI_P006.9443.t1		
APSI_P019.8195.t1		
APSI_P008.17140.t1	evm.model.NODE_214_length_45606_cov_0.34733.1;	g3424.t1
APSI_P009.18252.t1		g9283.t1
APSI_P005.10417.t1		
APSI_P005.10938.t1		
APSI_P015.12681.t1		
APSI_P023.8350.t1		g3551.t1
APSI_P023.8518.t1	evm.model.NODE_26533_length_6113_cov_2.23154.2;	g15265.t1
APSI_P006.9522.t1	evm.model.NODE_11794_length_9343_cov_0.50255.1;	g15193.t1
APSI_P004.3483.t1	evm.model.NODE_1717_length_23147_cov_0.744494.2;	
APSI_P005.10507.t1		
APSI_P007.13867.t1		
APSI_P009.18208.t1	evm.model.NODE_47421_length_4284_cov_0.770026.1;	g6831.t1
APSI_P004.3446.t1		g4160.t1
APSI_P008.16895.t1	evm.model.NODE_11912_length_9294_cov_0.491655.1;	g15702.t1
APSI_P022.4680.t1		
APSI_P009.17668.t1		g16952.t1
APSI_P012.8774.t1		
APSI_P005.11073.t1	evm.model.NODE_17650_length_7657_cov_0.811421.1;	g930.t1
APSI_P003.1924.t1	evm.model.NODE_31145_length_5605_cov_0.239321.1;	g14760.t1
APSI_P012.9139.t1	evm.model.NODE_37766_length_4983_cov_0.484349.1;	g11678.t1
APSI_P013.3895.t1	evm.model.NODE_34254_length_5289_cov_0.923867.1;	g9814.t1

APSI_P007.14189.t1	evm.model.NODE_1060_length_27712_cov_0.666751.1;	g3796.t1
APSI_P001.6438.t1	evm.model.NODE_5695_length_13335_cov_0.919443.1;	g17956.t1
APSI_P017.12449.t1		g13636.t1
APSI_P007.13786.t1	evm.model.NODE_17596_length_7670_cov_0.351982.1;	g549.t1
APSI_P005.10407.t1		
APSI_P001.6666.t1	evm.model.NODE_34381_length_5277_cov_0.283883.1;	
APSI_P018.7748.t1		
APSI_P002.15545.t1	evm.model.NODE_5238_length_13853_cov_0.473956.1;	g4213.t1
APSI_P023.8517.t1	evm.model.NODE_26533_length_6113_cov_2.23154.2;	g17175.t1
APSI_P018.7519.t1	evm.model.NODE_139_length_51599_cov_0.560033.2;	g13658.t1
APSI_P001.6422.t1		
APSI_P008.16939.t2	evm.model.NODE_31568_length_5559_cov_0.333211.1;	g13476.t1
APSI_P005.10528.t1	evm.model.NODE_13647_length_8711_cov_0.688956.4;	
APSI_P005.10668.t1		
APSI_P006.9601.t1	evm.model.NODE_3763_length_16150_cov_0.576671.1;	
APSI_P024.16506.t1		
APSI_P017.12375.t1	evm.model.NODE_42799_length_4595_cov_0.305282.1;	
APSI_P007.14181.t1	evm.model.NODE_4_length_99494_cov_0.351008.4;	g16911.t1
APSI_P002.14561.t2	evm.model.NODE_29272_length_5795_cov_1.39132.1;	g11407.t1
APSI_P001.5292.t1	evm.model.NODE_11428_length_9490_cov_0.763695.1;	g15514.t1
APSI_P004.3816.t1		
APSI_P001.7184.t1	evm.model.NODE_44175_length_4501_cov_0.595107.1;	g14173.t1
APSI_P008.16998.t1		
APSI_P009.18162.t1		
APSI_P014.1455.t1	evm.model.NODE_5026_length_14122_cov_0.672621.3;	
APSI_P008.17031.t1		
APSI_P013.4169.t1	evm.model.NODE_2744_length_18764_cov_0.703064.1;	
APSI_P007.13627.t1	evm.model.NODE_22544_length_6661_cov_0.699265.1;	
APSI_P003.1876.t1		
APSI_P007.13696.t1	evm.model.NODE_39355_length_4852_cov_0.340106.1;	g11280.t1
APSI_P009.17929.t1		g17682.t1
APSI_P003.2485.t1		g18421.t1
APSI_P017.12429.t1	evm.model.NODE_3559_length_16610_cov_0.298914.1;	g17136.t1
APSI_P004.2961.t1		
APSI_P004.3021.t1	evm.model.NODE_20239_length_7088_cov_0.730068.1;	g2154.t1
APSI_P004.3573.t1	evm.model.NODE_25723_length_6213_cov_1.77834.1;	
APSI_P002.15153.t1	evm.model.NODE_21040_length_6916_cov_0.875441.2;	g14717.t1
APSI_P019.8218.t1		
APSI_P017.12375.t2	evm.model.NODE_42799_length_4595_cov_0.305282.1;	
APSI_P005.10730.t1	evm.model.NODE_10152_length_10096_cov_0.832481.1;	g768.t1
APSI_P006.9653.t1		g5449.t1
APSI_P004.2937.t1		
APSI_P007.14430.t1		
APSI_P008.17394.t1		g17255.t1
APSI_P012.9030.t1		
APSI_P010.12120.t1		

APSI_P006.9736.t1		
APSI_P012.8606.t1	evm.model.NODE_53733_length_3913_cov_1.12097.1;	g14881.t2
APSI_H005.1788.t1	evm.model.NODE_4428_length_15041_cov_0.398283.1;	g11725.t1
APSI_H004.2917.t1	evm.model.NODE_19449_length_7248_cov_1.41983.2;	g11152.t1
APSI_H011.7922.t1		
APSI_H003.4396.t1	evm.model.NODE_42655_length_4604_cov_0.279875.1;	
APSI_H002.13098.t1		g2502.t1
APSI_H002.12351.t1	evm.model.NODE_214_length_45606_cov_0.34733.1;	g17078.t1
APSI_H020.87.t1	evm.model.NODE_24204_length_6402_cov_0.414343.1;	g1935.t1
APSI_H001.7110.t2		
APSI_H001.6138.t1	evm.model.NODE_10462_length_9942_cov_1.10912.2;	g17661.t1
APSI_H006.14420.t1		g16748.t1
APSI_H001.6253.t1	evm.model.NODE_4445_length_15006_cov_0.703475.2;	g17471.t1
APSI_H004.3191.t1		
APSI_H011.7909.t1	evm.model.NODE_47468_length_4281_cov_0.437891.1;	
APSI_H004.3438.t1		
APSI_H004.3166.t1	evm.model.NODE_2638_length_19144_cov_0.79755.1;	g17901.t1
APSI_H004.3327.t1		g10769.t1
APSI_H003.4728.t3		
APSI_H004.3321.t1		g495.t1
APSI_H016.15417.t2		
APSI_H005.1280.t1		
APSI_H011.7947.t1	evm.model.NODE_17812_length_7621_cov_1.97278.4;	g5886.t1
APSI_H020.373.t1	evm.model.NODE_10462_length_9942_cov_1.10912.2;	g2930.t1
APSI_H017.8136.t1	evm.model.NODE_3408_length_16981_cov_1.40977.3;	
APSI_H003.4610.t1		g14288.t1
APSI_H002.13405.t1		
APSI_H006.14609.t1	evm.model.NODE_31145_length_5605_cov_0.239321.1;	g14760.t1
APSI_H003.5320.t1		
APSI_H004.3315.t1		
APSI_H012.10730.t1		
APSI_H008.9266.t1	evm.model.NODE_4300_length_15213_cov_1.43309.2;	g889.t1
APSI_H011.7921.t1		
APSI_H005.1404.t1	evm.model.NODE_1401_length_25092_cov_0.323334.1;	g9384.t1
APSI_H008.9963.t1		
APSI_H014.2269.t1	evm.model.NODE_16851_length_7839_cov_0.835581.1;	g9203.t1
APSI_H003.5152.t1		
APSI_H004.3230.t1	evm.model.NODE_2099_length_21180_cov_0.647858.3;	g18071.t1
APSI_H005.1520.t1	evm.model.NODE_1060_length_27712_cov_0.666751.1;	g12670.t1
APSI_H006.15147.t2		
APSI_H001.6654.t1		
APSI_H002.12863.t1	evm.model.NODE_11428_length_9490_cov_0.763695.1;	g15514.t1
APSI_H019.11126.t1		
APSI_H007.8636.t1	evm.model.NODE_3763_length_16150_cov_0.576671.1;	
APSI_H006.14419.t1		g16748.t1
APSI_H003.5322.t1		

APSI_H002.13389.t2		
APSI_H003.4232.t1		g16463.t1
APSI_H013.5636.t1		
APSI_H006.14788.t2		
APSI_H004.3139.t1	evm.model.NODE_12201_length_9196_cov_0.656302.1;	g10530.t1
APSI_H017.8167.t1	evm.model.NODE_3408_length_16981_cov_1.40977.3;	
APSI_H017.8128.t1	evm.model.NODE_3408_length_16981_cov_1.40977.3;	
APSI_H002.13405.t3		
APSI_H008.9416.t1		g15597.t1
APSI_H004.3130.t1	evm.model.NODE_2099_length_21180_cov_0.647858.3;	g18071.t1
APSI_H009.11505.t1		
APSI_H016.15335.t1	evm.model.NODE_12201_length_9196_cov_0.656302.1;	g10530.t1
APSI_H015.402.t1	evm.model.NODE_4351_length_15142_cov_1.48465.1;	
APSI_H004.3254.t1	evm.model.NODE_40251_length_4784_cov_0.630878.1;	
APSI_H011.7549.t1		g13058.t1
APSI_H008.9936.t1	evm.model.NODE_34381_length_5277_cov_0.283883.1;	
APSI_H004.3137.t1	evm.model.NODE_12201_length_9196_cov_0.656302.1;	g10530.t1
APSI_H007.8902.t1	evm.model.NODE_47864_length_4256_cov_0.806733.1;	g13741.t1
APSI_H017.8139.t1		
APSI_H017.8334.t1		g17424.t1
APSI_H002.12434.t1		g1245.t1
APSI_H015.414.t1	evm.model.NODE_53034_length_3952_cov_1.53203.1;	g13990.t1
APSI_H011.7941.t1	evm.model.NODE_11232_length_9577_cov_1.54677.3;	g5938.t1
APSI_H004.3602.t1	evm.model.NODE_17596_length_7670_cov_0.351982.1;	g549.t1
APSI_H005.1601.t1	evm.model.NODE_17377_length_7721_cov_0.241375.1;	g10309.t1
APSI_H006.14364.t1	evm.model.NODE_24357_length_6382_cov_0.354117.1;	
APSI_H005.1650.t1		g1487.t1
APSI_H005.1156.t1		g11280.t1
APSI_H011.7445.t1	evm.model.NODE_47265_length_4293_cov_0.247.1;	g10611.t1
APSI_H008.9302.t1		
APSI_H005.958.t1	evm.model.NODE_4428_length_15041_cov_0.398283.1;	g4850.t1
APSI_H010.14291.t1		g18533.t1
APSI_H009.11834.t1		g15492.t1
APSI_H003.5224.t1	evm.model.NODE_17047_length_7793_cov_0.273379.1;	g10367.t1
APSI_H003.4333.t1		g5661.t1
APSI_H010.13775.t1	evm.model.NODE_4319_length_15189_cov_1.76232.8;	g4950.t1
APSI_H003.4419.t1	evm.model.NODE_17650_length_7657_cov_0.811421.1;	g16789.t1
APSI_H005.941.t1	evm.model.NODE_30167_length_5704_cov_0.64246.1;	g6986.t1
APSI_H006.15057.t1		g18421.t1
APSI_H001.5919.t1		
APSI_H001.6936.t1		g5402.t1
APSI_H007.8999.t1	evm.model.NODE_360_length_39094_cov_0.299261.2;	
APSI_H010.14175.t1	evm.model.NODE_2556_length_19410_cov_0.342789.1;	g13658.t1
APSI_H003.4229.t1		g16463.t1
APSI_H001.5956.t1	evm.model.NODE_5371_length_13696_cov_0.641241.1;	
APSI_H009.11923.t1	evm.model.NODE_10347_length_9998_cov_1.27474.2;	g9148.t1

APSI_H003.4925.t1		
APSI_H005.1524.t1	evm.model.NODE_1060_length_27712_cov_0.666751.1;	g3796.t1
APSI_H016.15662.t1		
APSI_H002.12594.t1		
APSI_H004.3630.t1		g2174.t1
APSI_H013.5580.t1		g13542.t1
APSI_H005.1704.t1		
APSI_H016.15382.t1		
APSI_H002.13062.t1		
APSI_H001.7055.t1	evm.model.NODE_11786_length_9347_cov_1.30542.1;	g12728.t1
APSI_H004.3192.t1		
APSI_H012.10628.t1	evm.model.NODE_12201_length_9196_cov_0.656302.1;	g16960.t1
APSI_H002.13295.t1	evm.model.NODE_14121_length_8545_cov_0.464531.1;	
APSI_H014.2201.t1	evm.model.NODE_26623_length_6099_cov_0.992802.1;	g10920.t1
APSI_H002.13034.t1	evm.model.NODE_50423_length_4101_cov_1.02718.1;	g12112.t1
APSI_H003.5003.t1		g3897.t2
APSI_H008.9977.t1	evm.model.NODE_4300_length_15213_cov_1.43309.2;	g889.t1
APSI_H010.14290.t1		g18533.t1
APSI_H014.2315.t1		g17727.t1
APSI_H005.1636.t1		
APSI_H006.15054.t1		g18421.t1
APSI_H012.10741.t1		g18289.t1
APSI_H010.13681.t1		g1482.t1
APSI_H016.15367.t1		g12043.t1
APSI_H006.15147.t3		
APSI_H007.8945.t1	evm.model.NODE_27074_length_6045_cov_1.07722.1;	g5808.t1
APSI_H016.15354.t1		
APSI_H007.8559.t1		g3151.t1
APSI_H002.12404.t1		
APSI_H011.7944.t1	evm.model.NODE_17812_length_7621_cov_1.97278.4;	g5886.t1
APSI_H002.12334.t1	evm.model.NODE_50324_length_4107_cov_0.0743719.1;	
APSI_H008.10082.t1		g14288.t1
APSI_H001.7323.t1		
APSI_H003.5243.t1	evm.model.NODE_37766_length_4983_cov_0.484349.1;	g11678.t1
APSI_H014.2402.t1		
APSI_H027.3774.t1	evm.model.NODE_10462_length_9942_cov_1.10912.2;	g2930.t1
APSI_H007.8961.t1		
APSI_H013.5633.t1		
APSI_H007.8761.t1		g15597.t1
APSI_H007.8744.t1	evm.model.NODE_12191_length_9196_cov_0.891534.1;	g14855.t1
APSI_H005.1565.t1	evm.model.NODE_2361_length_20081_cov_0.466553.1;	g3932.t1
APSI_H002.13097.t1		g2502.t1
APSI_H005.1816.t1		
APSI_H004.3650.t1	evm.model.NODE_33603_length_5352_cov_1.82086.2;	
APSI_H017.8250.t1		g3453.t1
APSI_H003.4226.t1		g16463.t1

APSI_H001.6793.t1	evm.model.NODE_38995_length_4882_cov_1.60126.4;	
APSI_H003.4473.t1	evm.model.NODE_1187_length_26556_cov_0.308868.2;	g11393.t2
APSI_H003.4621.t1	evm.model.NODE_31334_length_5585_cov_0.0443386.1;	
APSI_H002.12217.t1	evm.model.NODE_2556_length_19410_cov_0.342789.1;	g13658.t1
APSI_H019.10994.t1	evm.model.NODE_23109_length_6569_cov_0.855324.2;	g4969.t1
APSI_H003.4728.t1		
APSI_H012.10636.t1	evm.model.NODE_12201_length_9196_cov_0.656302.1;	g16960.t1
APSI_H010.14030.t1		
APSI_H008.9532.t1		
APSI_H020.197.t1		g15077.t1
APSI_H001.6977.t1		
APSI_H010.14266.t1	evm.model.NODE_41959_length_4652_cov_0.226519.2;	g16980.t1
APSI_H014.2421.t1	evm.model.NODE_21744_length_6797_cov_0.678561.2;	g17661.t1
APSI_H003.4491.t1	evm.model.NODE_214_length_45606_cov_0.34733.1;	g12843.t1
APSI_H020.150.t1		
APSI_H009.11351.t1		
APSI_H003.4911.t1	evm.model.NODE_10225_length_10054_cov_0.703536.1;	
APSI_H018.10277.t1	evm.model.NODE_13755_length_8677_cov_0.62.1;	g6327.t1
APSI_H002.13237.t1		
APSI_H008.9981.t1		g13814.t1
APSI_H006.14618.t1	evm.model.NODE_3753_length_16153_cov_0.416838.1;	
APSI_H004.2990.t1		
APSI_H020.265.t1	evm.model.NODE_2137_length_21017_cov_0.479943.1;	g1006.t1
APSI_H002.12188.t1		
APSI_H003.4911.t2	evm.model.NODE_10225_length_10054_cov_0.703536.1;	
APSI_H001.6016.t1		
APSI_H001.6500.t1		
APSI_H020.214.t1		
APSI_H009.11370.t1	evm.model.NODE_10530_length_9908_cov_0.717514.4;	g6647.t1
APSI_H014.2401.t1		
APSI_H001.6605.t1		
APSI_H002.13405.t5		
APSI_H003.4613.t1	evm.model.NODE_13633_length_8716_cov_0.215275.1;	g1121.t1
APSI_H020.352.t1	evm.model.NODE_10462_length_9942_cov_1.10912.2;	g2930.t1
APSI_H003.4166.t1		
APSI_H006.14750.t1	evm.model.NODE_10347_length_9998_cov_1.27474.2;	g9148.t1
APSI_H006.14979.t1	evm.model.NODE_1543_length_24159_cov_0.485562.1;	g15640.t1
APSI_H003.4583.t1	evm.model.NODE_47864_length_4256_cov_0.806733.1;	g15702.t1
APSI_H011.7469.t1		g9852.t1
APSI_H003.3953.t1		g5872.t1
APSI_H004.3151.t1	evm.model.NODE_36746_length_5068_cov_0.660393.1;	g3090.t1
APSI_H001.5883.t1		
APSI_H011.7875.t1		g3575.t1
APSI_H023.7995.t1		
APSI_H016.15346.t1	evm.model.NODE_12201_length_9196_cov_0.656302.1;	g10530.t1
APSI_H011.7901.t1		

APSI_H001.7002.t1		
APSI_H003.5302.t1		g15544.t1
APSI_H009.11786.t1		g133.t1
APSI_H016.15417.t1		
APSI_H017.8154.t1		g2424.t1
APSI_H012.10563.t1		
APSI_H011.7479.t1	evm.model.NODE_13415_length_8785_cov_0.517672.2;	g16998.t1
APSI_H001.7111.t2		
APSI_H001.6143.t1	evm.model.NODE_10462_length_9942_cov_1.10912.2;	g14881.t2
APSI_H018.10369.t1		g1477.t1
APSI_H003.5272.t1	evm.model.NODE_55_length_65597_cov_0.286605.1;	g17437.t1
APSI_H003.4519.t1		
APSI_H006.15147.t1		
APSI_H004.3417.t1	evm.model.NODE_2715_length_18873_cov_0.615565.1;	g12687.t1
APSI_H015.658.t1		
APSI_H002.12405.t1		
APSI_H013.5638.t1		
APSI_H002.12181.t1		
APSI_H006.15291.t1		
APSI_H004.2950.t1	evm.model.NODE_20451_length_7051_cov_0.568602.1;	g15687.t1
APSI_H006.15277.t1		
APSI_H004.3625.t1		
APSI_H011.7447.t1	evm.model.NODE_2137_length_21017_cov_0.479943.1;	g10611.t1
APSI_H009.11522.t1	evm.model.NODE_2876_length_18335_cov_0.47221.3;	g3021.t1
APSI_H008.9642.t1		g1326.t1
APSI_H004.3432.t1	evm.model.NODE_23552_length_6500_cov_0.90805.1;	g12687.t1
APSI_H005.1083.t1	evm.model.NODE_13939_length_8621_cov_1.12668.3;	g4948.t1
APSI_H008.9972.t1	evm.model.NODE_4300_length_15213_cov_1.43309.2;	g889.t1
APSI_H004.3737.t1		g12300.t1
APSI_H013.5578.t1	evm.model.NODE_12169_length_9205_cov_0.451481.1;	g16342.t1
APSI_H002.12403.t1		
APSI_H015.607.t1	evm.model.NODE_21468_length_6852_cov_0.295613.1;	g11292.t1
APSI_H014.2116.t1	evm.model.NODE_30385_length_5682_cov_0.453105.1;	g2856.t1
APSI_H002.13405.t2		
APSI_H010.13761.t1	evm.model.NODE_5615_length_13416_cov_0.518602.2;	g836.t1
APSI_H008.9895.t1		g15597.t1
APSI_H001.7110.t1		
APSI_H002.13439.t1	evm.model.NODE_10061_length_10145_cov_0.0507087.1;	
APSI_H003.4924.t1		g9283.t1
APSI_H018.10384.t1		g1477.t1
APSI_H009.11254.t1		
APSI_H001.6259.t1	evm.model.NODE_4445_length_15006_cov_0.703475.2;	g17471.t1
APSI_H001.7111.t1		
APSI_H019.11152.t1	evm.model.NODE_1768_length_22731_cov_0.761502.2;	g2914.t1
APSI_H002.12498.t1		g149.t1
APSI_H012.10577.t1	evm.model.NODE_14478_length_8456_cov_1.05451.2;	g2699.t1

APSI_H018.10205.t1	evm.model.NODE_35185_length_5204_cov_1.13098.1;	g14932.t1
APSI_H001.6143.t2	evm.model.NODE_10462_length_9942_cov_1.10912.2;	g14881.t2
APSI_H004.2779.t1	evm.model.NODE_57798_length_3696_cov_0.819277.1;	
APSI_H004.2904.t1	evm.model.NODE_19449_length_7248_cov_1.41983.2;	g11152.t1
APSI_H001.5864.t1	evm.model.NODE_41959_length_4652_cov_0.226519.2;	g16748.t1
APSI_H007.8619.t1	evm.model.NODE_33933_length_5321_cov_0.561995.1;	
APSI_H004.2977.t1		
APSI_H002.12864.t1		
APSI_H003.4422.t1	evm.model.NODE_17650_length_7657_cov_0.811421.1;	g16789.t1
APSI_H010.13570.t2	evm.model.NODE_29272_length_5795_cov_1.39132.1;	g11407.t1
APSI_H007.9034.t1		g1245.t1
APSI_H007.9071.t1		g2616.t1
APSI_H013.5415.t1		
APSI_H005.990.t1		g2331.t1
APSI_H014.2232.t1		g18208.t1
APSI_H001.6153.t1	evm.model.NODE_53733_length_3913_cov_1.12097.1;	g14881.t2
APSI_H001.6954.t1	evm.model.NODE_35140_length_5210_cov_0.691324.1;	
APSI_H009.11931.t1		
APSI_H024.9216.t1	evm.model.NODE_139_length_51599_cov_0.560033.2;	g13658.t1
APSI_H003.4866.t1		g544.t1
APSI_H014.2291.t1		g14240.t1
APSI_H008.9486.t2		g3485.t1
APSI_H003.4898.t1	evm.model.NODE_10225_length_10054_cov_0.703536.1;	
APSI_H016.15485.t1		g11599.t1
APSI_H013.5645.t1	evm.model.NODE_17070_length_7788_cov_0.437671.1;	g10302.t1
APSI_H002.12785.t1	evm.model.NODE_43077_length_4576_cov_0.219825.1;	g14456.t1
APSI_H004.2899.t1	evm.model.NODE_30484_length_5672_cov_0.655005.1;	g13520.t1
APSI_H002.12353.t1	evm.model.NODE_214_length_45606_cov_0.34733.1;	g17078.t1
APSI_H014.2344.t1		g645.t1
APSI_H002.12843.t1	evm.model.NODE_11209_length_9589_cov_0.266751.1;	
APSI_H007.8820.t1	evm.model.NODE_42655_length_4604_cov_0.279875.1;	
APSI_H011.7462.t1	evm.model.NODE_44719_length_4465_cov_1.06524.2;	
APSI_H017.8151.t1		g2422.t1
APSI_H009.11760.t1	evm.model.NODE_215_length_45608_cov_0.342099.2;	g3569.t1
APSI_H010.14187.t1	evm.model.NODE_11112_length_9643_cov_0.62768.1;	g17758.t1
APSI_H008.9395.t1	evm.model.NODE_135553_length_1546_cov_1.04299.2;	
APSI_H002.12958.t1	evm.model.NODE_50423_length_4101_cov_1.02718.1;	g12112.t1
APSI_H015.770.t1		
APSI_H011.7407.t1	evm.model.NODE_31568_length_5559_cov_0.333211.1;	g13476.t1
APSI_H002.12354.t1	evm.model.NODE_214_length_45606_cov_0.34733.1;	g17076.t1
APSI_H003.4928.t1		
APSI_H012.10664.t1	evm.model.NODE_47016_length_4308_cov_0.743902.1;	g1911.t1
APSI_H010.13570.t1	evm.model.NODE_29272_length_5795_cov_1.39132.1;	g11407.t1
APSI_H011.7930.t1	evm.model.NODE_11232_length_9577_cov_1.54677.3;	g11403.t1
APSI_H007.9111.t1		g13719.t1
APSI_H005.1264.t1	evm.model.NODE_1172_length_26737_cov_0.188193.1;	g17973.t1

APSI_H001.6018.t1		
APSI_H011.7881.t1	evm.model.NODE_47265_length_4293_cov_0.247.1;	
APSI_H020.290.t1	evm.model.NODE_4319_length_15189_cov_1.76232.8;	g14475.t1
APSI_H002.13389.t1		
APSI_H009.12003.t1	evm.model.NODE_10347_length_9998_cov_1.27474.2;	g5740.t1
APSI_H010.13613.t1		g2073.t1
APSI_H005.1513.t1	evm.model.NODE_4_length_99494_cov_0.351008.4;	g16911.t1
APSI_H012.10558.t1		
APSI_H008.9467.t1		
APSI_H018.10350.t1	evm.model.NODE_16423_length_7930_cov_0.859926.2;	g15043.t1
APSI_H003.5318.t1	evm.model.NODE_15472_length_8166_cov_1.05996.1;	g16531.t1
APSI_H006.14775.t5		
APSI_H004.2981.t1		
APSI_H004.3033.t1	evm.model.NODE_43844_length_4524_cov_1.04298.2;	g9005.t1
APSI_H016.15598.t1	evm.model.NODE_17742_length_7635_cov_0.85895.1;	g1647.t1
APSI_H005.1070.t1		g11131.t1
APSI_H001.6817.t1	evm.model.NODE_471_length_36147_cov_0.628061.4;	g3300.t1
APSI_H006.14597.t1	evm.model.NODE_11232_length_9577_cov_1.54677.3;	g11403.t1
APSI_H002.12402.t1		
APSI_H002.13405.t4		
APSI_H010.14016.t1		
APSI_H012.10637.t1	evm.model.NODE_12201_length_9196_cov_0.656302.1;	g16960.t1
APSI_H003.4206.t1		
APSI_H004.3492.t1		
APSI_H020.197.t2		g15077.t1
APSI_H007.9186.t1		
APSI_H020.231.t1		
APSI_H001.6945.t1	evm.model.NODE_21756_length_6789_cov_0.714179.1;	g8972.t1
APSI_H004.3379.t1	evm.model.NODE_25723_length_6213_cov_1.77834.1;	
APSI_H017.8157.t1	evm.model.NODE_17650_length_7657_cov_0.811421.1;	g930.t1

APPENDIX E. Blast local of effector candidates from MF-1 and SA biotypes; parameters used: e-value: 10-5 and identity ≥ 40%

MF-1	SA
evm.model.NODE_10061_length_10145_cov_0.0507087.1	
evm.model.NODE_10152_length_10096_cov_0.832481.1	g768.t1
evm.model.NODE_10225_length_10054_cov_0.703536.1	
evm.model.NODE_10347_length_9998_cov_1.27474.2	g9148.t1
evm.model.NODE_10399_length_9973_cov_17.2373.3	
evm.model.NODE_104004_length_2112_cov_1.66801.1	g13741.t1
evm.model.NODE_10462_length_9942_cov_1.10912.2	g17661.t1
evm.model.NODE_10530_length_9908_cov_0.717514.4	g5660.t1
evm.model.NODE_10569_length_9889_cov_0.720242.1	g2183.t1
evm.model.NODE_105_length_55253_cov_0.45355.1	g16373.t1
evm.model.NODE_1060_length_27712_cov_0.666751.1	g12670.t1
evm.model.NODE_1074_length_27621_cov_1.26717.2	g845.t1
evm.model.NODE_11108_length_9646_cov_0.920475.1	
evm.model.NODE_11112_length_9643_cov_0.62768.1	g17758.t1
evm.model.NODE_11176_length_9608_cov_0.896003.1	g16369.t1
evm.model.NODE_11209_length_9589_cov_0.266751.1	
evm.model.NODE_11232_length_9577_cov_1.54677.3	g11403.t1
evm.model.NODE_11274_length_9557_cov_0.67561.2	g317.t1
evm.model.NODE_11428_length_9490_cov_0.763695.1	g15514.t1
evm.model.NODE_114746_length_1891_cov_0.502268.1	
evm.model.NODE_11687_length_9385_cov_1.54699.2	g13487.t1
evm.model.NODE_1172_length_26737_cov_0.188193.1	g17973.t1
evm.model.NODE_11786_length_9347_cov_1.30542.1	g12728.t1
evm.model.NODE_11794_length_9343_cov_0.50255.1	g15193.t1
evm.model.NODE_1187_length_26556_cov_0.308868.2	g11393.t2
evm.model.NODE_11912_length_9294_cov_0.491655.1	g15702.t1
evm.model.NODE_11_length_86909_cov_0.133459.3	g13487.t1
evm.model.NODE_12087_length_9232_cov_0.709061.1	g15687.t1
evm.model.NODE_12169_length_9205_cov_0.451481.1	g16342.t1
evm.model.NODE_12191_length_9196_cov_0.891534.1	g14855.t1
evm.model.NODE_12201_length_9196_cov_0.656302.1	g10530.t1
evm.model.NODE_123330_length_1735_cov_1.20522.1	
evm.model.NODE_12378_length_9131_cov_0.962914.1	g5081.t1
evm.model.NODE_12491_length_9093_cov_0.505688.1	g14173.t1
evm.model.NODE_12507_length_9082_cov_0.159058.2	
evm.model.NODE_12611_length_9049_cov_0.544945.3	g6826.t1
evm.model.NODE_127356_length_1668_cov_0.0661908.1	
evm.model.NODE_12741_length_9006_cov_0.176484.1	
evm.model.NODE_12743_length_9006_cov_0.699628.1	
evm.model.NODE_12793_length_8993_cov_0.571622.3	
evm.model.NODE_128173_length_1656_cov_0.691302.1	
evm.model.NODE_131451_length_1605_cov_1.44655.1	
evm.model.NODE_133257_length_1578_cov_1.36527.1	

evm.model.NODE_13415_length_8785_cov_0.517672.2	g16998.t1
evm.model.NODE_13447_length_8775_cov_0.4493.2	
evm.model.NODE_135553_length_1546_cov_1.04299.1	
evm.model.NODE_135553_length_1546_cov_1.04299.2	
evm.model.NODE_13633_length_8716_cov_0.215275.1	g1121.t1
evm.model.NODE_13647_length_8711_cov_0.688956.4	
evm.model.NODE_13752_length_8677_cov_0.852865.1	g12728.t1
evm.model.NODE_13755_length_8677_cov_0.62.1	g768.t1
evm.model.NODE_137688_length_1516_cov_1.0036.1	
evm.model.NODE_13939_length_8621_cov_1.12668.3	g4948.t1
evm.model.NODE_139_length_51599_cov_0.560033.2	g13658.t1
evm.model.NODE_1401_length_25092_cov_0.323334.1	g9384.t1
evm.model.NODE_14121_length_8545_cov_0.464531.1	
evm.model.NODE_14478_length_8456_cov_1.05451.2	g2699.t1
evm.model.NODE_14556_length_8430_cov_0.588582.2	g3709.t1
evm.model.NODE_14970_length_8304_cov_0.597261.1	g2616.t1
evm.model.NODE_15002_length_8298_cov_0.549137.1	g13868.t1
evm.model.NODE_15054_length_8284_cov_1.25043.1	
evm.model.NODE_150611_length_1345_cov_0.1	g12473.t1
evm.model.NODE_15174_length_8249_cov_0.443487.1	
evm.model.NODE_1521_length_24252_cov_1.0121.1	
evm.model.NODE_15340_length_8203_cov_0.106625.1	
evm.model.NODE_15375_length_8185_cov_0.378348.2	g265.t1
evm.model.NODE_1543_length_24159_cov_0.485562.1	g15640.t1
evm.model.NODE_154410_length_1299_cov_0.384812.1	g18071.t1
evm.model.NODE_15472_length_8166_cov_1.05996.1	g16531.t1
evm.model.NODE_15519_length_8153_cov_0.999377.2	
evm.model.NODE_15626_length_8122_cov_1.19235.1	g989.t1
evm.model.NODE_15688_length_8108_cov_1.01428.1	g14051.t1
evm.model.NODE_15804_length_8083_cov_0.214429.1	g13581.t1
evm.model.NODE_15836_length_8076_cov_0.739338.1	g845.t1
evm.model.NODE_15944_length_8047_cov_1.14973.1	
evm.model.NODE_1600_length_23783_cov_1.50397.5	
evm.model.NODE_161229_length_1221_cov_4.3766.1	
evm.model.NODE_16422_length_7909_cov_0.220044.1	g9764.t1
evm.model.NODE_16423_length_7930_cov_0.859926.2	g15043.t1
evm.model.NODE_16665_length_7877_cov_0.280351.1	g13308.t1
evm.model.NODE_16670_length_7878_cov_1.91511.2	g17580.t1
evm.model.NODE_16740_length_7856_cov_0.165482.1	g16500.t1
evm.model.NODE_167661_length_1151_cov_0.768555.1	
evm.model.NODE_16776_length_7854_cov_0.763427.3	
evm.model.NODE_16851_length_7839_cov_0.835581.1	g9203.t1
evm.model.NODE_17047_length_7793_cov_0.273379.1	g10367.t1
evm.model.NODE_17070_length_7788_cov_0.437671.1	g10302.t1
evm.model.NODE_1717_length_23147_cov_0.744494.2	
evm.model.NODE_17345_length_7727_cov_0.360395.1	g1490.t1

evm.model.NODE_17377_length_7721_cov_0.241375.1	g10309.t1
evm.model.NODE_17418_length_7712_cov_0.404087.1	g17575.t1
evm.model.NODE_17469_length_7699_cov_0.658743.1	
evm.model.NODE_1747_length_22938_cov_1.23273.1	g2331.t1
evm.model.NODE_1751_length_22899_cov_0.396259.2	g11431.t1
evm.model.NODE_17596_length_7670_cov_0.351982.1	g549.t1
evm.model.NODE_17650_length_7657_cov_0.811421.1	g16789.t1
evm.model.NODE_1768_length_22731_cov_0.761502.2	g2914.t1
evm.model.NODE_17742_length_7635_cov_0.85895.1	g1647.t1
evm.model.NODE_17766_length_7629_cov_0.216742.1	g2726.t1
evm.model.NODE_17812_length_7621_cov_1.97278.4	g5886.t1
evm.model.NODE_17921_length_7595_cov_0.373058.1	
evm.model.NODE_1793_length_22625_cov_0.6064.2	
evm.model.NODE_18203_length_7530_cov_0.816831.2	
evm.model.NODE_18659_length_7423_cov_1.75308.2	
evm.model.NODE_18723_length_7409_cov_1.43408.1	
evm.model.NODE_18795_length_7393_cov_0.537022.1	
evm.model.NODE_18838_length_7381_cov_0.855114.1	g17469.t1
evm.model.NODE_19449_length_7248_cov_1.41983.2	g11152.t1
evm.model.NODE_20012_length_7131_cov_0.803969.1	
evm.model.NODE_20016_length_7129_cov_0.858183.1	
evm.model.NODE_20061_length_7120_cov_1.91105.4	g15460.t1
evm.model.NODE_20239_length_7088_cov_0.730068.1	g2154.t1
evm.model.NODE_20426_length_7056_cov_0.480445.1	g14078.t1
evm.model.NODE_20451_length_7051_cov_0.568602.1	g15687.t1
evm.model.NODE_20477_length_7046_cov_0.544154.1	g10438.t1
evm.model.NODE_20576_length_7027_cov_1.6387.2	
evm.model.NODE_2061_length_21333_cov_0.314864.1	g14108.t1
evm.model.NODE_20670_length_7007_cov_0.489971.1	
evm.model.NODE_20733_length_6994_cov_1.04733.1	g13646.t1
evm.model.NODE_2075_length_21285_cov_0.389734.2	g3296.t1
evm.model.NODE_2099_length_21180_cov_0.647858.3	g18071.t1
evm.model.NODE_21040_length_6916_cov_0.875441.2	g14717.t1
evm.model.NODE_2137_length_21017_cov_0.479943.1	g1006.t1
evm.model.NODE_21468_length_6852_cov_0.295613.1	g11292.t1
evm.model.NODE_214_length_45606_cov_0.34733.1	g12843.t1
evm.model.NODE_215_length_45608_cov_0.342099.2	g3569.t1
evm.model.NODE_2160_length_20942_cov_0.93375.2	g2930.t1
evm.model.NODE_21744_length_6797_cov_0.678561.2	g17661.t1
evm.model.NODE_21756_length_6789_cov_0.714179.1	g8972.t1
evm.model.NODE_21773_length_6791_cov_0.847539.1	g3653.t1
evm.model.NODE_22544_length_6661_cov_0.699265.1	
evm.model.NODE_2266_length_20454_cov_0.872091.3	
evm.model.NODE_22848_length_6612_cov_1.14079.1	g13542.t1
evm.model.NODE_2287_length_20383_cov_0.512243.1	
evm.model.NODE_23109_length_6569_cov_0.855324.2	g4969.t1

evm.model.NODE_23344_length_6532_cov_0.712769.1	g10309.t1
evm.model.NODE_23552_length_6500_cov_0.90805.1	g12687.t1
evm.model.NODE_2361_length_20081_cov_0.466553.1	g3932.t1
evm.model.NODE_24204_length_6402_cov_0.414343.1	g1935.t1
evm.model.NODE_24357_length_6382_cov_0.354117.1	
evm.model.NODE_2488_length_19599_cov_1.25.3	
evm.model.NODE_2496_length_19561_cov_0.842996.3	
evm.model.NODE_25339_length_6259_cov_1.47048.2	
evm.model.NODE_2556_length_19410_cov_0.342789.1	g13658.t1
evm.model.NODE_25723_length_6213_cov_1.77834.1	
evm.model.NODE_25911_length_6188_cov_0.873618.2	g6743.t1
evm.model.NODE_262_length_42745_cov_0.94878.1	
evm.model.NODE_2638_length_19144_cov_0.79755.1	g17901.t1
evm.model.NODE_2644_length_19126_cov_0.597874.1	g11445.t1
evm.model.NODE_26533_length_6113_cov_2.23154.2	g17175.t1
evm.model.NODE_26623_length_6099_cov_0.992802.1	g10920.t1
evm.model.NODE_26741_length_6086_cov_0.331096.1	
evm.model.NODE_27074_length_6045_cov_1.07722.1	g5808.t1
evm.model.NODE_2715_length_18873_cov_0.615565.1	g12687.t1
evm.model.NODE_2744_length_18764_cov_0.703064.1	
evm.model.NODE_2770_length_18665_cov_1.63449.1	g13476.t1
evm.model.NODE_27877_length_5954_cov_0.473314.1	g889.t1
evm.model.NODE_28014_length_5936_cov_0.422104.1	
evm.model.NODE_28303_length_5903_cov_0.666551.1	
evm.model.NODE_2856_length_18375_cov_1.15493.1	g15702.t1
evm.model.NODE_28608_length_5870_cov_0.279122.1	g15193.t1
evm.model.NODE_28763_length_5852_cov_0.907265.1	g836.t1
evm.model.NODE_2876_length_18335_cov_0.47221.3	g3021.t1
evm.model.NODE_28797_length_5848_cov_0.290509.1	
evm.model.NODE_28950_length_5829_cov_1.03016.1	
evm.model.NODE_29272_length_5795_cov_1.39132.1	g11407.t1
evm.model.NODE_29340_length_5789_cov_1.35694.2	g10334.t1
evm.model.NODE_2985_length_18064_cov_0.808674.5	
evm.model.NODE_30167_length_5704_cov_0.64246.1	g6986.t1
evm.model.NODE_30292_length_5692_cov_0.54583.1	
evm.model.NODE_30385_length_5682_cov_0.453105.1	g2856.t1
evm.model.NODE_30437_length_5676_cov_0.30474.1	g15702.t1
evm.model.NODE_30470_length_5673_cov_1.08186.1	
evm.model.NODE_30484_length_5672_cov_0.655005.1	g13520.t1
evm.model.NODE_306_length_40808_cov_0.610555.1	
evm.model.NODE_31145_length_5605_cov_0.239321.1	g14760.t1
evm.model.NODE_31334_length_5585_cov_0.0443386.1	
evm.model.NODE_31345_length_5584_cov_0.223016.1	
evm.model.NODE_31408_length_5577_cov_0.620367.1	
evm.model.NODE_31568_length_5559_cov_0.333211.1	g13476.t1
evm.model.NODE_31591_length_5557_cov_0.401105.1	g2183.t1

evm.model.NODE_31592_length_5557_cov_0.88232.1	
evm.model.NODE_31678_length_5549_cov_0.815382.1	
evm.model.NODE_3255_length_17366_cov_0.286377.1	
evm.model.NODE_3285_length_17284_cov_0.699598.2	g17398.t1
evm.model.NODE_32908_length_5423_cov_1.11782.2	
evm.model.NODE_33375_length_5373_cov_1.81395.1	
evm.model.NODE_33392_length_5371_cov_0.889207.2	g8042.t1
evm.model.NODE_33603_length_5352_cov_1.82086.2	
evm.model.NODE_33895_length_5326_cov_0.483362.1	
evm.model.NODE_33933_length_5321_cov_0.561995.1	
evm.model.NODE_3408_length_16981_cov_1.40977.3	
evm.model.NODE_34254_length_5289_cov_0.923867.1	g9814.t1
evm.model.NODE_3425_length_16954_cov_1.12177.2	g15269.t1
evm.model.NODE_34381_length_5277_cov_0.283883.1	
evm.model.NODE_34818_length_5238_cov_0.799452.1	
evm.model.NODE_34859_length_5234_cov_0.768357.1	
evm.model.NODE_3491_length_16812_cov_1.27576.3	g3834.t1
evm.model.NODE_35022_length_5219_cov_0.809505.2	
evm.model.NODE_35140_length_5210_cov_0.691324.1	
evm.model.NODE_35185_length_5204_cov_1.13098.1	g14932.t1
evm.model.NODE_35347_length_5190_cov_0.343935.1	
evm.model.NODE_35350_length_5186_cov_0.240221.1	
evm.model.NODE_354_length_39246_cov_0.895862.1	g12271.t1
evm.model.NODE_3559_length_16610_cov_0.298914.1	g17136.t1
evm.model.NODE_35654_length_5164_cov_0.948978.1	
evm.model.NODE_360_length_39094_cov_0.299261.2	
evm.model.NODE_36327_length_5104_cov_0.212578.1	g5561.t1
evm.model.NODE_36746_length_5068_cov_0.660393.1	g3090.t1
evm.model.NODE_37124_length_5036_cov_1.03585.1	
evm.model.NODE_3753_length_16153_cov_0.416838.1	
evm.model.NODE_3763_length_16150_cov_0.576671.1	
evm.model.NODE_37766_length_4983_cov_0.484349.1	g11678.t1
evm.model.NODE_38089_length_4957_cov_0.561698.1	
evm.model.NODE_38840_length_4894_cov_1.57562.1	
evm.model.NODE_38995_length_4882_cov_1.60126.4	
evm.model.NODE_39355_length_4852_cov_0.340106.1	g3741.t1
evm.model.NODE_39546_length_4840_cov_0.859962.1	g16975.t1
evm.model.NODE_3999_length_15719_cov_1.10076.1	g3290.t1
evm.model.NODE_4004_length_15711_cov_0.468848.2	
evm.model.NODE_40050_length_4800_cov_0.812326.1	g15424.t1
evm.model.NODE_40251_length_4784_cov_0.630878.1	
evm.model.NODE_41125_length_4715_cov_0.45728.1	
evm.model.NODE_41221_length_4707_cov_0.434061.2	
evm.model.NODE_41239_length_4704_cov_0.740991.1	
evm.model.NODE_41885_length_4657_cov_0.907506.1	
evm.model.NODE_41959_length_4652_cov_0.226519.2	g16980.t1

evm.model.NODE_42552_length_4612_cov_0.33913.1	g15809.t1
evm.model.NODE_42655_length_4604_cov_0.279875.1	
evm.model.NODE_4272_length_15245_cov_1.3394.7	
evm.model.NODE_4275_length_15239_cov_1.17988.2	
evm.model.NODE_42799_length_4595_cov_0.305282.1	
evm.model.NODE_4300_length_15213_cov_1.43309.2	g889.t1
evm.model.NODE_43077_length_4576_cov_0.219825.1	g14456.t1
evm.model.NODE_4319_length_15189_cov_1.76232.5	
evm.model.NODE_4319_length_15189_cov_1.76232.8	g14475.t1
evm.model.NODE_4351_length_15142_cov_1.48465.1	
evm.model.NODE_43844_length_4524_cov_1.04298.2	g9005.t1
evm.model.NODE_44175_length_4501_cov_0.595107.1	g14173.t1
evm.model.NODE_4428_length_15041_cov_0.398283.1	g11725.t1
evm.model.NODE_4445_length_15006_cov_0.703475.2	g17471.t1
evm.model.NODE_44719_length_4465_cov_1.06524.2	
evm.model.NODE_47016_length_4308_cov_0.743902.1	g1911.t1
evm.model.NODE_471_length_36147_cov_0.628061.4	g3300.t1
evm.model.NODE_47265_length_4293_cov_0.247.1	g10611.t1
evm.model.NODE_47421_length_4284_cov_0.770026.1	g11350.t1
evm.model.NODE_47468_length_4281_cov_0.437891.1	
evm.model.NODE_47535_length_4276_cov_0.0556627.2	
evm.model.NODE_47864_length_4256_cov_0.806733.1	g13741.t1
evm.model.NODE_48455_length_4220_cov_0.780601.1	g16800.t1
evm.model.NODE_487_length_35803_cov_0.914396.3	
evm.model.NODE_49333_length_4167_cov_0.681188.1	
evm.model.NODE_4936_length_14262_cov_0.336753.1	
evm.model.NODE_49674_length_4146_cov_0.940035.1	
evm.model.NODE_4_length_99494_cov_0.351008.4	g16911.t1
evm.model.NODE_5026_length_14122_cov_0.672621.3	
evm.model.NODE_50324_length_4107_cov_0.0743719.1	
evm.model.NODE_50423_length_4101_cov_1.02718.1	g12112.t1
evm.model.NODE_51001_length_4068_cov_1.38848.1	
evm.model.NODE_51346_length_4048_cov_2.22494.1	
evm.model.NODE_5144_length_13967_cov_0.811199.2	g14813.t1
evm.model.NODE_5174_length_13932_cov_0.457081.3	
evm.model.NODE_5238_length_13853_cov_0.473956.1	g4213.t1
evm.model.NODE_52444_length_3985_cov_0.487818.2	
evm.model.NODE_52873_length_3961_cov_0.143453.1	g12530.t1
evm.model.NODE_53034_length_3952_cov_1.53203.1	g13990.t1
evm.model.NODE_5371_length_13696_cov_0.641241.1	
evm.model.NODE_53733_length_3913_cov_1.12097.1	g14881.t2
evm.model.NODE_54407_length_3875_cov_0.682836.1	g10144.t1
evm.model.NODE_54623_length_3866_cov_0.69671.1	
evm.model.NODE_54833_length_3853_cov_7.91814.1	
evm.model.NODE_55075_length_3839_cov_0.0344828.1	
evm.model.NODE_55497_length_3818_cov_1.60634.1	g15287.t1

evm.model.NODE_5556_length_13483_cov_0.842554.2	g14855.t1
evm.model.NODE_5586_length_13452_cov_2.96878.4	
evm.model.NODE_55_length_65597_cov_0.286605.1	g17437.t1
evm.model.NODE_5615_length_13416_cov_0.518602.2	g836.t1
evm.model.NODE_56533_length_3763_cov_0.503575.1	g14667.t1
evm.model.NODE_5695_length_13335_cov_0.919443.1	g17956.t1
evm.model.NODE_5720_length_13298_cov_0.474148.1	g3727.t1
evm.model.NODE_573_length_34048_cov_0.387171.1	
evm.model.NODE_57798_length_3696_cov_0.819277.1	

4 CONCLUDING REMARKS

In a complex pathosystem as the *A. psidii* and *Eucalyptus*, the *in vitro* assays allowed simulate nearest the conditions *in planta* and enable to elucidate slightly the molecular mechanisms involved during the host infection. Our results showed that there is a differential expression of the candidate effectors comparing cuticular waxes from species resistant and susceptible. The suppression or increasing of candidate effector expression depends on the host susceptibility or resistance, and cuticular wax as a stimulus to fungi growth rises as an alternative to the *in vivo* assays, in which the challenge is access fungi material genetic. The candidate Ap28303 accumulated in the nucleus of epidermic cells of *N. benthamiana*. Although this candidate was predicted as a protease inhibitor, our findings showed that probably this candidate develops another function during the infection. This is the first study of localization subcellular of effector in *A. psidii* and a step forward in the study of genes associated with infection of myrtle rust. However, further studies are necessary to characterize the Ap28303 as an effector of *A. psidii*, and its function.

There are several biotypes of *A. psidii*, though the evolutionary mechanisms involved to explain the several hosts of *A. psidii* are still unclear. The effector's study may provide information about the genetic variability among the biotypes. Our findings in Chapter 2, showed effector candidates conserved and non-conserved among the biotypes Au, MF-1, and SA, as well unique and shared protein clusters to the biotypes. This work provided evidence of variability on effector candidates of *A. psidii* biotypes, however, it is necessary to solve the limitation about genome information from the biotypes. Therefore, our findings lay a strong foundation for further studies to characterize the variability among the effector candidates of *A. psidii* biotypes.